UTILISATION OF AN EXISTING NATURAL GAS STORAGE FIELD FOR HYDROGEN STORAGE: NORTHERN MARMARA DEPLETED GAS FIELD SIMULATION STUDY

A THESIS SUBMITTED TO
THE GRADUATE SCHOOL OF NATURAL AND APPLIED SCIENCES
OF
MIDDLE EAST TECHNICAL UNIVERSITY

BY

HASAN GÜRSEL

IN PARTIAL FULFILLMENT OF THE REQUIREMENTS
FOR
THE DEGREE OF MASTER OF SCIENCE
IN
PETROLEUM AND NATURAL GAS ENGINEERING

SEPTEMBER 2022

Approval of the thesis:

UTILISATION OF AN EXISTING NATURAL GAS STORAGE FIELD FOR HYDROGEN STORAGE: NORTHERN MARMARA DEPLETED GAS FIELD SIMULATION STUDY

submitted by **HASAN GÜRSEL** in partial fulfillment of the requirements for the degree of **Master of Science** i**n Petroleum and Natural Gas Engineering, Middle East Technical University** by,

Prof. Dr. Halil Kalıpçılar
Dean, Graduate School of **Natural and Applied Sciences** _____

Assist. Prof. Dr. İsmail Durgut
Head of the Department, **Petroleum and Natural Gas Eng, METU** _____

Assoc. Prof. Dr. Çağlar Sınayuç
Supervisor, **Petroleum and Natural Gas Eng, METU** _____

Murat Fatih Tuğan PhD.
Co-Supervisor, **Turkiye Petrolleri Anonim Ortaklığı** _____

Examining Committee Members:

Assist. Prof. Dr. İsmail Durgut
Petroleum and Natural Gas Eng, METU _____

Assoc. Prof. Dr. Çağlar Sınayuç
Petroleum and Natural Gas Eng, METU _____

Assist. Prof. Dr. Doruk Alp
Petroleum and Natural Gas Eng, METU NCC _____

Date: 02.09.2022

I hereby declare that all information in this document has been obtained and presented in accordance with academic rules and ethical conduct. I also declare that, as required by these rules and conduct, I have fully cited and referenced all material and results that are not original to this work.

Name, Surname : Hasan Gürsel

Signature :

ABSTRACT

UTILISATION OF AN EXISTING NATURAL GAS STORAGE FIELD FOR HYDROGEN STORAGE: NORTHERN MARMARA DEPLETED GAS FIELD SIMULATION STUDY

Gürsel, Hasan
Master of Science, Petroleum and Natural Gas Engineering
Supervisor : Assoc. Prof. Çağlar Sinayuç
Co-Supervisor: Murat Fatih Tuğan, PhD

September 2022, 163 pages

The time window for energy transition gets narrower each day under the pressure of climate change. Underground hydrogen storage (UHS) can play a cruicial role in future energy systems as it may hit two birds with one stone by assuring energy security and mitigating climate change.

In this study, a UHS simulation is conducted using data from the Northern Marmara Field. A commercial compositional flow simulator is used for simulating methane and hydrogen storage periods of 25 years each. As the current simulation techniques are insufficient to eradicate numerical dispersion at the field scale, it was minimized by numerical controls and assumed to be a substitution for physical dispersion.

Results showed that, for a field of such a large scale with multiple wells, each well would produce significantly different streams depending on well location and time.

With each hydrogen cycle, the separation between the total injected and produced amounts has increased, leaving 2.61% of hydrogen to be remaining in the reservoir. However, the remaining portion could be retrieved by further depleting the reservoir with an extended production.

The total withdrawn energy has been calculated as 371 TWhs for the methane storage period and 119 TWhs for the hydrogen. To compare respectively, during the methane storage period, 2.6 times more energy was withdrawn in the first cycles, raising to 6.2 times more energy for the 25^{th} cycles. As the fraction of methane that has been produced during the hydrogen cycles decreased, the energy content of the produced stream also decreased.

Keywords: Underground Hydrogen Storage, Hydrogen Reservoir Simulation, Climate Change Mitigation, Energy Security

ÖZ

MEVCUT BİR DOĞAL GAZ DEPOLAMA SAHASININ HİDROJEN DEPOLAMA İÇİN DEĞERLENDİRİLMESİ: KUZEY MARMARA SAHASI SİMÜLASYON ÇALIŞMASI

Gürsel, Hasan
Yüksek Lisans, Petrol ve Doğal gaz Mühendisliği
Tez Yöneticisi: Doç. Dr. Çağlar Sinayuç
Ortak Tez Yöneticisi: Dr. Murat Fatih Tuğan

Eylül 2022, 163 sayfa

İklim değişikliği baskısı altında enerji dönüşümü için kullanılabilecek zaman penceresi her geçen gün daralmaktadır. Enerji dönüşümünün yeri doldurulması zor parçalarından biri olması mümkün olan yeraltı hidrojen depolama (UHS), enerji güvenliğini desteklemekle birlikte iklim değişikliğiyle mücadeleye de katkı sunarak bir taşla iki kuş vurabilir.

Bu çalışmada, Kuzey Marmara Tükenmiş Doğal Gaz Sahası'nın verileriyle, ticari bir bileşimsel akış simülatörü kullanılarak, her biri 25 yıllık, metan ve takiben hidrojen depolama simülasyonu yapılmıştır. Mevcut simülasyon yöntemlerinin saha ölçeğinde nümerik dispersiyonu engellemekte yetersiz olması sebebiyle, nümerik kontroller kullanılarak bu etki en aza indirilmiş ve bu şekilde fiziksel dispersiyonu ikame ettiği varsayılmıştır.

Sonuçlar bu büyüklükte ve birden çok kuyu içeren sahalarda her kuyunun ötekilere kıyasla, kuyunun yerine ve zamana bağlı olarak kayda değer ölçüde farklı akışlar ürettiğini göstermiştir.

Her döngüde enjekte edilen ve üretilen hidrojen miktarları arasındaki makas açılmış ve son döngüden sonra %2.61 hidrojen rezervuarda kalmıştır. Kalan

miktarın, sahayı uzatılmış bir üretim periyodu ile tüketerek geri üretilmesi mümkün olabilir.

Üretilen toplam enerji metan depolama periyodu için 371 terawattsaat, hidrojen periyodu içinse 119 terawattsaat olarak hesaplanmıştır. Karşılıklı olarak kıyaslandığında, metan depolanması döneminde ilk döngüde 2.6 kat, yirmi beşinci döngüde ise 6.2 kat daha fazla enerji geri üretilmiştir. Hidrojen döngüleri esnasında üretilen metanın oranının düşmesiyle birlikte akışın ihtiva ettiği enerji de düşmüştür.

Anahtar Kelimeler: Yer Altı Hidrojen Depolama, Hidrojen Rezervuar Simulasyonu, İklim Değişikliği ile Mücadele, Enerji Güvenliği

To my family with whom I wish I could have spent more time…

ACKNOWLEDGMENTS

I am genuinely thankful to my supervisor Assoc. Prof. Çağlar Sinayuç and co-supervisor Dr. Murat Fatih Tuğan for their guidance, criticism, and advice. Without their suggestions, this thesis would not be what it is.

I want to thank the whole faculty and staff of the METU Petroleum and Natural Gas Engineering Department to whom I owe a lot for the trust and feeling of home they gave to me throughout all these years.

I am indebted to Computer Modelling Group Ltd. Support Team for providing the help in no time when required. I should especially note Ali Kasraian and Faraj Zarei who have kindly responded to me.

I want to thank Barış Sanlı for taking the time and sharing his knowledge with me on the issue of hydrogen. He is a unique source of vast open knowledge that every student interested in energy should benefit from.

I also want to thank my wife Buse for her patience and for the joy she brings to my life. She has been the best partner in science all the way.

I am filled with the deepest of gratitudes towards my parents Aysu and Tunç, and my sister Ceren for their unconditional support and love that has enabled me up to this point in my life.

Due to having limited space and being afraid of missing someone out, I wish to thank altogether to all the acquaintances who have aided and encouraged me throughout the journey.

TABLE OF CONTENTS

LIST OF TABLES

TABLES

LIST OF FIGURES

FIGURES

LIST OF ABBREVIATIONS AND NOMENCLATURE

ABBREVIATIONS

AE - Alkaline Electrolysis

AIChE - American Institute of Chemical Engineers

AR6 - Assessment Report 6

BOTAS - Boru Hatları ile Petrol Taşıma Anonim Şirketi

BTX - Benzene, Toluene, Xylene

CAPEX - Capital Expenditure

CCU - Carbon Capture and Utilisation

CMG - Computer Modeling Group

DECE - Designed Exploration and Controlled Evolution

ENTSOG - The European Network of Transmission System Operators for Gas

EOS - Equation of State

ERD - Extended Reach Drilling

FCH2JU - Fuel Cells and Hydrogen 2 Joint Undertaking

GHG - Greenhouse Gas

HyUSPRe - Hydrogen Underground Storage in Porous Reservoirs

IEA - International Energy Agency

Inj. – Injection

IMPES – Implicit Pressure Explicit Saturation

IPCC - Intergovernmental Panel on Climate Change

LF - Load Factor

LOHC - Liquid Organic Hydrogen Carriers

LRVC - Long Run Variable Cost

MOF - Metal Organic Framework

NBP - Normal boiling Point

NMGF - Northern Marmara Gas Field

NTP - Normal Temperature and Pressure

OPEX - Operational Expenditure

P/T Change - Pressure and Temperature Change

PEM - Proton Exchange Membrane

PR-1978 - Peng Robinson Equation of State (1978)

Prod. - Production

PSA - Pressure Swing Adsorption

R&D - Research and Development

SCTR - Standard Conditions

SDG - Sustainable Development Goal

SMR - Steam Methane Reforming

SNG - Synthetic Natural Gas

SOE - Solid Oxide Electrolysis

SOFC - Solid Oxide Fuel Cell

SSRM - Sulfur Species Reducing Microorganisms

T&D - Transmission and Distribution

TPAO - Türkiye Petrolleri Anonim Ortaklığı

TVD - Total Variation Diminishing

UHS - Underground Hydrogen Storage

UK - United Kingdom

UKCDR - United Kingdom Collaborative on Development Research

UN - United Nations

UNDRR - United Nations Office for Disaster Risk Reduction

UNECE - United Nations Economics Commission for Europe

UPS - Uninterruptible Power Supply

USDOE - United States Department of Energy

WEF - World Economic Forum

NOMENCLATURE

CPOR - rock compressibility, 1/psi

geofac - geometry factor

GWh - gigawatthour

krg - relative permeability to gas in the liquid/gas system

krog -Relative permeability to oil in the presence of gas and connate water for the given saturation

krow - relative permeability to oil in the water/oil system

krw - relative permeability to water at the given water saturation

KvKh Ratio - ratio of vertical permeability to horizontal permeability

KWh - kilowatthour

MWh - megawatthour

OGIP - original gas in place

P - pressure

PRPOR - reference pressure for rock compressibility, psi

Sg - gas saturation

Sw - water saturation

TWh - terawatthour

wfrac - well fraction

CHAPTER 1

INTRODUCTION

World Economic Forum identifies “Climate Action Failure” as the most severe risk the earth faces today (WEF, 2022). For many decades, climate change has been under the spotlight as one of the major problems of humankind (Bolin, 2007). The United Nations recognised the problem as a dire risk in the Sendai Framework and set it as a Sustainable Development Goal (SDG) to combat climate change in the 2030 agenda (UN, 2016; UNDRR, 2015). The sixth assessment report (AR6) produced by the Intergovernmental Panel on Climate Change (IPCC) states that anthropogenic greenhouse gas emissions (GHGs) are a significant driver for the hastening variations of the climate across the globe (Masson-Delmotte et al., 2021), and it points out the need for energy carriers such as hydrogen to mitigate the effects (Shukla et al., 2022).

Since fossil fuel emissions are the root cause of the problem, nearly all countries have been trying to transition their energy mix into a more environmentally sustainable basket of energy sources by setting up goals, developing road maps, and enacting policies such as incentives and taxes to promote the expansion of renewable energy sources and climate-friendly processes (Fekete et al., 2021; IEA, 2022a).

Unfortunately, even though their share has been growing steadily, renewables only take up a limited portion of the total primary energy supply (IEA, 2022b). Barriers to renewables’ market penetration have been studied, and there is a large consensus over their further development to be expected in the future (Asante et al., 2020; Kabel & Bassim, 2020; Nasr et al., 2020). However, the problems with hard-to-abate sectors remain on the table (Åhman, n.d.). Furthermore, integrating a large share of renewable electricity into the grid requires storage in order to have the flexibility to fulfill demand-response requirements (Denholm, 2015; Tong et al.,

2021). Solar and wind reliability of countries' electrical systems in an optimistic case can be viewed at the Appendix J.

On top of its role in the chemicals industry as a feedstock, hydrogen can be used as a medium to carry energy. It can be blended into natural gas grid to be used for heating purposes, it can be used to lower the carbon footprint of energy-intensive industries, and beyond everything, it can be stored to be used when it is most needed (IEA, 2019; Luna, 2019; Mcdonald, 2018; Shukla et al., 2022). In this way, hydrogen can replace fossil alternatives while enhancing energy security and aiding climate change mitigation at the same time (Hughes, 2009; Sheffield, 2007).

Sad to say, hydrogen brings about many problems of its own. In particular how storage can be achieved on large scale (Heinemann et al., 2021). The literature points out a few options, namely, salt caverns, depleted fields, and aquifers. Since hydrogen's role as an energy carrier is still at developmental stages many of the storage examples in practice are salt caverns leeched for the chemicals industry's needs. As a common practice not hydrogen but town gas is known to be stored at depleted gas reservoirs (Foh et al., 1979; Kruck et al., 2013; Lord et al., 2011; Zivar et al., 2021). In the recent past, two promising active projects that store 10% hydrogen that is blended with methane in sandstone reservoirs returned good results (Pérez et al., 2016; RAG et al., 2017). Although no known project has been implemented for storing 100% hydrogen in depleted gas reservoirs, their advantages such as data, infrastructure and geological availabilities make them worth considering (worldwide projects of UHS can be viewed at Appendix K).

In the Literature Survey chapter, under the Hydrogen Life Cycle heading, an introductory level of information regarding the round-trip of the hydrogen starting from the production until the end-use is presented together also with parts for the thermodynamic efficiency and cost. Since this study mainly focuses on underground hydrogen storage (UHS), this aspect of the life cycle is addressed in a separate heading within the same chapter. The salt cavern and porous media options for UHS, and the possible issues to be encountered are addressed. Following that, a comparison of H_2, CH_4, and CO_2 is presented as they might also

be competing candidates for the limited number of subsurface structures for storage.

The last heading in Literature Survey gives the field description. Northern Marmara Gas Field (NMGF) located in the Marmara Sea in Turkey, which is a depleted gas field that is currently being used to store natural gas, might be suitable for hydrogen storage (BOTAŞ, 2022; Cavanagh et al., 2022). Before beginning the modelling, possible issues that might be associated with simulating UHS in Northern Marmara Field are evaluated.

In this study, the field is modelled based solely on the previously published data in prior studies (Abravcı, 2017; Bagci & Öztürk, 2007; Çalışgan, 2005; Gumrah et al., 2005; Kaptanoğlu et al., 1998; Karaalioğlu, 1997; Özkiliç, 2005; Öztürk, 2004; Sahin et al., 2012; Yildirim et al., 2009). The model is fine-tuned and uncertainty in input parameters are minimised by history matching the past production performance of the field from 1997 to 2002. The model validity is checked by solving the gas material balance analytically using the field data that is extracted from Sahin et al., (2012) by Grabit (see Appendix B).

Subsequently, starting from 2007, additional wells are added to the model to simulate 25 years of cyclic methane storage between 2007-2032. This period is followed by 25 years of cyclic hydrogen storage between 2032-2057. Both periods have one cycle per year consisting of four parts to mimic the field practice (Abravcı, 2017). An extended production period is simulated to show that the remaining hydrogen at the reservoir is reproducible by further depletion of the field. Lastly, a simulation until the year 3500 is run to see for the diffusion effects which are minuscule compared to the dispersion.

In the penultimate chapter, the obtained results are shared and discussed. Lastly, based on these discussions, conclusions are drawn and suggestions are given for further studies.

CHAPTER 2

LITERATURE SURVEY

Made up of just one electron and one proton, hydrogen is the simplest and the most abundant element in the universe (EIA, n.d.). The two naturally occurring isotopes of hydrogen, namely deuterium and tritium, which are commonly used in nuclear applications, are left beyond the scope of this study (Housecroft, n.d.). Although it is believed not to be naturally found in the molecular form in large amounts here on Earth, there are coincidental geological discoveries of hydrogen accumulations that might point out otherwise (Zgonnik, 2020).

The element was discovered by Henry Cavendish in 1776. The word 'hydrogen' is coined as a French word coming from the Greek hudro (water) and genes (born) (Oxford Learner's Dictionaries, n.d.; Royal Society of Chemistry, n.d.). 'Hydrogen' throughout this text is used to denote the hydrogen molecule (H_2) which is a colorless, odorless, and highly flammable gas for which the properties are available in Appendix F.

Hydrogen has the highest energy content per mass among all fuels, however, its low density in ambient conditions require advanced storage methods to be developed (USDOE, 2022). Moreover, research and development of "production of hydrogen from water" has been in the International Energy Program since the founding of the International Energy Agency (IEA) in 1974 (Scott, 2004).

2.1 Hydrogen Life Cycle

To create a more wholesome picture, and to develop a more solid intuition, not just the porous media storage aspect but the whole life cycle of hydrogen was investigated. Needless to say, each heading requires multidisciplinary expertise and could have a thesis dedicated just to itself. Nevertheless, at an introductory level, this thesis might hopefully point out the key subjects related to the processes leading to the large scale storage of hydrogen in the subsurface porous medium.

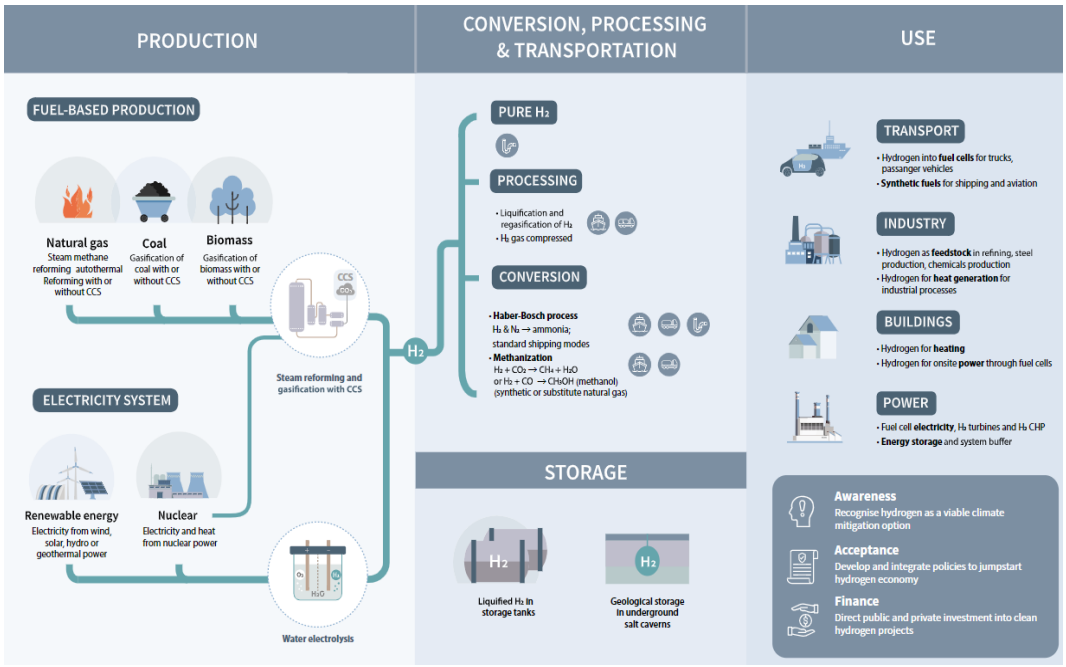

Figure 2.1. Hydrogen Value Chain (UNECE Task Force on Hydrogen, 2022)

Even though hydrogen can also be used to synthesize other energy carriers that might also be viable in the future sustainable energy systems, such as ammonia, methanol, ethanol, SNG, etc. (Acar, 2018; Knoors et al., 2019), these secondary options are left outside the scope of this thesis.

2.1.1 Production

As part of the clean hydrogen value chain, electrolysis is the most favored method of producing hydrogen. Although it was thought to be too costly before, hydrogen production from renewable electricity is already price competitive in niche applications, and in this decade it is expected to expand even more into other areas (Glenk & Reichelstein, 2019).

During electrolysis, the only inputs to the electrolyser are water and electricity. Even though the system requires fresh water not to corrode the equipment, it is a surmountable problem since desalination of seawater with the current technologies barely adds up to the production cost (Beswick et al., 2021; IEA, 2021). Nevertheless, Steam Methane Reforming (SMR) is the most ubiquitous method for the time being (IEA, 2021; Treese et al., 2015).

Despite being out of the scope of this study, there are many other promising studies that are being conducted on hydrogen production methods ranging from biological to radioactive methods (Dawood et al., 2020; Dincer & Acar, 2014; Gupta Ram B., 2009; Martino et al., 2021; Subramani et al., 2012).

2.1.1.1 Steam Methane Reforming (SMR)

Currently, most of the demand for hydrogen comes from refineries and ammonia producers (IEA, 2021). Hydrogen generation unit is the heart of a refinery since a problem at this unit could stop the entire operation. Hydrogen is needed to produce clean fuels that meet environmental regulation criteria, to produce demanded amounts of middle distillates, and to process heavy, sour crudes (Mandal, 2021). The most common method for obtaining hydrogen that is used by the refineries is the SMR (Treese et al., 2015). The conventional method involves cracking heavier hydrocarbons into methane, desulfurization, reforming, water-gas shift, and lastly, purification which is usually conducted by the pressure swing adsorption (PSA) (Mandal, 2021; Subramani et al., 2012; Treese et al., 2015).

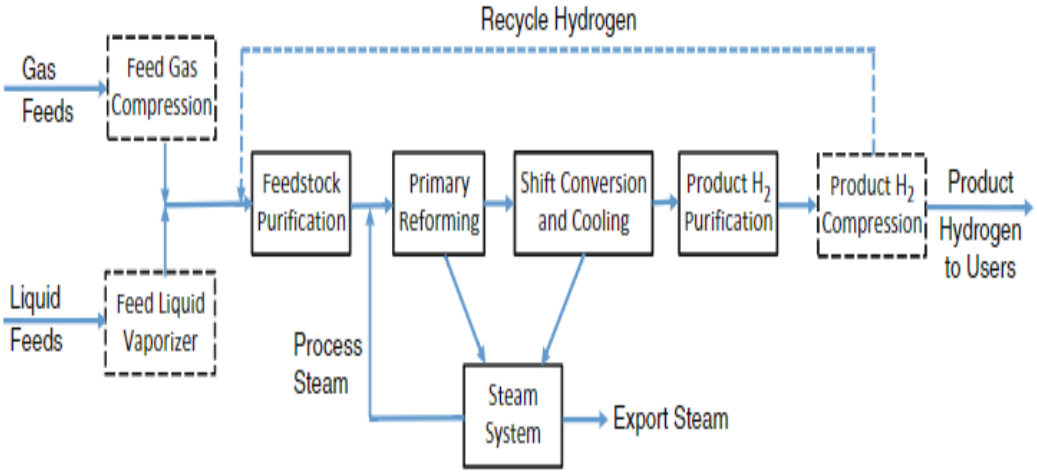

Figure 2.2. SMR Block Flow Diagram Example (Treese et al., 2015)

Despite its common usage, SMR has the downsides of having CO, CO_2, and NO_x emissions, hard to clean residue, harsh operating conditions, and the requirements of stable boiling water and operation conditions to be beyond certain potential (Treese et al., 2015).

2.1.1.2 Electrolysis

Technology outlook shows that, among all options for electrolysis, three technologies that grab the most attention are Alkaline Electrolysis (AE), Proton Exchange Membrane (PEM), and Solid Oxide Electrolysis (SOE) cells (Guo et al., 2019; Schmidt et al., 2017; Taibi et al., 2020). While SOE is still in the developmental stages, AE has been a mature technology for many years (Taibi et al., 2018). On the other hand, PEM is expected to further commercialise and surpass the AE as the dominant technology by 2030 (Schmidt et al., 2017). As can be seen from Table 2.1, each technology has its advantages and disadvantages.

Table 2.1 Comparison of AE, PEM, and SOE (Pivovar, 2021)

Type	Pros	Cons	Temperature
Alkaline	• Well established • Lower capital cost • More material choice at high pH • High manufacturing readiness • Can leverage existing supply chains • Demonstrated in larger capacity	• Corrosive liquid electrolyte is used • Higher ohmic drop • Lack of differential pressure operation • Shunt currents • Limited intermittency capability • Efficiency	Low (0-200 °C)
Polymer Electrolyte Membrane	• Low ohmic losses/High power density operation • Differential pressure operation • DI water only operation • Leverages PEM fuel cell development and supply chain • Load following capability	• Requires expensive materials (Ti, Pt, Ir, perfluorinated polymers) • Lower manufacturing and technology readiness • Efficiency	Low (0-200 °C)
Solid Oxide	• High efficiency • Low-cost materials • Integration with continuous, high temperature electricity sources (e.g. nuclear energy) • Leverages SOFC development and supply chain • Differential pressure operation	• High temperature materials challenges • Limited intermittency capability • Thermal integration • Lower manufacturing and technology readiness • Steam conversion and separation challenges	High (>500 °C)

A notable argument for PEM's expected market expansion is its ability to deal with intermittent currents, and thereby with renewables, better than the other options. PEM also gives pressurised hydrogen as output and has a more solid design (Schmidt et al., 2017). However, its dependency on platinum group metals (especially iridium) raises questions about its widespread manufacturing and usage (Minke et al., 2021). SOE, despite potentially offering higher efficiencies and the ability to work reversibly as a fuel cell, is not yet commercial. It is noted that high temperature working conditions for SOE cells bring about material problems, and it is currently not much competitive regarding the lifetime of the system (Schmidt et al., 2017). Since there is a trade-off between efficiency, durability, and cost, obtaining the correct electrolysis method is an optimisation problem that should be tailored for the project at hand (Taibi et al., 2020).

2.1.2 Purification

A critical step from production to the utilisation of hydrogen is the purification. Although the cost of purifying water for electrolysis is marginal (Beswick et al., 2021; IEA, 2021), the separation of hydrogen from gas streams might add to the cost significantly (Melaina et al., 2013).

Purification becomes especially crucial when it comes to the operating range of the fuel cells, and therefore, vehicle applications. For that reason, specific standards of purity were needed to be developed. (Du et al., 2021).

Even though there are diverse methods of purification, involving but not limited to catalytic methods, metal hydrides as a storage media, and membrane based separations, the most common method used for large streams is the Pressure Swing Adsorption (PSA) (Gupta Ram B., 2009; Subramani et al., 2012).

During PSA, by the periodical pressure change, the gas stream goes through various adsorption beds (widely used ones being zeolites, activated carbon beds, and metal organic frameworks (MOFs)) which are designed to remove certain impurities with a specific concentration and order (Mandal, 2021).

It is noted that if and when hydrogen is used as a more mainstream fuel, there might be a need for using multiple hydrogen purification methods in combination (Du et al., 2021).

2.1.3 Distribution

Hydrogen can be transported with different methods (pipelines, tube trailers, ships, trucks, railroads, etc.) in many different forms (compressed, liquefied, or by hydrogen carriers such as ammonia, ethanol, methanol, etc.) (Gupta et al., 2016; Gupta Ram B., 2009). Since this study focuses on large scale storage, it explores the large scale distribution case which might be possible with the existing pipeline network (Quintino et al., 2021).

On one side, blending natural gas with hydrogen is thought to be a cleaner solution in terms of emissions, but on the other side, it lowers the energy density of the gas stream. For the same energy content to be delivered with the same pressure drop between the compressing stations, about three times the volume of hydrogen should be flowing instead of natural gas. (Gupta et al., 2016; Quintino et al., 2021).

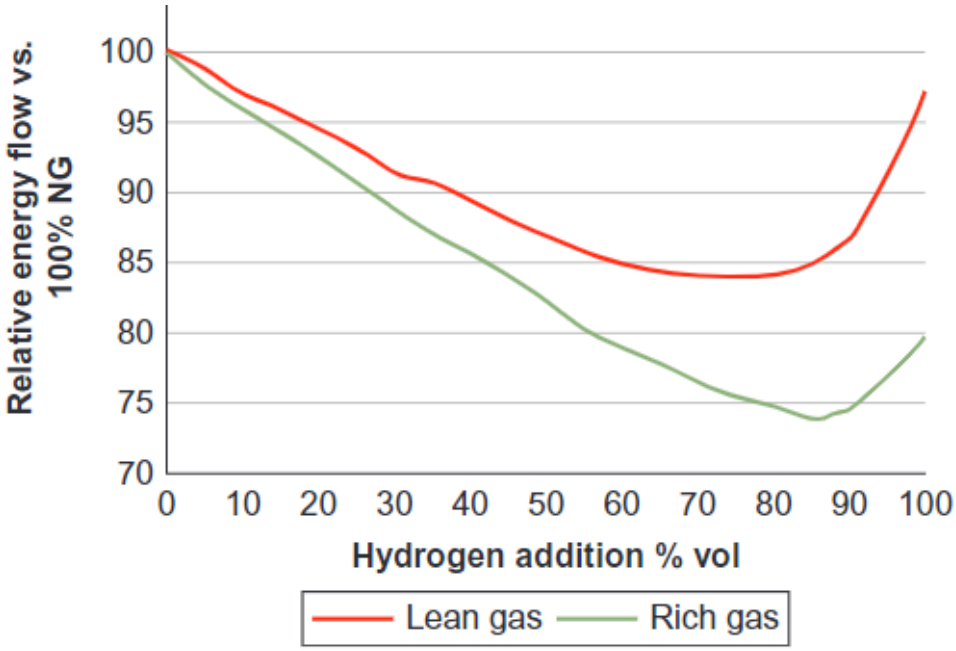

Figure 2.3. The energy content of hydrogen containing streams in comparison with lean gas and rich gas with constant pressure drop (Gupta et al., 2016)

Furthermore, the use of blended gas in daily household appliances requires thorough investigations of safety against situations like flashback/blowoff, flame (see Appendix I), and leakage detections (Dinçer et al., 2021; Glanville et al., 2022). In addition, since the sulfur in thiols is not suitable for fuel cells, new odorants need to be developed for hydrogen containing streams instead of the commonly used mercaptans (Mouli-Castillo et al., 2020).

Hydrogen embrittlement of the metals is another issue with hydrogen transport. Though the mechanism behind the phenomena is still under investigation, it is known that by penetrating into the lattices at the molecular level, hydrogen causes metals to lose their bearing ability due to reduced ductility (Wu et al., 2022). The

hydrogen causing embrittlement can have external (occurring due to corrosion, H_2 presence, or H_2S presence) or internal (occurring during the material processes such as welding, smelting, pickling, and plating) origins, and the origin in turn determines the prevention strategy. Whilst microstructure modification for the materials (adjusting the alloy composition) studies are continued, for the externally originated embrittlement, surface coating and other surface modifications are considered as the combatting approach (Li et al., 2020).

Lastly, in order to be distributed via pipeline and later on to be used, for example in a filling station, hydrogen needs to be compressed up to high pressures. Industry experience shows that reciprocating compressors are the optimal tools for such tasks since they are the only option for comfortably delivering such pressures at a varying rate. It is probably good to note a few incidents when lubricating oil has caused cavitation due to evaporating and then recondensing during the hydrogen flow. Therefore, nonlubricated options might be considered to be more suitable for the job (Hoff, 2020).

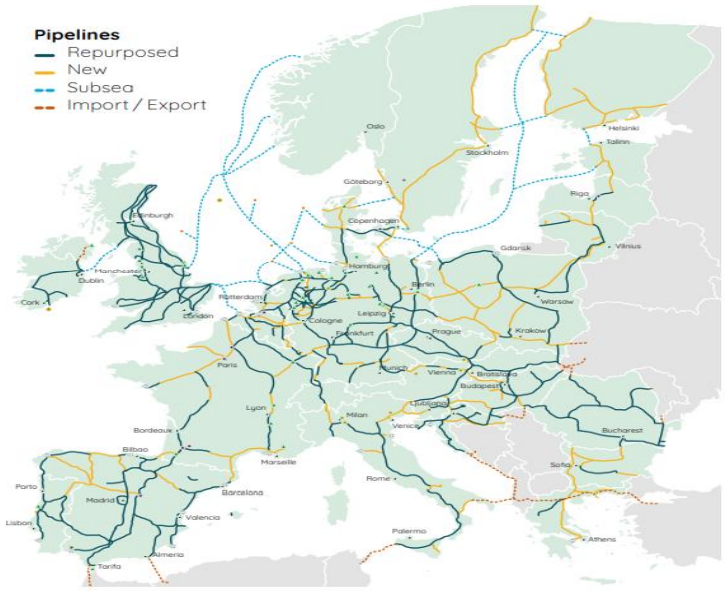

Figure 2.4. Envisioned hydrogen pipeline infrastructure for Europe by 2040 (Modified from Amber Grid et al., 2022)

2.1.4 Consumption

Hydrogen as an energy carrier can be burned directly or used by a fuel cell to generate electricity. Nevertheless, as Figure 2.5 shows, hydrogen is used more as a feedstock rather than an energy carrier for the refining and chemicals sectors.

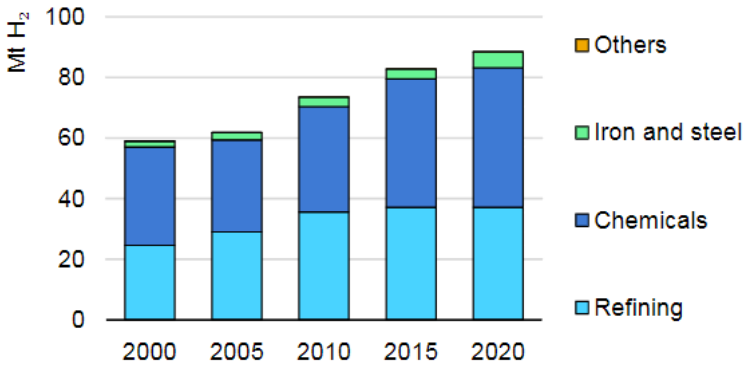

Figure 2.5. H_2 demand by sector (IEA, 2021)

In the future, demand is expected to be diversified with the increasing amount of applications (IEA, 2019). Since there is a large overlap between these sectors and hard-to-abate/hard-to-electrify sectors (see Figure 2.6 and Figure 2.7), hydrogen might play an inimitable role in the future energy transition into a net-zero scenario (FCH2JU, 2019).

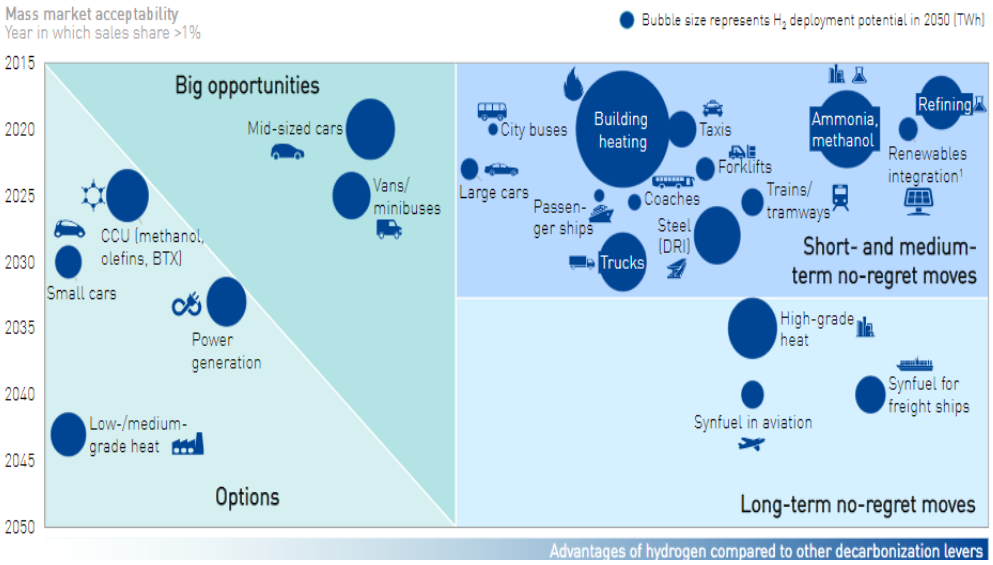

Figure 2.6. Hydrogen end-uses roadmap for Europe (FCH2JU, 2019)

Last but not least, hydrogen as a storage medium for renewable energy could possibly benefit isolated places such as islands to become self-sufficient in terms of their electricity needs (Karlsson, 2021; Luna, 2019).

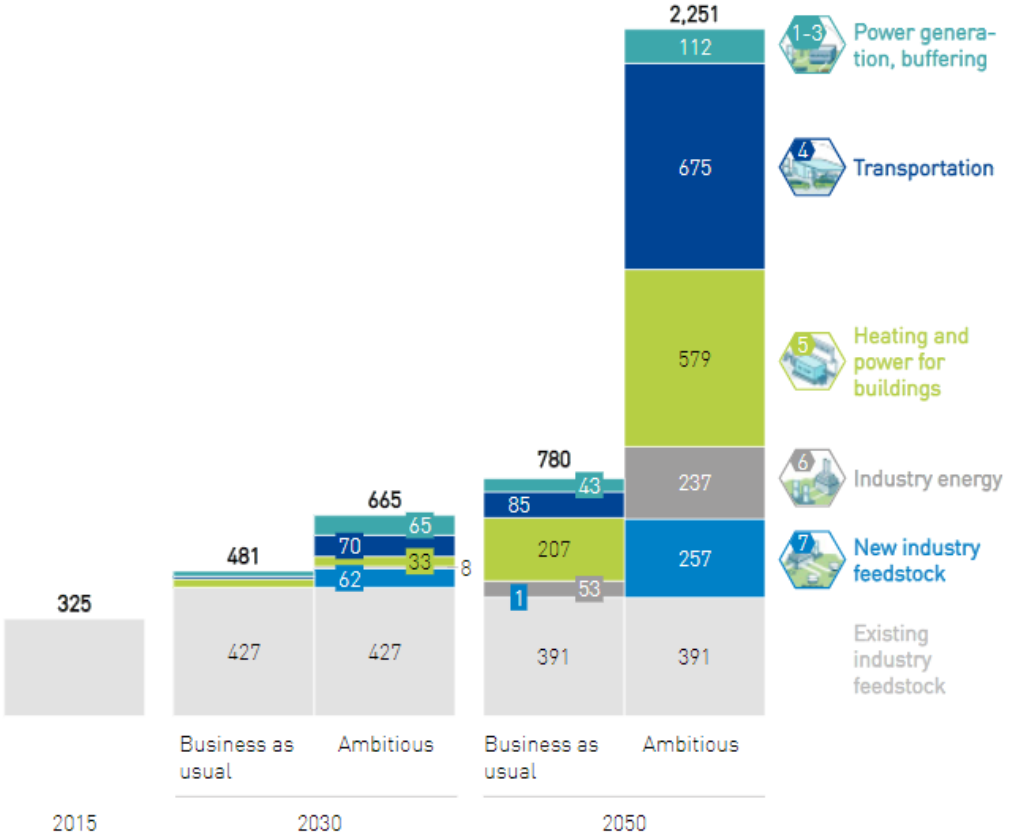

Figure 2.7. Hydrogen energy demand (TWh) projection for Europe (FCH2JU, 2019)

2.1.5 Surface Storage

Surface storage options can go up to MWh scales, but if large scale, bulk amounts of hydrogen storage is needed in GWh ranges, the viable options are the subsurface choices which are addressed in a separate heading (Heinemann et al., 2021). It might also be noted that if the hydrogen is to be transported with the pipeline

networks, depending on the size and the material of the infrastructure, the pipes themselves might act a as storage medium in GWh ranges (Gupta et al., 2016).

While the conventional methods for storing hydrogen (see Table 2.2) are physical, either as a compressed gas at ambient temperature or as a cryogenic liquid at low pressure, many material-based options are under development, such as adsorbents like carbon materials, metal organic frameworks (MOFs), and hydrides to name a few (Gupta et al., 2016; Gupta Ram B., 2009; Hassan et al., 2021; USDOE, 2022).

Depending on the end-use, different requirements would arise for the surface storage and there is no single best option for all applications (Hassan et al., 2021).

Table 2.2 Hydrogen storage options for mobility (Rivard et al., 2019)

Method	Gravimetric Energy Density (%wt)	Volumetric Energy Density (MJ/L)	Temperature (K)	Pressure (barg)	Remarks
Compressed	5.7	4.9	293	700	Current industry standard
Liquid	7.5	6.4	20	0	Boil-off constitutes a major disadvantage
Cold/cryo compressed	5.4	4.0	40-80	300	Boil-off constitutes a major disadvantage
Metal Organic Frameworks (MOFs)	4.5	7.2	78	20-100	Attractive densities only at very low temperatures
Carbon nanostructures	2.0	5.0	298	100	Volumetric density based on the power density of 2.1 g/mL and 2.0 wt % storage capacity
Metal hydrides	7.6	13.2	260-425	20	Requires thermal management system
Metal borohydrides	14.9–18.5	9.8-17.6	130	105	Low temperature high pressure thermal management required
Kubas type	10.5	23.6	293	120	-
Liquid Organic Hydrogen Carriers (LOHCs)	8.5	7	293	0	Highly endo/exothermal requires processing plant and catalyst. Not suitable for mobility
Chemical	15.5	11.5	298	10	Requires SOFC

2.2 Efficiency and Cost

2.2.1 Thermodynamic Efficiency

Low round-trip efficiency (see Table 2.3) might sometimes make hydrogen's potential as an energy carrier to be overlooked (Pellow et al., 2015). Even if the other processes (heating, cooling, water purification, etc.) are ignored, the overall round-trip efficiency of a hydrogen system is about 30% due to production, compression, distribution, and fuel cell conversions (Kelly, 2014; Pellow et al., 2015; Wanner, 2021). Since compressors are already close to their ideal efficiencies, an enhancement in terms of efficiency might be expected from the fuel cells and electrolysers. However, this is also unlikely to change the overall efficiency dramatically (Wanner, 2021). In comparison, natural gas combined cycle power plants' efficiency lies around 45% - 57% (Boyce, 2012).

Table 2.3 Minimum and real energies for 1 Nm^3 of hydrogen (Wanner, 2021)

	Ideal Energy (KWh/Nm^3)	Real Energy (KWh/Nm^3)
Electrolyzer (20 bar, purification)	3.17	4.0-5.5
Compression (150 bar)/ Liqeufication	0.16/0.36	0.23/0.90
Handling/Distribution/Storage	0.00	0.15
Fuel cell output	3.00	1.33
Input energy/Output energy	1.1-1.2	3.3-4.9

A scenario where electricity is converted into hydrogen to be later converted back into electricity, despite being low on CO2 intensity, loses 39-80% of the invested exergy (Farajzadeh et al., 2022). Yet still, based on energy return on investment calculations, underground hydrogen storage (UHS) might be the only sensible non-fossil option capable of storing at a seasonal level (Clerjon & Perdu, 2019).

2.2.2 Cost

Although, round trip cost of hydrogen can vary considerably at each step of the life cycle, many studies conducted for separate cases agree that the major component of the cost arises from the production phase (Kennedy et al., 2019; le Duigou et al., 2017; Song et al., 2021; Viktorsson et al., 2017; Zhao et al., 2019).

For the time being, SMR is the cheaper production method compared to the electrolyser options, and a cost reduction is necessary for green hydrogen to become widespread (Cembalest, 2020; Taibi et al., 2020). Moreover, there seems to be no consensus over an accurate cost of electrolysis as it significantly varies depending on numerous factors including type of electrolyser, electricity price, capacity factors, and financing costs to name but a few (Poljak, 2022).

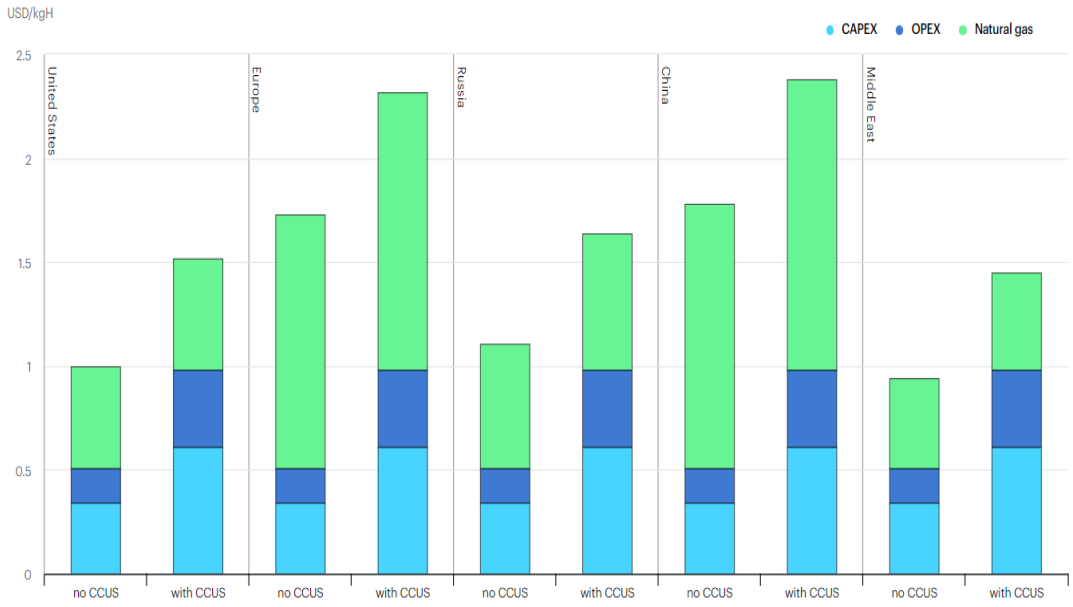

Figure 2.8. H_2 production from natural gas costs for different regions (IEA, 2019)

A cost reduction in electrolyser prices is expected with technological advancement, and scaling up (Taibi et al., 2020). However, another significant cost driver for electrolysis, which is the electricity price can vary greatly based on the location (Poljak, 2022; Terwel & Kerkhoven, 2019; Viktorsson et al., 2017).

Pipeline transport and underground storage costs seem to be much less significant compared to the production costs. A study conducted for France used 1 €/kg for distribution cost and concluded that underground storage takes up no more than 5% of the total cost (le Duigou et al., 2017).

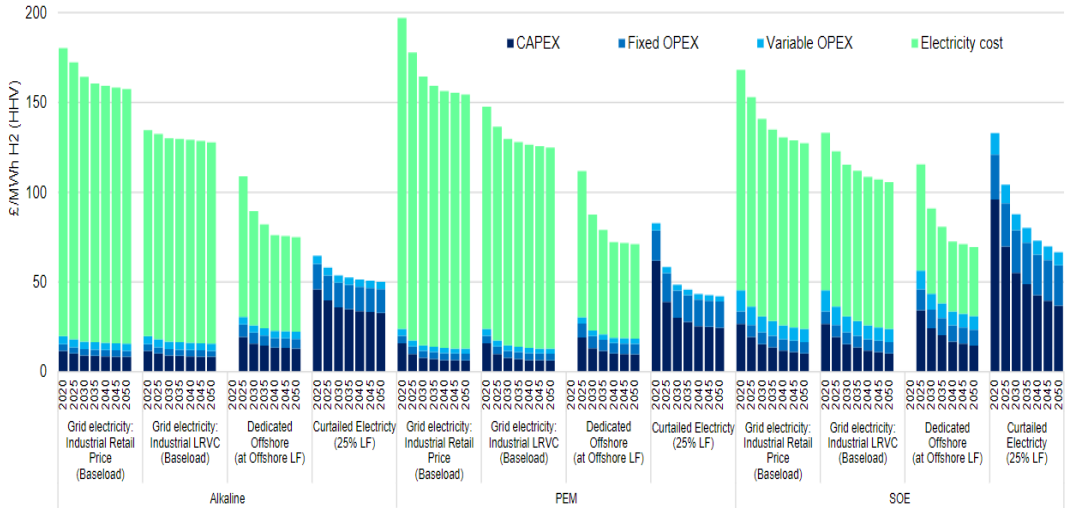

Figure 2.9. Levelised cost of hydrogen estimates for AE, PEM, and SOE connected to different electricity sources, commissioning from 2020 to 2050 (UKCDR, 2021)

Another study investigated the cost for a scenario of distribution by the existing pipeline network coupled with geological storage. For 1.6 kilotons of hydrogen delivered per year, 2.73 $/kg was estimated. The study has also pointed out the cost of refueling stations (approx. 2.5 million $/station). According to the findings, if the cost for refueling stations were not considered, the cost for delivering and storing hydrogen would be just above 1 $/kg (Demir & Dincer, 2018).

2.3 Underground Hydrogen Storage (UHS)

For bulk energy management and electricity storage, UHS is an option in the pilot stages which might offer high capacities with high flexibility in discharge times (Møller et al., 2017; Mondial L, 2016).

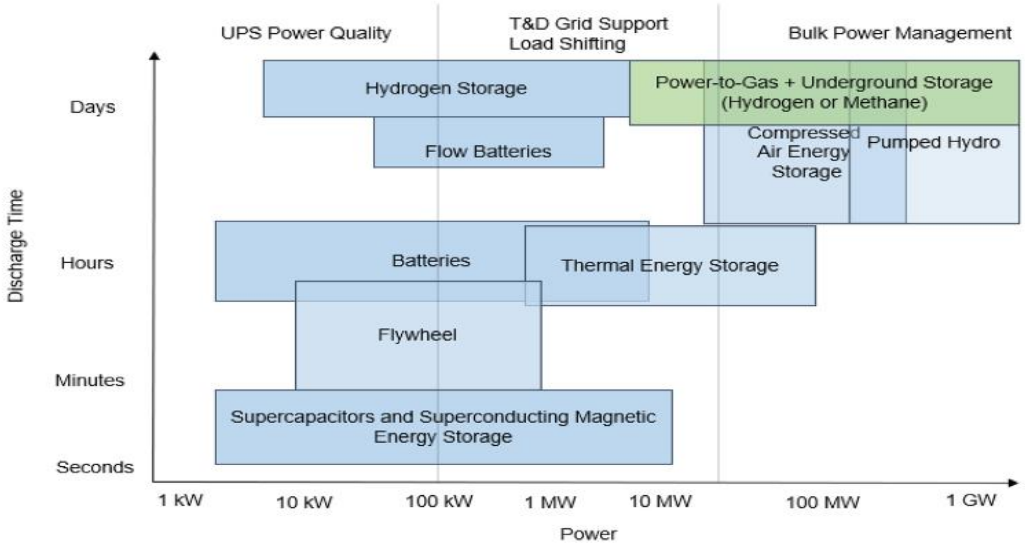

Figure 2.10. Discharge time vs power for electrical storage (Wallace et al., 2021)

2.3.1 Storage Options for Hydrogen

An overview of all known UHS technologies, including pipe storage, rock caverns, and abandoned mines, has been conducted and a large selection of existing projects were compiled with the HyUnder project (Kruck et al., 2013). A compilation made for this study can be seen in Appendix K.

Comparatively three geological options, namely aquifers, salt caverns, and depleted fields stand out to be more viable than the others (see Table 2.4 and Table 2.5) (Lord et al., 2011; Matos et al., 2019; Muhammed et al., 2022; Zivar et al., 2021).

Table 2.4 Characteristics of UHS options (Muhammed et al., 2022; Visser, 2020)

Characteristic	Storage Media		
	Salt Caverns	Depleted Reservoirs	Aquifers
Storage Capacity	Based on cavern size	High	High
Discharge Rate	High	Average	Low
Initial Cost	High	Average	Average
Cyclic Cost	Low	Average	Average
Seismic Risk	Low	Average	High
Chemical Conversion Rate	Low	Average	High
Cushion Gas Requirement	Low	Average	High
Leakage Risk	Low	High	High
Usability Purpose	Frequent	Seasonal	Seasonal

There are two recent projects of UHS in depleted gas reservoirs, namely, the Underground Sun in Austria, and the Patagonia Wind in Argentina. Neither project has reported any insurmountable problem that might get in the way of UHS (Pérez et al., 2016; RAG et al., 2017).

Table 2.5 Operational Parameters modified from (Abravcı, 2022)

Parameter	Storage Media		
	Salt Caverns	Depleted Fields	Aquifers
Cushion Gas/Working Gas (% by volume)	30-50	100-150	150-200
Injection Duration (days)	20-40	200-250	200-250
Withdrawal Duration (days)	10-20	100-150	100-150
Number of Cycles (per year)	5-6	1-2	1-2
Contamination of Water or Gas	Negligible after a few cycles	Critical	Critical

Since geographical availability and feasibility for each structure is case dependent, each option might be more viable depending on the circumstances and goals. As for the offshore gas depleted reservoirs, a study conducted for the UK concluded that offshore depleted gas fields have the potential to easily meet the need for seasonal storage many times over the demand (Mouli-Castillo et al., 2021). Meanwhile, a feasibility study conducted in the Netherlands for the North Sea concluded that offshore fields can be an option, but require further studies and pilot projects need to be implemented. (van Gessel et al., 2022).

Ultimately, some barriers exist for UHS no matter the storage media. Since the practice involves dealing with the subsurface uncertainties, all projects would inherit some risks. An exemplary list of risk factors can be found in Appendix G. Due to embrittlement, well equipment must be chosen appropriately, and the recognition of seismic risks and prevention of potential leakage requires careful examination of the geology. Furthermore, all three types of storage media might suffer from microbial activity that could result in methane, acetic acid, hydrogen sulfide production, and/or iron reduction (Dopffel et al., 2021). Lastly, all projects would require preliminary work on the issues of social acceptance, legislation, economics, and safety (Tarkowski & Uliasz-Misiak, 2022; Visser, 2020).

2.3.2 Salt Cavern Storage

Despite the examples of incidents with salt cavern storage (Yang et al., 2013), they are perceived as the safest storage option (Muhammed et al., 2022; Visser, 2020).

Salt deposits can be found either as bedded or diapiric structures with the first being less favorable because of being more prone to stability issues (Han et al., 2006). Due to the salts' healing ability, pure salt storages are expected to provide a good seal (Kumar et al., 2021; Laban, 2020). Compared with the porous media counterparts, salt caverns provide more frequent cycles, less cushion gas to working gas ratio, and less risk of contamination (Abravcı, 2022; Muhammed et al., 2022; Visser, 2020).

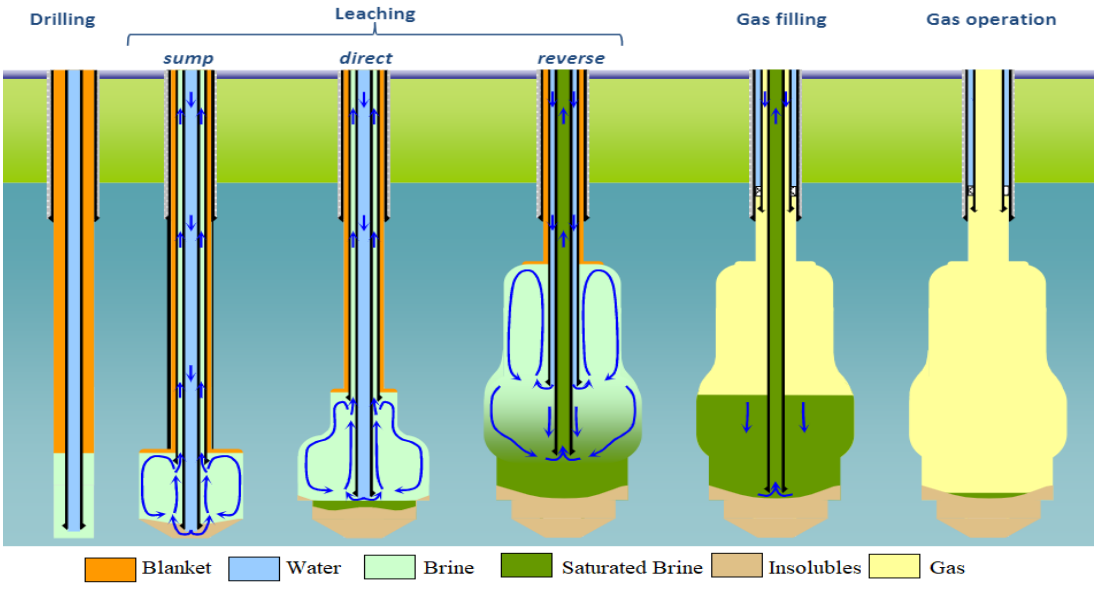

Figure 2.11. Steps of Cavern Creation (Hévin, 2019)

Although the type of the formation significantly affects the cavern design (Caglayan et al., 2020; Habibi, 2019) the main cavern creation process that includes leeching, debrining, and filling phases is the same (see Figure 2.11) (Laban, 2020).

There are two common practices of cavern storage, either wet or dry. In wet storage the required pressure is supplied by brine, whereas for dry storage it is supplied by the cushion gas which makes it more costly (British Geological Survey, 2008; Passaris, 2022).

2.3.2.1 Issues Associated with Salt Cavern Storage

Even though a large portion of the literature is focused on the microbial contamination aspects (Laban, 2020), geomechanics also plays an important role in salt cavern storage. Heterogeneity of the formation can have a significant effect on the cavern design and tertiary creep deformation. Although it might not be a serious risk in the first cycle, it can possibly lead to failure in the long term storage (Kumar et al., 2021).

While salt is usually considered as a good seal, anomalous salt zones which have variations in features of textures, inclusions, compositions, and structures also exist. Such zones might be prone to leakage no matter whether they are diapiric or bedded (Warren, 2017).

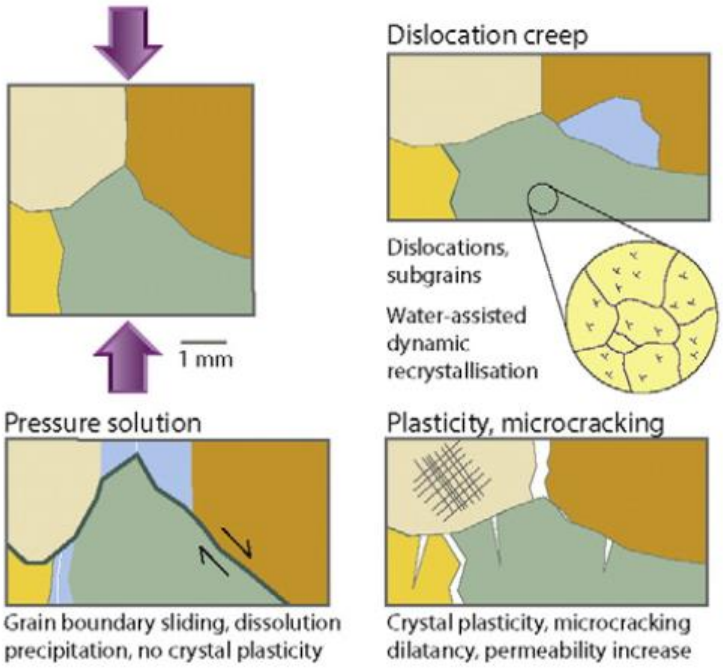

Figure 2.12. Crystal Scale Representation of Rock Salt Deformation (Warren, 2017) as cited in (Gholami, 2022)

Moreover, solution mining, i.e. leaching, requires eight to ten times the volume of water for a single volume of the cavern (Londe, 2021). The transport and discharge of such large amounts of water is costly and environmentally sensitive. As an example, such problems with Tuz Gölü Storage Project in Turkey were surmounted by supplying the fresh water from the Hirfanlı Dam and discharging the brine into the Tuz Gölü, reanimating the drying lake (BOTAS, n.d.).

2.3.3 Porous Media Storage

Aquifers offer large volumes of storage capacity and they are more geographically available compared to the depleted fields. Since there is no host gas, gas mixing might be less of an issue for the aquifers. However, most of the aquifers are not characterised yet, and storing gas in them might induce seismicity or result in leakage (Zoback, 2022). Also since they lack the existing infrastructure and reservoir data, their development might require more investment than the depleted fields (Foh et al., 1979; Kruck et al., 2013; Zivar et al., 2021).

Although gas **storage in oil fields** is a known practice (usually to enhance oil production), they are generally not considered as an option for storing hydrogen because of the lack of field experience and the additional complexity they bring to the design. If hydrogen was to be stored in an oil field, it would push the oil meanwhile dissolving in it, which might cause the solution gas to flash. Mixing with the solution gas and dissolving in the oil would presumably cause impurities and irrecoverable hydrogen losses (Ennis-King et al., 2021; RISC, 2021). Moreover, oil fields generally contain some amount of sulfur which can be detrimental to hydrogen operations. For the time being, literature can be said to be insufficient for the oil fields as a storage media, and to the best of the author's knowledge, there is only one simulation study (Kanaani et al., 2022).

Depleted gas fields might be a favorable option for seasonal storage due to the benefits they offer such as existing data and infrastructure (Mouli-Castillo et al., 2021; Visser, 2020). Although there are questions about the purity of hydrogen due to gas mixing, there exist some projects in development stages (Pérez et al., 2016; RAG Austria AG et al., 2017; Zivar et al., 2021).

Bio-methanation is another means for hydrogen to be utilised in a depleted gas reservoir (Strobel et al., 2020). Projects have validated the existence of the concept, and are trying to commercialise it. For the time being, microbial reactions seem to be too slow and the biofilm formed during them poses an issue. (Perez, 2022; Pérez et al., 2016; Pichler, 2022; RAG et al., 2017; Zauner et al., 2022).

2.3.3.1 Issues Associated with UHS in Porous Media

Possible problems with the storage of hydrogen in porous media have been extensively investigated (Heinemann et al., 2021). Feldmann et al. (2016) suggested that although diffusion into the aqueous phase does not seem to be a critical problem. However, gas mixing can significantly lower hydrogen concentration in the withdrawn gas. The same study also foresees that, unlike depleted gas field storage, gravity override and viscous fingering could play a major role in aquifer storage (Feldmann et al., 2016).

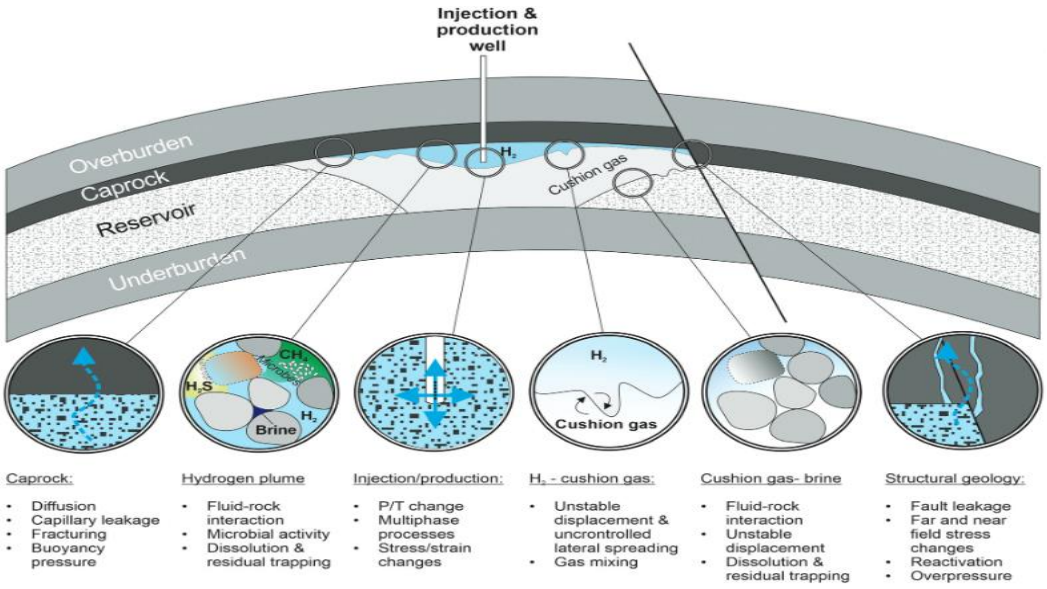

Figure 2.13. Issues Related to Porous Media Storage (Heinemann et al., 2021)

Lateral spreading is another major problem that could result in the loss of hydrogen. In comparison with methane, hydrogen spreads faster and further into the reservoir possibly passing the spill point. This could especially become problematic for the aquifer structures where there is less data (Hagemann et al., 2015).

Hydrogen-rock-water interactions have also been examined. Pichler (2013) has shown that especially for carbonate rocks an increase in pH, dissolution of dolomite, and precipitation of calcite were observed (Pichler, 2013). Another study

used heterogeneous rock to study the effects and found out that hydrogen interaction with the rock could result in a slight reduction in porosity which could enhance the sealing capacity of cap rock while reducing the available storage capacity (Hemme & van Berk, 2018). Both studies agreed with the previously mentioned argument that diffusion in the aqueous phase is insignificant compared to other possible losses (Feldmann et al., 2016; Hemme & van Berk, 2018; Pichler, 2013).

Many possible interactions of hydrogen with the reservoir and cap rocks have been investigated and evaluated as possible problems (Hagemann et al., 2015; Hemme & van Berk, 2018). A more recent case study, however, has concluded that abiotic reactions with reservoir minerals are much less effective than the previous assumptions when realistic kinetic conditions are applied (Hassannayebi et al., 2019). Also agreeing that equilibrium models might overestimate the reaction rates, it was suggested that a geochemical database like the ones for CO_2 should be built also for hydrogen (Heinemann et al., 2021).

Ultimately, all studies seem to agree that reduction of pyrite to pyrrhotite is a valid reason for hydrogen loss meanwhile releasing H_2S (Hassannayebi et al., 2019; Hemme & van Berk, 2018; Pichler, 2013; Reitenbach et al., 2015).

Knowing the thermo-physical properties of streams containing hydrogen and other gases are of vital importance for modelling the multiphase flow. Alternative viscosity models might be required for hydrogen unlike other non-polar gases (Hassanpouryouzband et al., 2020; Heinemann et al., 2021). Time dependent relative permeability and wettability changes, capillary pressure, and hysteresis effects should be considered for an accurate model, and for the time being there are only a handful of studies on this subject (Eller et al., 2022; Hashemi et al., 2021).

Finally, it is noted that cyclic hydrogen storage might have negative effects on the geomechanic storage integrity. Although possible threats to geomechanic integrity have been extensively studied for other gases, little is known about a hydrogen case (Hangx, 2022).

Joule-Thompson effect (the cooling of real gases when passing through a throttle) which can be a serious problem for CO_2 storage is expected to be far less of a problem for hydrogen. But still, due to being more heat conductive and possibly reactive, hydrogen could cause deformation of the grain structure, opening of leakage pathways, and mechanical failure in the long run (Heinemann et al., 2021).

2.3.4 Previous Work

There exist multiple reviews of the literature in various works (Muhammed et al., 2022; Thiyagarajan et al., 2022; Visser, 2020; Zivar et al., 2021). The only example found for simulation of long term storage in a large gas field with multiple wells was published earlier in 2022 (Zamehrian & Sedaee, 2022). This study by Zameherian and Sadaee (2022) simulated ten years of cyclic storage with a prolonged production period after the last cycle, and focused on the dissolution of H_2 into the condensate phase and the utilisation of various cushion gas alternatives. Although it had 16 wells, the study did not give information about the individual well production performances in terms of purity. Still, it provides a benchmark to this study.

2.4 Comparison of Gases (H_2-CH_4-CO_2) for Storage

Although other gases, such as helium, compressed air, etc., can also be stored underground, the main candidates for subsurface storage are hydrogen, carbon dioxide, and methane.

All three of these gases are expected to be in supercritical conditions at the subsurface conditions. As shown in Figure 2.14, the minimum reservoir pressure (86 bar) and reservoir temperature (68.8 °C) for NMGF are above the critical point of CO_2.

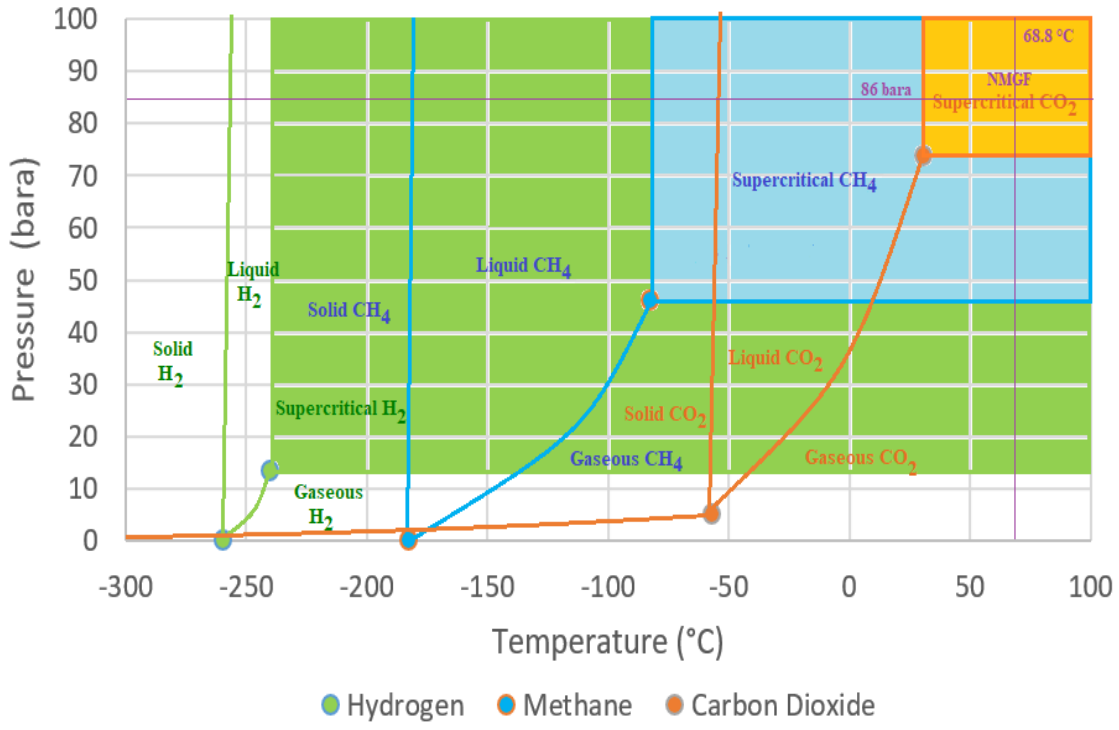

Figure 2.14. Phase diagrams for H_2, CO_2, and CH_4 (data from (The Engineering Toolbox, n.d.))

Since CO_2 is not stored with the intention of withdrawal, the aim is to trap as much CO_2 as possible for a much longer time than what is considered for H_2 and CH_4.

Figure 2.15 shows that the density of CO_2 increases significantly in a narrow depth (pressure) range. Therefore, it is desired to store it beyond a threshold depth to have more CO_2 stored per subsurface volume. Change of density with depth is much more gradual for methane and even more so for hydrogen, enabling them to be stored at shallower depths (Sarah Gasda, 2022).

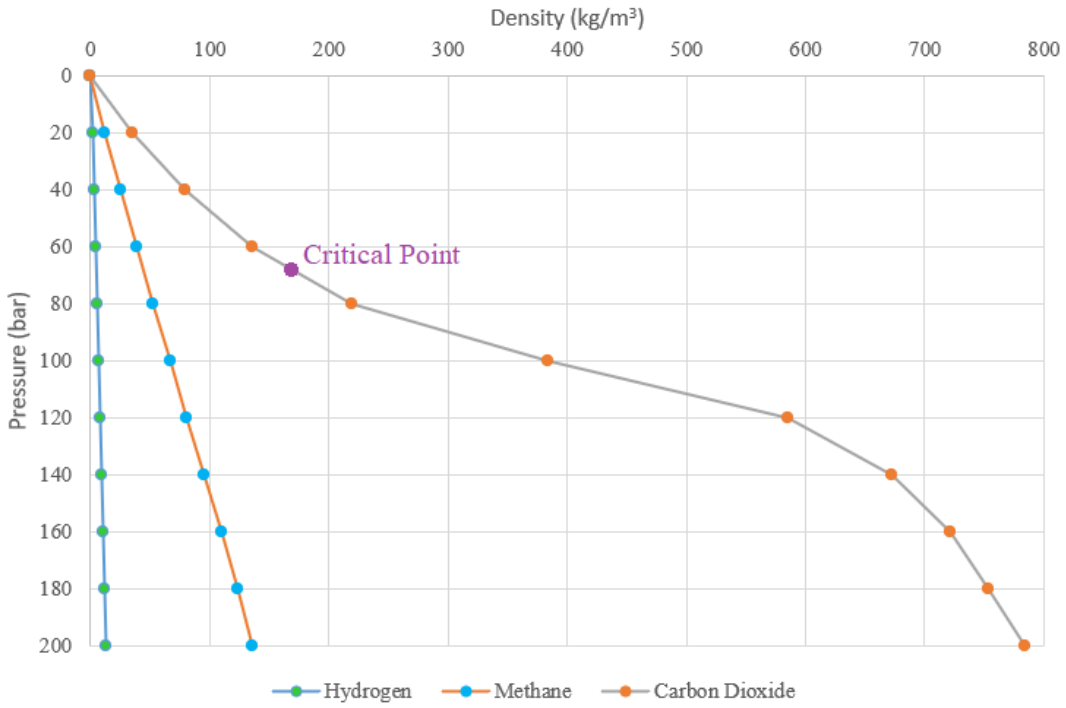

Figure 2.15. Pressure vs Density for H_2, CO_2, and CH_4 at 50 °C (image created from (Sarah Gasda, 2022) with data from (NIST Chemistry WebBook, 2022)

Rather than CO_2 storage, natural gas storage is a better analog for hydrogen. Needless to say, as they are separate compounds, hydrogen and methane exhibit different chemical and physical properties. For example, methane is more easily compressed than hydrogen. As can be seen from Figures 2.16 and 2.17 with increasing pressure, hydrogen's z factor, which is greater than 1, tends to increase, whereas for methane it is less than one and tends to decrease.

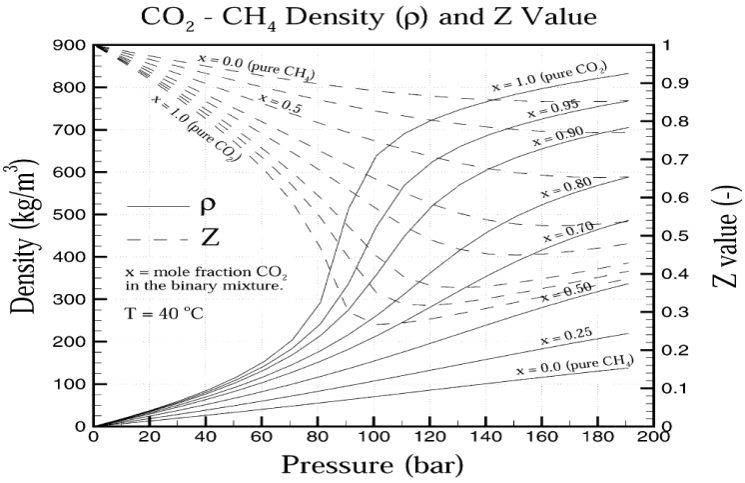

Figure 2.16. Density and Z compressibility factors at 40 °C - CH_4 & CO_2 (Oldenburg, 2003; as cited in Peters, 2022)

Deeper storage means more gas per subsurface volume (i.e. more energy per m^3 of reservoir rock) to be stored for both CH_4 and H_2 (Edlmann, 2022). Assuming all other parameters are the same, CH_4 storage would benefit more from deeper storage since it has better compressibility than H_2. One study conducted for investigating the optimum storage depth for hydrogen has asserted that maximum storage is attainable around 1100 meters (Iglauer, 2022).

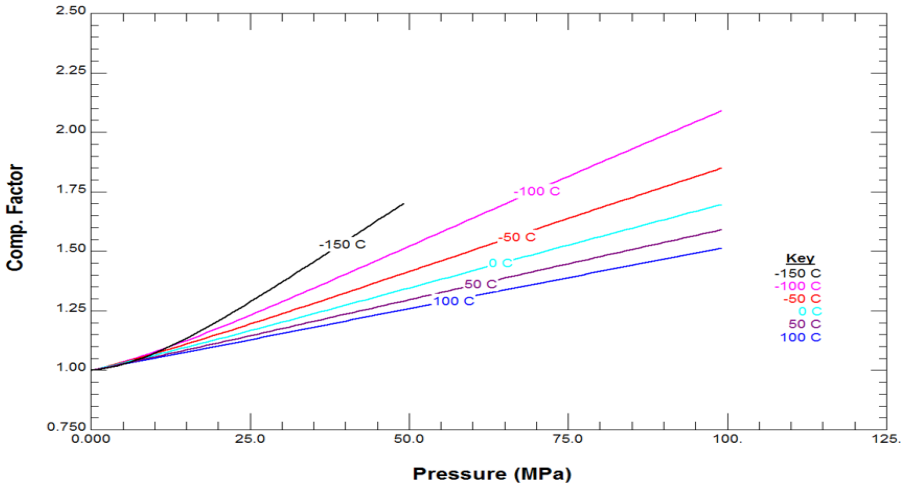

Figure 2.17. Hydrogen Z (compressibility factor) at different temperature and pressures (Hydrogen Analysis Resource Center, 2022)

Due to its energy density being higher, methane can store roughly three times the energy that can be stored with hydrogen at the same reservoir volume (Heinemann, 2021). Densities and compressibilities of three gases can be compared using Figures 2.16, 2.17, and 2.18.

Furthermore, since hydrogen is a universal electron donor, it is much more prone to being consumed by microorganisms (Dopffel et al., 2021). Using biocides is a common practice in oil and gas fields (Turkiewicz et al., 2013). However, no study has been found for a hydrogen storage case. This might be because of the questionable penetration of the biocide into the reservoir to eradicate all biological activity, or the additional purification needs and complexity it brings.

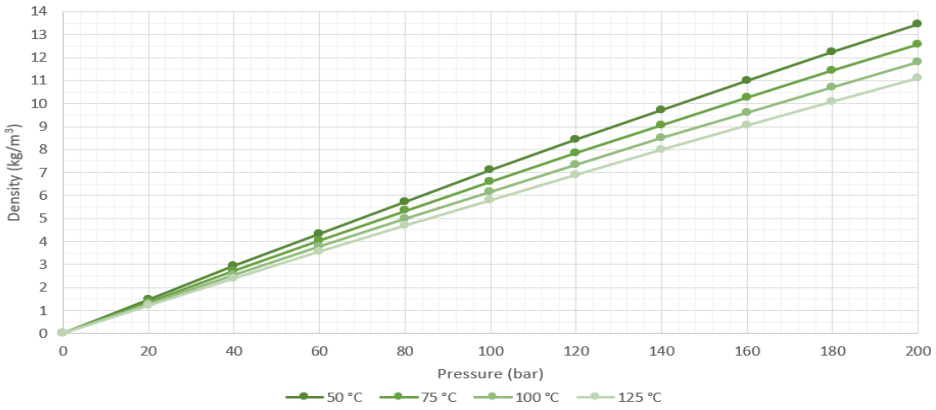

Figure 2.18. Hydrogen density for 0-200 bar 50-125 °C. Data from:(NIST Chemistry WebBook, 2022)

Saline aquifers, most of which are not well characterised, have proven to be good storages for CO_2 before. In that case, the high solubility of CO_2 in brine acts as a trapping mechanism aiding the purpose (Riaz & Cinar, 2014). However, for CH_4 and H_2, the utilisation of an aquifer requires a much more thorough investigation including seismicity studies (Zoback, 2022).

In the end, there are numerous external factors that might affect the site selection process for gas storage or the gas selection for the storage site. Therefore, all options on the table should be considered based on the project targets and many simulations should be carried out before a conclusion is drawn.

2.5 The Northern Marmara Gas Field (NMGF)

This study uses the Northern Marmara depleted gas field, which has been used as an active natural gas storage, to simulate hydrogen storage.

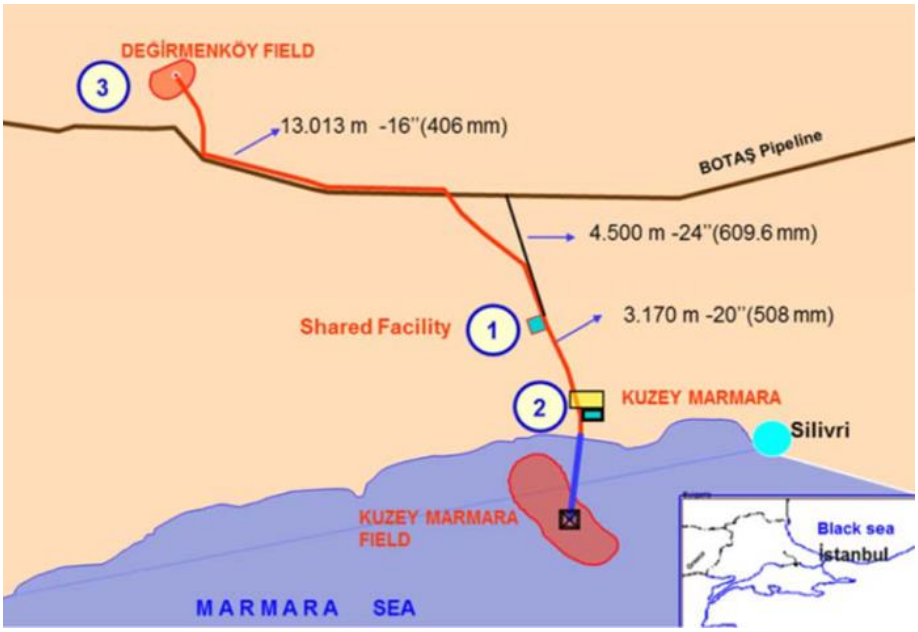

Figure 2.19. Project Layout of Northern Marmara & Değirmenköy Fields' Shared Facility (Sahin et al., 2012)

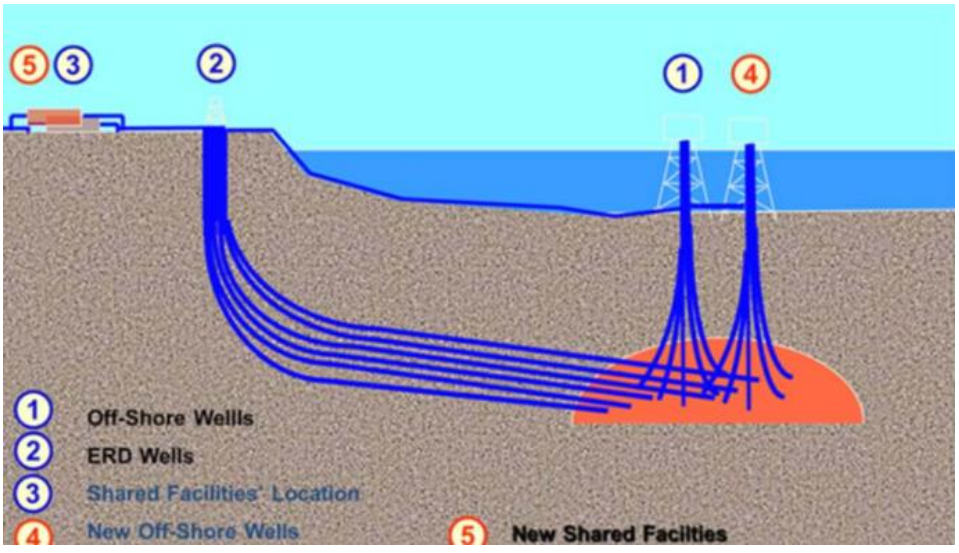

Figure 2.20. Cross Section View of the Northern Marmara Field (Sahin et al., 2012)

2.5.1 Field Development History

Regarded as the first offshore discovery of the Turkish Petroleum (TPAO), NMGF struck gas in 1988 at the NM-1 well (TPAO, 2022). Also considering the possibility for it to become a future storage site, the field was developed with five wells (Kaptanoğlu et al., 1998). Extended reach drilling (ERD) was attempted for NM-2 well, but due to poor rig performance, and problems with the leasing of the land, it was unsuccessful. In the end, NM-2 was logged and abandoned as a dry hole. Other wells were drilled from the same offshore platform with NM-1 to cover four directions around it making a total of 5 wells. After completions, production began as of September 1997 (Kaptanoğlu et al., 1998; Öztürk, 2004; Sahin et al., 2012; Yildirim et al., 2009).

The production was terminated at the end of 2001 leaving the remaining gas as cushion. After the feasibility, engineering design, and optimisation studies, Northern Marmara was set to be a storage field and six Extended Reach Drilling (ERD) wells were drilled by mid-2004. The wells drilled later exceeded the expectations. As a result, initial estimations of 3.7 billion m^3 Original Gas In Place (OGIP) and 1.6 billion m^3 working gas capacity were revised to 5.5 billion m^3 and 2.25 billion m^3, respectively (Sahin et al., 2012; Yildirim et al., 2009).

As of 2022, the field serves as the largest natural gas storage field in Turkey (Abravcı, 2017; BOTAŞ, 2022).Further field development with 18 additional wells is commissioned with the goal to increase the storage capacity to 4.6 billion m^3 with 75 million m^3/day withdrawal capacity (Kolin, 2022).

2.5.2 Reservoir Description

Stratigraphy of NMGF is given in Table 2.6, and additional information about the reservoir rock and the cap rock are given below.

Table 2.6 Lithological Data (Kaptanoğlu et al., 1998)

Formation	Depth (m)	Thickness (m)	Lithology
Water Column	0	40	-
Sea Bed	40	50	-
Osmancık	90	310	shale, sandstone, slitstone
Mezardere	400	710	mudstone, sandstone, shale, tuff
Ceylan	1110	40	shale, marn, limestone (cap rock)
Soğucak	1150	50	limestone (reservoir rock)
Final	1200	-	-

The salinity for the NM1 well was given as 30.000 ppm (Çalışgan, 2005) and the reservoir temperature is given as 68.8° celsius (Sahin et al., 2012).

2.5.2.1 Cap Rock

The cap rock belongs to Ceylan Formation. The shale dominated formation also contains marl, clayey limestone, turbidites, and tuff that is silicated between some places which can be mapped as guide layers (Altıner et al., 2006).

2.5.2.2 Reservoir Rock

The reservoir rock belongs to the Soğucak Formation which mostly consists of carbonates deposited in a shelf environment. Limestones of this formation exhibit medium to good porosity with dissolution pores. Some sandstone and marl are also encountered between layers, and at the basin bottom, pelagic clayey limestone and tuffs were detected with well data (Altıner et al., 2006).

CHAPTER 3

STATEMENT OF THE PROBLEM

Climate change is recognized as one of the most critical problems for humankind to tackle. Although electricity from renewable energy sources helps for reducing emissions, not all end-uses are able to get electrificated for the time being. Moreover, integrating a large share of intermittent sources into the grid makes it harder to balance the supply to meet the changing demand. Hydrogen as an energy carrier could enable the energy produced from renewable sources to be carried and stored, consequently, adding time and space flexibility to the energy system. Moreover, when produced and stored locally it could ehnance energy security by guaranteeing supply availability.

When it comes to the bulk storage of hydrogen, underground storage is the prominent option. There are a few choices (salt caverns, depleted fields, aquifers, etc.) for underground hydrogen storage. Each of these choices might be viable depending on the scale and the aims of the specific project at hand.

It is known that UHS projects inherit a high risk arising from dealing with a highly reactive molecule in highly uncertain geologic settings. Since the concept of hydrogen as an energy carrier is still in its infancy, the financially safest applications are prioritized. Even though, salt caverns (especially domal structures) are perceived as safer and have more examples of field practice, depleted natural gas fields can also be valid candidates for UHS site selection.

There are multiple modelling and simulation studies of UHS in depleted natural gas reservoirs that investigate the possible risks and try to quantify their effects. Moreover, there are two recent projects of UHS in depleted natural gas reservoirs that produced hopeful results for future operations.

Nevertheless, these real world applications were carried out in relatively small fields targeting only 10% hydrogen mixed with natural gas. If hydrogen is to become a key part of the energy transition, there will be a need for larger projects covering longer durations. Simulating long term storage of pure hydrogen at a larger field with multiple wells could provide valuable insight into the possible outcomes.

By simulating 25 years of cyclic hydrogen storage in Northern Marmara Field, this thesis aims to shed a light on the possible outcomes while also communicating the limitations to capture a realistic picture.

It should be noted that, this study leaves the financial feasibility aspect out of the scope, and makes no suggestions for any project to be implemented or not. NMGF is used merely as an example for a large, depleted natural gas field.

CHAPTER 4

METHODOLOGY

This work simulates long term hydrogen storage in a depleted natural gas reservoir with multiple wells to evaluate the outcomes. CMG GEM 2020.11 compositional flow simulator was selected to be the most suitable, readily available software for the task (see Appendix C).

Possible problems related to numerical modelling, and simulating the field are addressed. Subsequently, reservoir and fluid models are built using data from prior studies (Abravcı, 2017; Bagci & Öztürk, 2007; Çalışgan, 2005; Gumrah et al., 2005; Kaptanoğlu et al., 1998; Karaalioğlu, 1997; Özkiliç, 2005; Öztürk, 2004; Sahin et al., 2012; Yildirim et al., 2009).

History matching with the field data was performed to reduce subsurface uncertainty. An analytical solution of gas material balance was done and the P/z vs Gp graph was used to check the history matched model validity.

With the finalized model at hand, a cyclic storage design followed by an extended production period was simulated. Lastly, a simulation until the year 3500 was simulated to observe the diffusion and dissolution effects.

CHAPTER 5

EVALUATION OF THE NORTHERN MARMARA GAS FIELD FOR UHS

5.1 Examination of Site Specific Factors

HyUSPRe project documented the Northern Marmara Field as the only porous UHS site in Turkey (Cavanagh et al., 2022). Moreover, the reservoir lies around the optimum depth (1100m) for storing H_2 (Iglauer, 2022).

Based on the study by Thaysen et al. (2021), the reservoir is prone to different sorts of biological contamination (see Figure 5.1. where every point represents a group of microbial organisms). However, since the field has not been sampled for microorganisms and the critical values might be subject to change when both salinity and temperature stresses are acting togethe, firm conclusions can be made only after lab work and field monitoring.

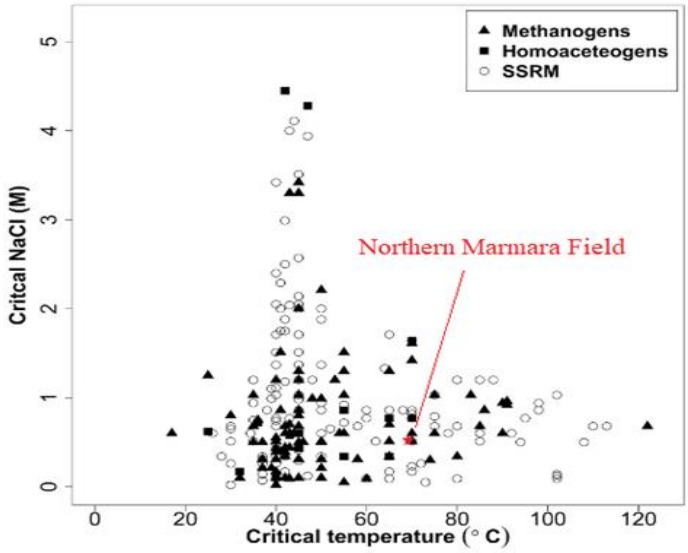

Figure 5.1. Critical temperature (without salinity stress) versus critical salinity (without temperature stress) for methanogens, homoacetogens and SSRM. (modified from Thaysen et al., 2021)

H_2S production by microorganisms and/or geochemical reactions is a serious worry for hydrogen storage projects (Dopffel et al., 2021; Hassannayebi et al., 2019). Even though some H_2S production was encountered with the Underground Sun Project, which had some pyrite in the formation, it was not a vital issue since the amount was not really significant. Moreover, H_2S production did not show any exponential growth behaviour as one would expect from microbial activity (Pichler, 2022). As there is no mention of pyrite in the formation and there is no data about microorganisms, this study assumes that the field is free of any geochemical or biological activity that would result in conversion of the hydrogen.

Some microbial activity in the reservoir might enable it to be used as an underground bio-tmethanation plant as well (Strobel et al., 2020). Examples of such projects, which are not yet commercial, can be found in Argentina and Austria (Perez, 2022; Pérez et al., 2016; Pichler, 2022; RAG et al., 2017).

In terms of geochemical reactions, the literature matches the field experience (Hassannayebi et al., 2019; Perez, 2022; Pichler, 2022). This strengthens the expectation for no fast-reaction to occur, however, site specific lab work can be useful to see whether pyrite to pyrrhotite reaction or any other reaction takes place.

The composition of formation water can potentially increase hydrogen dissolution which is normally a minuscule issue (RAG et al., 2017). Formation water should be sampled and experimented on to measure the exact solubility.

Another issue, which has not been a problem in the two aforementioned fields but still requires attention, is the cap rock integrity. Although, the studies and the field data showed no sign of leakage, some examinations and tests should be carried out beforehand to build confidence (Hemme & van Berk, 2018; Perez, 2022; Pichler, 2022).

When the issues mentioned above are examined, and the field equipment is inspected for replacement/maintenance, there seems to be no irresolvable problem for UHS in the Northern Marmara Field.

CHAPTER 6

NUMERICAL MODELLING AND SIMULATION

6.1 Shortcomings of the Model

The model for this study was based solely on the data obtained from the aformentioned, previously published studies.

Since log data was not available, the reservoir properties, such as porosity, permeability, and thickness were assumed to be constant throughout the reservoir creating a homogenous structure. Therefore, reservoir heterogeneity is not represented, which might result in optimistic estimations for some parts of the reservoir.

As this is the first study considering the field for UHS, there was no study regarding the investigation of microbial biota or any lab work about the possible biological reactions. Since it is a highly site-specific issue, no assumptions were made and the modelling of possible biological reactions was left outside the scope of this work. However, it is noted that, the field lies in a temperature-salinity region which might give way to biological reactions. Also since there is CO_2 presence, bio-methanation is a strong possibility which could end up in biofilm forming.

Although the dissolution of hydrogen in brine is not neglected, it might be subject to change depending on the mineral composition of the formation water. This aspect of the model can be improved with experimental work providing more data about the formation water.

Geochemical reactions also required lab work to be conducted before they were modelled. No fast-geochemical reactions were observed in the aformentioned UHS in porous media projects agreeing with the literature research (Hassannayebi et al., 2019; Pérez et al., 2016; Pichler, 2022). An exception to that could have been

pyrite to pyrrhotite reaction, but it was not expected for the Northern Marmara Field as there was no mention of pyrite in the reservoir. Still, geochemical reactions is a possible issue that might have been not captured with this model.

Peng-Robinson (PR-1978) was assumed to be a good enough EOS for the fluid model which also comes into play for the calculation of gravitational effects and gas mixing by the simulator. Diffusion, although it has a minuscule effect on mixing, was also accounted for by using approximate values for the diffusivity constants.

There were no data available regarding dispersivity. However, even if there were data on dispersivity, it would probably be futile since its effects would be overshadowed by numerical dispersion (Terstappen, 2021; Yildirim et al., 2009). Hence, as suggested by Terstappen (2021), numerical dispersion was minimized by applying numerical controls and assumed to be a substitution for physical dispersion. Nevertheless, the validity of this substitution would highly depend on field properties, grid and time step size for the model. Therefore, despite the author's best efforts, the modelled gas mixing might not reflect reality.

6.2 Model Creation Process

The steps followed for the model creation process can be listed as below:

1) Sifting and formatting the data into a useful format (see Appendix D).
2) Setting the dimensions considering the software license and processing power limits, and creating a preliminary reservoir model to be optimized later on.
3) Creating the fluid model.
4) History matching and setting the final model parameters.
5) Checking the model validity with an analytical solution.

6.2.1 Preliminary Model

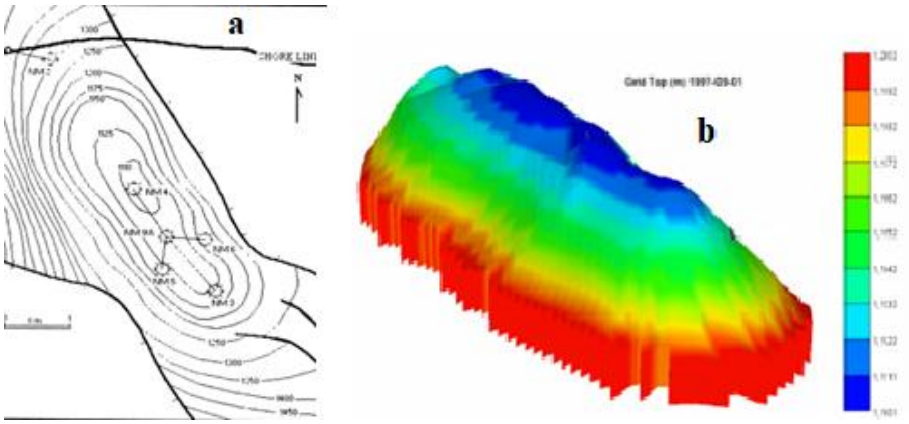

Figure 6.1. a) Contour Map (Kaptanoğlu et al., 1998) b) The Preliminary Model

The contour map taken from Kaptanoğlu, Atalay, and Yörük (1998) was digitized using Surfer (see Appendix A), and imported into the Builder. A cartesian grid consisting of 12444 blocks was placed on top of the map and the null blocks were cut out. The first five producer wells were perforated according to the digitized map, and the 'Create Trajectories from Completions(PERF)' command was used to construct the trajectories. Lastly, a gas cap with the composition given in Table 6.1. is defined.

Table 6.1 Composition of the Native Gas (Özkiliç, 2005)

Component	Mole Fraction (%)
C1	91.45
C2	3.21
C3	1.21
iC4	0.24
nC4	0.30
iC5	0.09
nC5	0.07
CO_2	2.28
N_2	1.15

6.2.2 Fluid Model

Although GERG-2008 EOS was shown to be superior to Peng Robinson in terms of accuracy, PR has been shown to yield faster calculations (Baladão et al., 2018). There also is a novel model (PC-SAFT EOS) asserting even further improvements to GERG-2008 (Eller et al., 2022). In the end, since the reservoir temperature is above 200 Kelvin many EOS could be used with reasonable accuracy (Nasrifar, 2010). For this study, PR (1978) was used since it is a widely used option for the industry and it is readily available in the simulator.

WinProp Fluid Property Characterization Tool was used to model the fluids. Most properties were determined by Peng Robinson (PR-1978) equation of state (EOS) by WinProp, while a few parameters were needed to be manually entered. CMG included hydrogen in the WinProp library as a default compound starting from the 2021 version (Faraj Zarei, 2021). However, since the 2020 version of WinProp was available, hydrogen properties were entered manually using the properties from CMG's workshop (Ali Kasraian, 2020).

For solubility, Henry's Constant values were calculated by WinProp at reservoir temperature and pressure. However, since the 2020 version was not tuned for hydrogen, the values were adjusted according to the CMG's workshop (Ali Kasraian, 2020). Diffusion of compounds into the aqueous phase (DIFFC-AQU command in GEM) other than methane and hydrogen were neglected and 3.75×10^{-5} cm^2/sec and 8.5×10^{-5} cm^2/sec were entered as diffusion constants, respectively. For gas diffusivity (DIFFC-GAS command in GEM) 4.46×10^{-5} cm^2/sec was used. Lastly, 'HYSKRG' keyword was entered into the .dat file manually, to account for the hysteresis effects in relative permeability.

Two other gases, namely 'Trace H2' and 'Trace CH4' were defined to visualise the effects of the injection/production more clearly. These gases had the exact same properties as hydrogen and methane, respectively. They were injected with a trace amount (10^{-5} of the total stream) to be able to separate the injected gas' behaviour from the host gas, in other words, to create better resolution (see Figures 7.3&7.4).

6.2.3 History Matching and the Final Model

To match the OGIP of 5.5 billion m^3 reported by the field engineers' (Sahin et al., 2012), porosity and thickness were needed to be set. Although most other studies (Bagci & Öztürk, 2007; Gumrah et al., 2005; Özkiliç, 2005; Öztürk, 2004) used a cnstant thickness value of 65 meters, it is denoted in Sahin, Abravci, and Tirek (2012) that 65 meters is the maximum thickness. Concluding that the thickness value might be variable, and since the average porosity was known to be 20%, a constant thickness of 34 (8.5x4) meters was used in the model as it matched the OGIP.

Table 6.2 Model Reservoir Volume

	Unit	Quantity
Total Bulk Reservoir Volume	reservoir m^3	225 million
Total Pore Volume	reservoir m^3	44.88 million
Total Hydrocarbon Pore Volume	reservoir m^3	40.39 million
Original Gas in Place	standard m^3	5.5 billion

Production data from Öztürk (2004) were fed to the model and wellhead pressures were matched while staying loyal to the data extracted from Şahin, Abravcı, and Tırek (2012) (see Appendix B). Error margins of wellhead pressures were checked to make sure they were lower than 5%, and the properties were adjusted. No satisfactory explanation was found from the references for the produced water. Therefore, relative permeability values and the initial water saturation were adjusted to match the cumulative water production.

Table 6.3 Relative Permeability Tables used in the Model

Water-Oil Table			Liquid Gas Table		
Sw	krw	krow	Sg	krg	krog
0	0	1	0	0	1
0.1	0.007	0.9	0.1	0.1	0.9
0.9	0.9	0.1	0.9	0.9	0.007
1	1	0	1	1	0

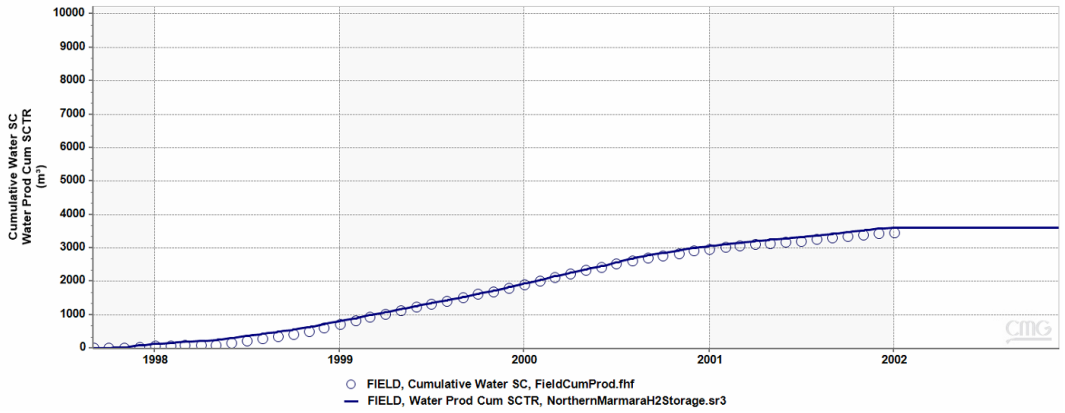

Figure 6.2. Model Match of the Cumulative Water Production

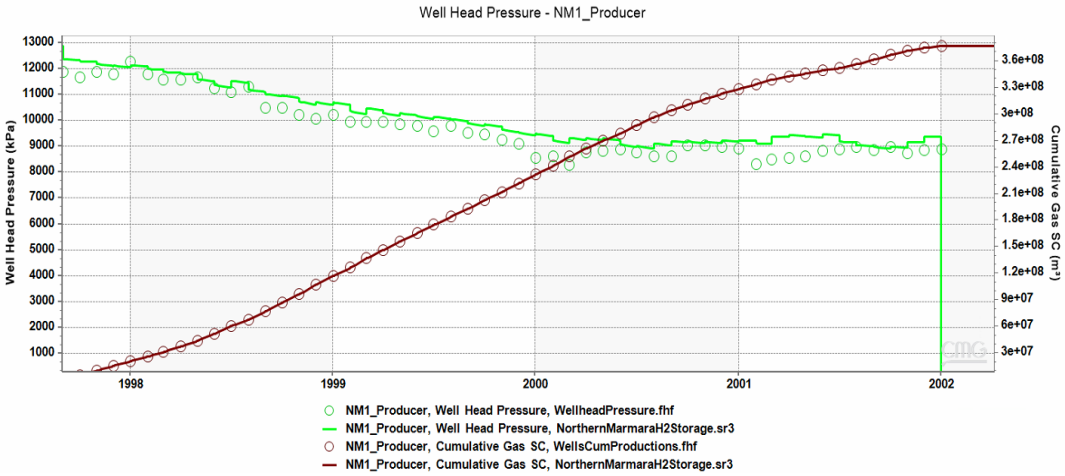

Figure 6.3. Model Match for NM-1 Well (Pwh & Cum. Gas. Production)

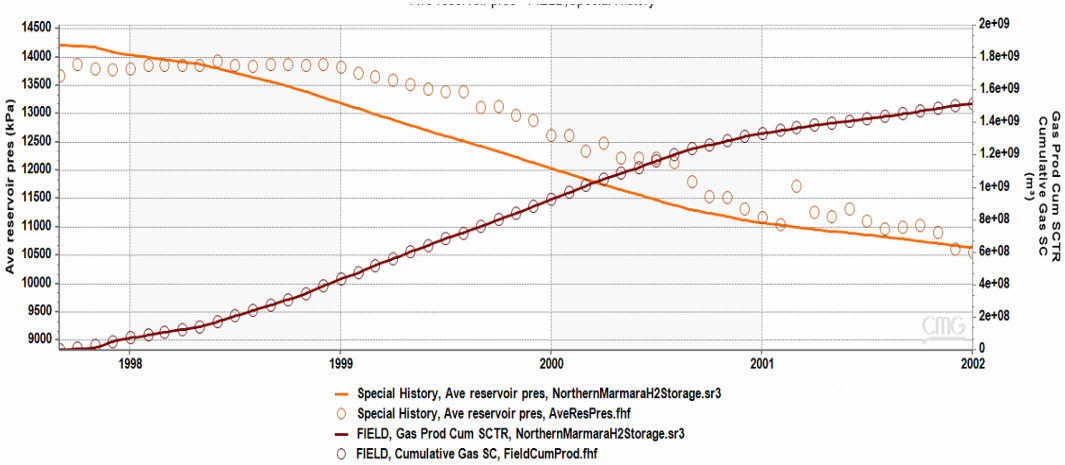

Figure 6.4. Model Match of the Field (Average Res. Pressure & Cum. Gas Prod.)

Since the real locations for the wells drilled after 2002 were not known, the locations in Gumrah et al. (2005) were used and six additional wells were added.

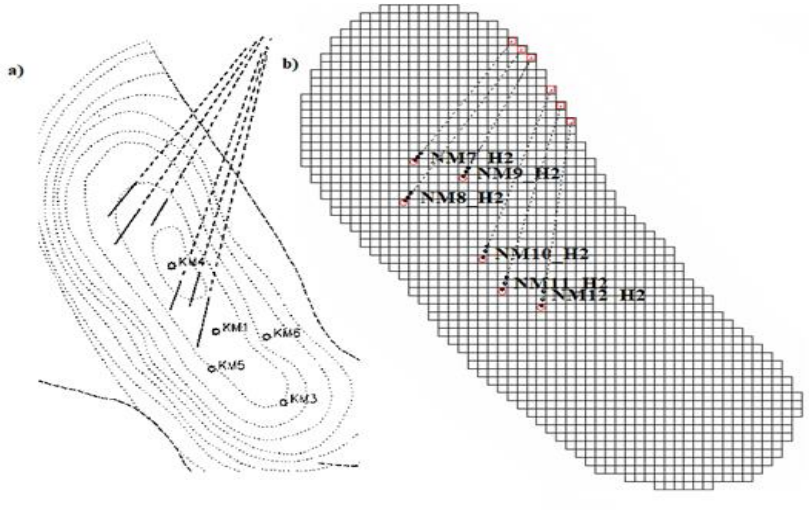

Figure 6.5. Additional wells' trajectories a) From (Gumrah et al., 2005) b)Model

Well Properties are given in Table 6.4, where rad corresponds to the tubing diameter. Geofac is a dimensionless number depending upon the wells placement within the grid block, and 0.37 corresponds to the center of a square block. Wfrac is a number between 0 and 1 that is used to define the fraction of a circle that the well models, and 1 corresponds to a full circle.

Table 6.4 Well Properties

Property	Unit	Value
Relative Roughness (Özkiliç, 2005)	-	0.000742
Wellhead Temperature	°C	15
Bottomhole Temperature	°C	68.8
Geometry	Direction	K or I
Well Radius	m	0.2032
rad	m	0.0762
geofac	-	0.37
wfrac	0 to 1	1.0
skin	-	0.0

Reservoir properties that were used for the model are given in Table 6.5. where CPOR is the rock compressibility and PRPOR is the reference pressure for determination of the CPOR.

Table 6.5 Reservoir Properties

Property	Unit	Value
Porosity	%	20
Permeability	mD	50
KvKh Ratio	-	0.37
Reference Depth	m	1259
Reference Pressure	kPa	14300
CPOR (Öztürk, 2004)	1/psi	$4x10^{-6}$
PRPOR (Öztürk, 2004)	kPa	14500
$Sw_{initial}$	%	0.2
$Sw_{critical}$ (Öztürk, 2004)	%	0.1
Reservoir Temperature (Sahin et al., 2012)	°C	68.8

6.2.4 Analytical Gas Material Balance Solution

A double check on the model was done by solving the material balance equation for dry gas reservoirs (Samura et al., 2021). P/z vs Gp graph was compared with the real field data from Sahin, Abravci, and Tirek (2012) covering the 2007 to 2012 period and the original field design. Required z compressibility factor values for the model were calculated using Standing-Katz correlations (as the same with the software) using pseudocritical values adjustment factor of 2.5 for the CO_2 presence in the gas composition (Mccain, 1991). Since the graph showed a good enough approximation to the data, the model was accepted for forward simulations.

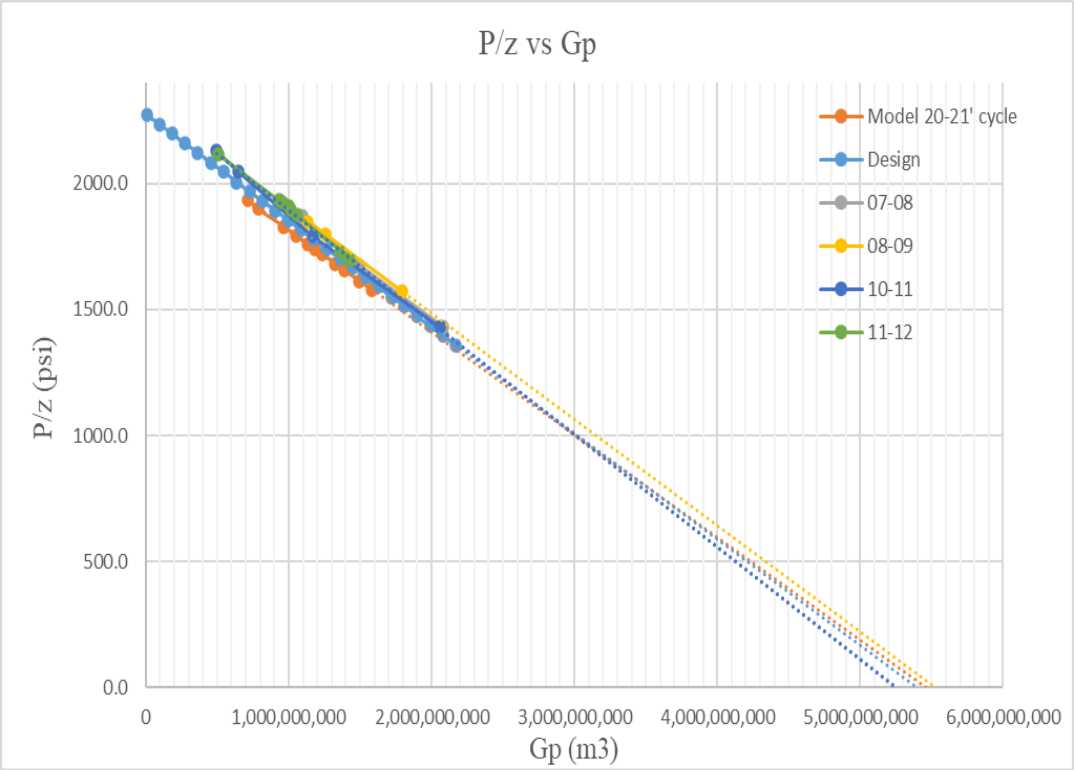

Figure 6.6. P/z vs Gp plot for the Northern Marmara Gas Storage Field Model (Values except the "Model 20-21' cycle" were extracted from (Sahin et al., 2012) using Grabit (see Appendix B)

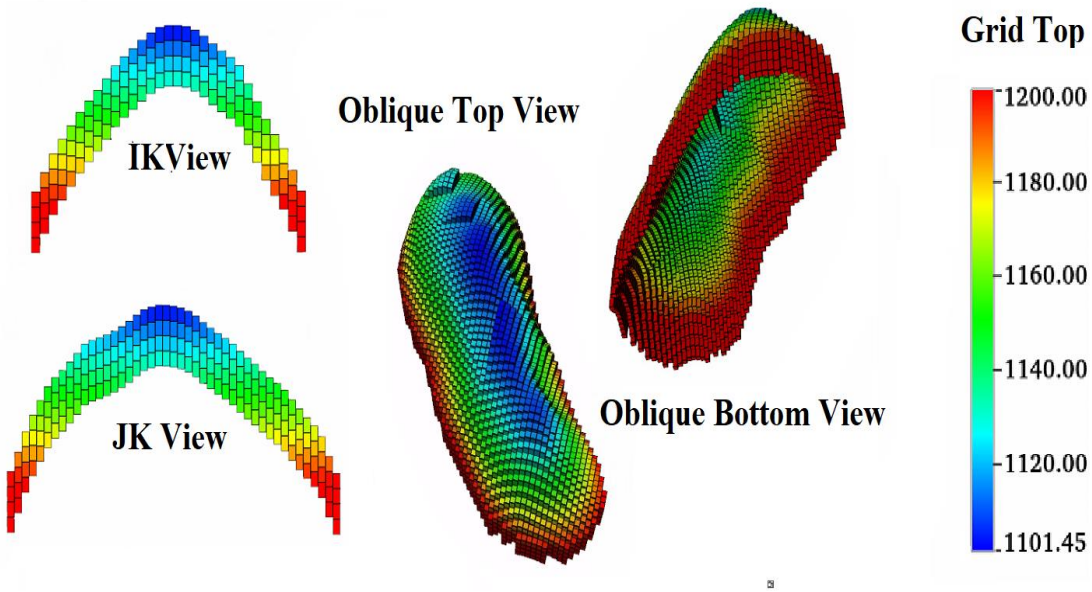

Figure 6.7. Final Model from various views

6.3 Numerical Dispersion

Discretization of continua on time and/or space for numerical calculations results in a truncation error. Replacing the derivatives with finite differences by the Taylor series approximations causes spatial gradients to be smeared. The smearing of the simulated front (see Figure 6.9) causes it to diverge from the actual front impacting the modeling of the displacement (Fanchi, 2018).

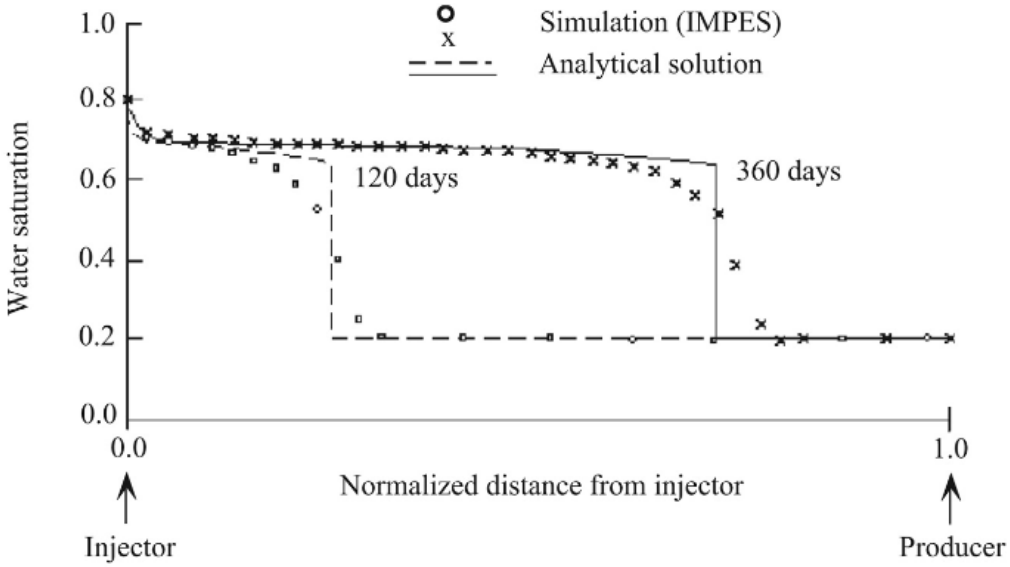

Figure 6.8. Front smearing for a linear Buckley-Levertt Waterflood Model (Fanchi, 2018)

In other words, dividing the reservoir into grid blocks and the time into time-steps homogenizes the spatial properties causing numerical errors to accumulate. This situation causes the simulated model to have a higher dispersivity than the real reservoir. (Dentz, 2022; Terstappen, 2021).

The dispersion introduced by the numerical errors is of the same order of magnitude as the physical dispersion or higher (Shrivastava, 2003). For large grid-cell and time-step sizes the numerical dispersion overpowers the physical dispersion (Terstappen, 2021).

Theoretically, this problem could be resolved by using cell sizes and time step lengths so small that the effect becomes almost negligible, however, this is not practicle as it increases the computational time to an insensible level (Terstappen, 2021).

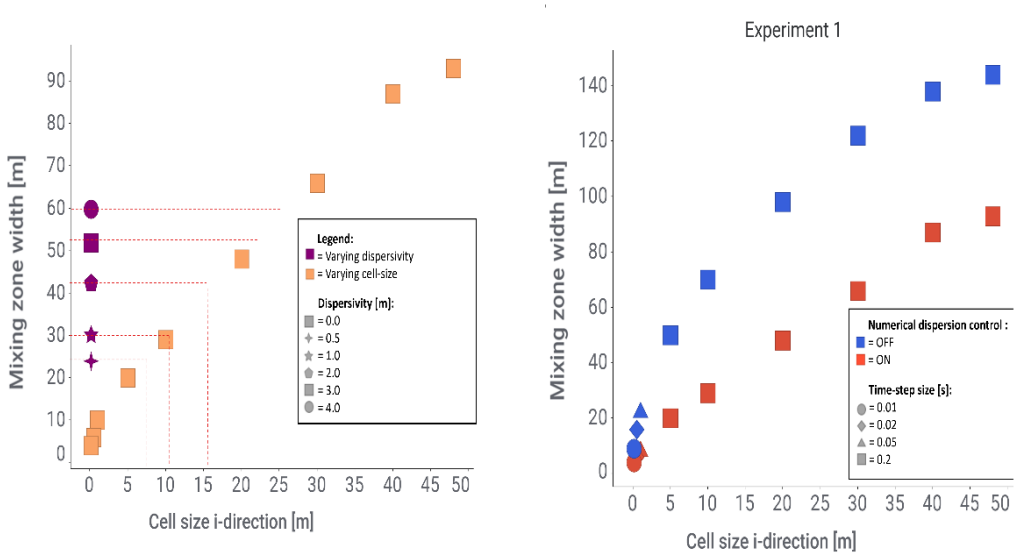

Figure 6.9. Mixing zone width versus cell sizes for varying dispersivities (on the left), and for varying time-step sizes with and without flux limiter (on the right) (Terstappen, 2021)

GEM has the built in command 'TWOPTFLUX' to activate the Total Variation Limiting flux limiter (TVD) (Shrivastava, 2003; Terstappen, 2021). By activating this numerical control, overshooting and undershooting of calculations are eliminated and numerical stability is ensured in the overall numerical scheme (Computer Modelling Group, n.d.). As shown on the right hand side of the Figure 6.10 flux limiter was effective to minimize the mixing zone width to its 40% for a 5-meter cell size and to its 54% for a 50-meter cell size (Terstappen, 2021).

For the time being there is no known method in any reservoir simulator that completely eliminates numerical dispersion at field scale. Even if numerical dispersion could have been eliminated, modelling macroscopic dispersion still would not be possible for this study. As dispersivity is highly dependent on

heterogeneity and scale, long duration tracer tests would be required to obtain a realistic field value (Terstappen, 2021).

Numerical dispersion can be used to compensate for the physical dispersion (Shrivastava, 2003; Terstappen, 2021). This study assumes for grid blocks with dimensions 65x65x8.5 meters, when the flux limiter is activated, numerical dispersion accounts for the physical dispersion. Hence, physical dispersion was not incorporated in the main model. It is noted that, applying the flux limiter decreased the amount of hydrogen that is left in the reservoir after the cycling period from 4.705% to 2.609%. Comparatively, incorporating physical dispersivity of 4 meters (the upper limit used in Terstappen (2021)) in a seperate model only increased this amount to 2.647%.

6.4 Forward Simulations

To approximate the real field practice, the schedule that was presented at the World Petroleum Congress (2017) was used (Abravcı, 2017). The simulations consisted of four parts, namely, the methane storage period, the hydrogen storage period, the extended production period to retrieve the hydrogen that has been left behind, and the shut-in period afterward to observe the effect of diffusion and gravitational segregation.

The first two periods, which are the cyclic storage of methane and hydrogen, were run for 25 years each. Every cycle consisted of a withdrawal period of 120 days starting from the 15th of November, and an injection period of 215 days starting from April 1st. There were 15 days of break in between withdrawal and injections. Starting from 2007, cyclic methane storage was realized with the pressure constraints of 8400-14300 kPa as given in Abravcı (2017). Starting from 2032, methane was switched with pure hydrogen, and cyclic storage continued for another 25 years.

Since the injected/produced gases, especially in the methane cycles, were not clearly distinct from the host gas at the reservoir, trace amounts (10^{-5} of the total

stream) of distinctive gases with the same fluid properties were injected in another copy of the model. Since their concentrations changed on a narrower scale, these gases, named ‘Trace CH4’ and ‘Trace H2’ helped for visualising the transport of the injected/produced gases with better sensitivity.

Table 6.6 Cycling Constraints

Constraint	Production	Injection
Duration (days)	120	215
Pressure (kPa)	Min. 8400	Max. 14300
Max. Stream Rate (m3/day)	16 million	9 million
15 days breaks are left between the production and injection periods		

Following the cyclic storage periods, an extended production with the constraint of total production up to 5 million m^3/day was realized together with the minimum reservoir pressure constraint of 3000 kPa.

In the first production period (the history matched period) only 5 production wells were used. For the methane production period, 6 wells were added, and each of them were copied as injector wells making 22 active wells (11 injection-11 production). With the 5 shut-in ones belonging to the first production period, 27 wells were defined in total. For the hydrogen storage period, 11 wells were again copied to define hydrogen producer and injectors. This makes the total number of wells 49 with 22 of them being active. For the extended production period, 11 wells were copied again.

In short, except for the first production period with 5 wells, there were 11 active wells in the field at any given time. The wells were copied as part of the workflow merely for better control over the model.

CHAPTER 7

RESULTS AND DISCUSSION

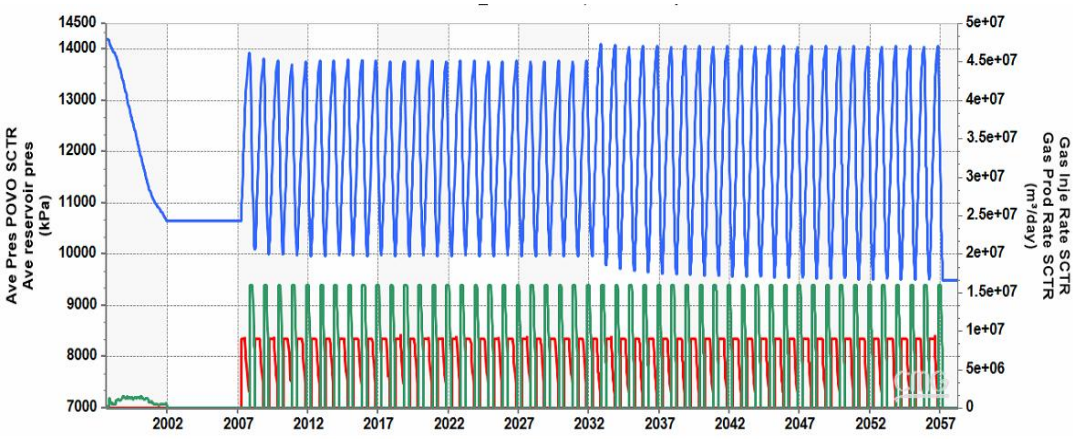

Figure 7.1. Average Reservoir pressure, Prod. Rate, Inj. Rate for 1997-2058

The first depletion period of the field between 1997-2002 produced 1.5 billion m^3 of gas resulting in a drop in the field average pressure from 14200 to 10650 kPa. The methane storage period started with the first injection in 15.April.2007 and ended with the last withdrawal in 01.April.2032. Starting from 15.April.2032 hydrogen injections began ending in 01.April.2057. Each year had 1 injection/withdrawal cycle as denoted in Table 6.6.

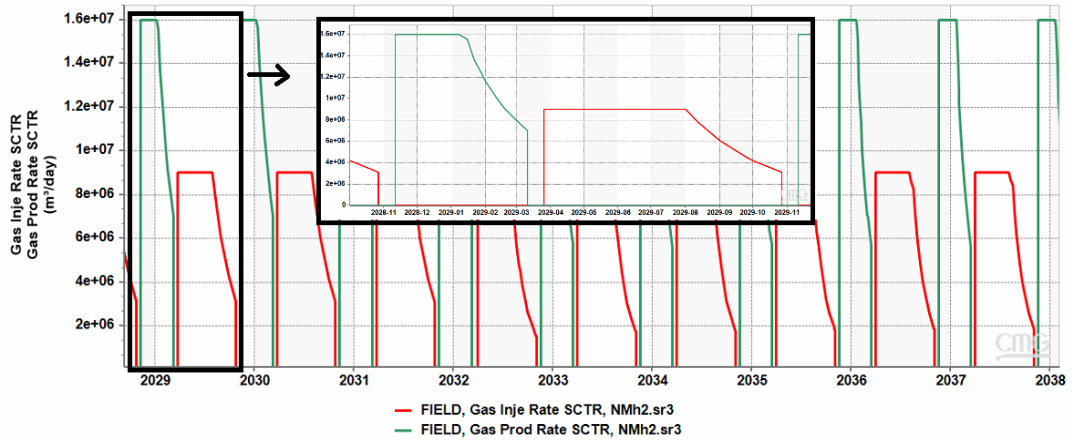

Figure 7.2. Field Prod. and Inj. Rates 2029-2038 (2029 cycle is enlarged)

Since the wells' bottomhole pressure constraints (8400-14300 kPa) were triggered, the injection and withdrawal targets were not fully satisfied with 9-16 million m^3, but rather the rates fell towards the end of each period as seen in Figure 7.2. As shown in Figure 7.1, during the methane cycles, the average reservoir pressure fluctuated around 13800-10000 kPa. Since hydrogen is less viscous it penetrated into the reservoir further than methane causing average pressure to fluctuate around 14000-9500 kPa.

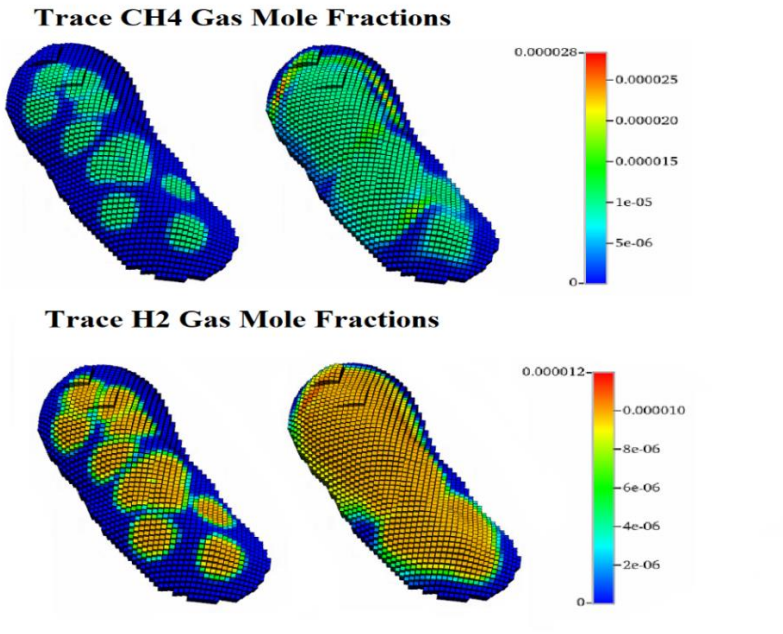

Figure 7.3. Trace gases penetration into the reservoir after the first and the last injections

As a result of 25 cycles, 3.259 million tons of hydrogen was injected and 3.174 million tons of hydrogen was withdrawn. Even when the geochemical and biological reactions are neglected, approximately 2.61% of the hydrogen was left behind in the reservoir as a result of cyclic storage. On the other hand, for methane, the cumulative withdrawal/injection amounts matched each other after the cycles. In fact, some portion of the 'injected methane' also remained in the reservoir, but since the native gas also had a high methane concentration, it made up for the remaining injected gas (Please see Figure 7.4). 26 million tons of methane was injected and withdrawn during the methane storage period.

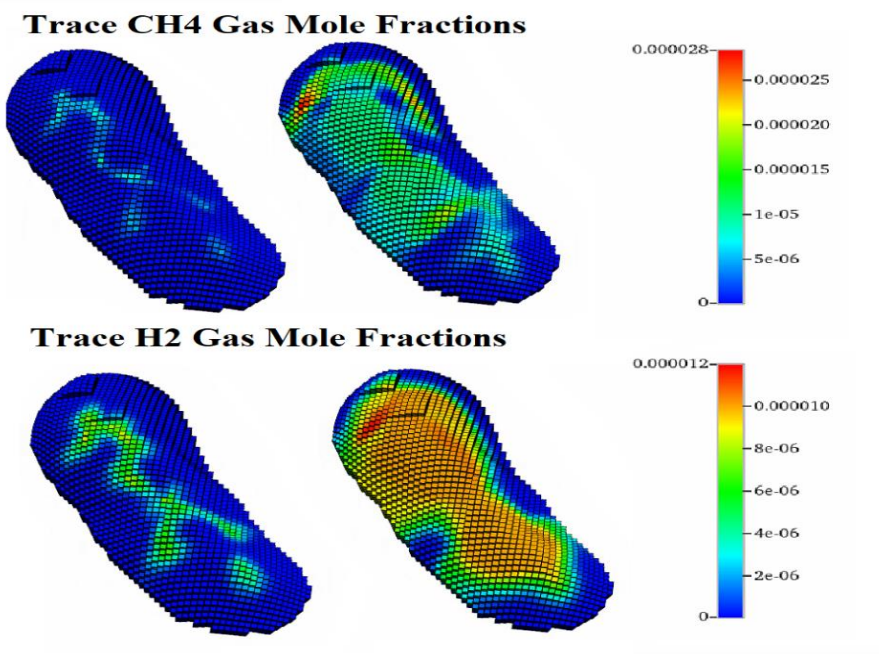

Figure 7.4. Remaining portion of injected gases shown after the first and last productions by the defined trace gases

Comparing the 25 years of cycle periods for both methane and hydrogen, approximately 371 TWhs of energy was reproduced for methane cycles and 119 TWhs (106.65 from H_2 and 12.25 from CH_4) was reproduced from hydrogen cycles (see Appendix H for calculations).

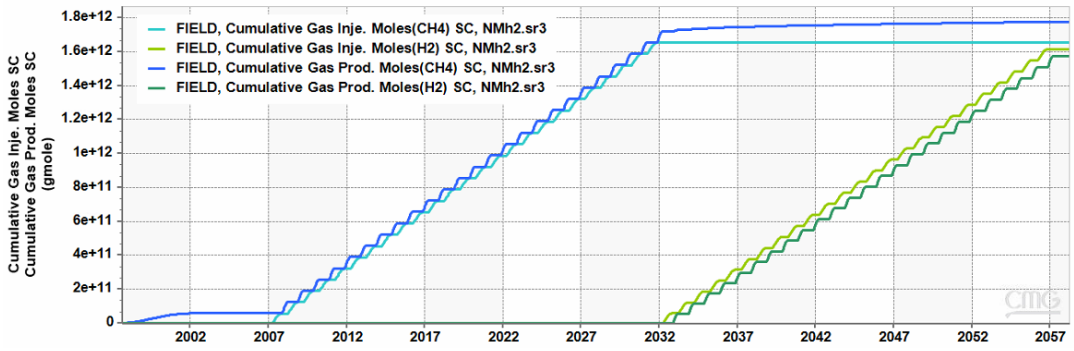

Figure 7.5. Cumulative Production and Injection for CH_4 and H_2 (gmole) between 01.09.1997 – 01.04.2057

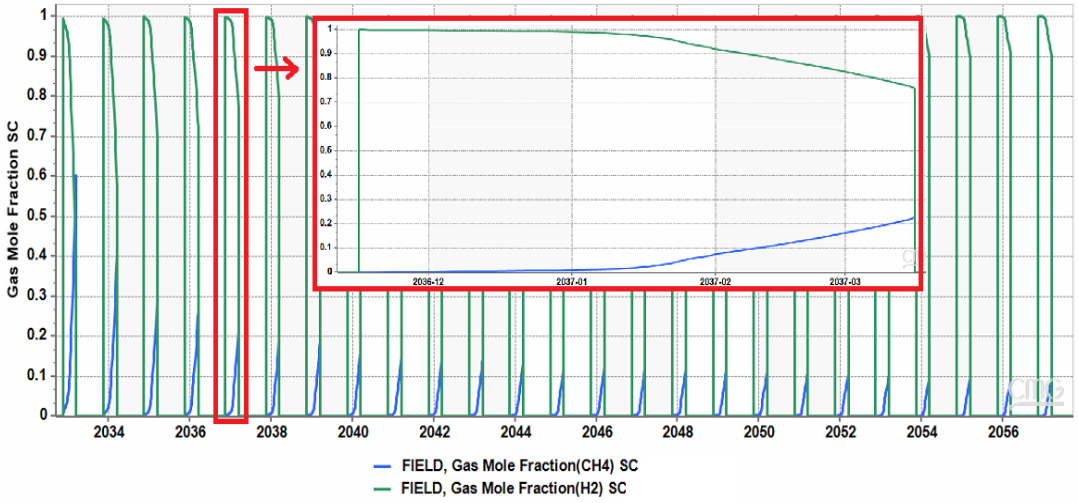

Figure 7.6. Methane and Hydrogen Volume Fractions, 2037 cycle is enlarged

The molar fraction of methane that is withdrawn during hydrogen cycles seems to persist at around 8% even after 25 hydrogen cycles. Moreover, other gases that were present in the reservoir gas composition are also produced with the withdrawn gas with their molar fractions within parts per thousand scale. Despite the molar fraction of the gases decreasing with each cycle, a total of 0.5% of ethane, propane, butane, pentane, carbon dioxide, and nitrogen from the native gas were present in the withdrawn gas in the last withdrawal period.

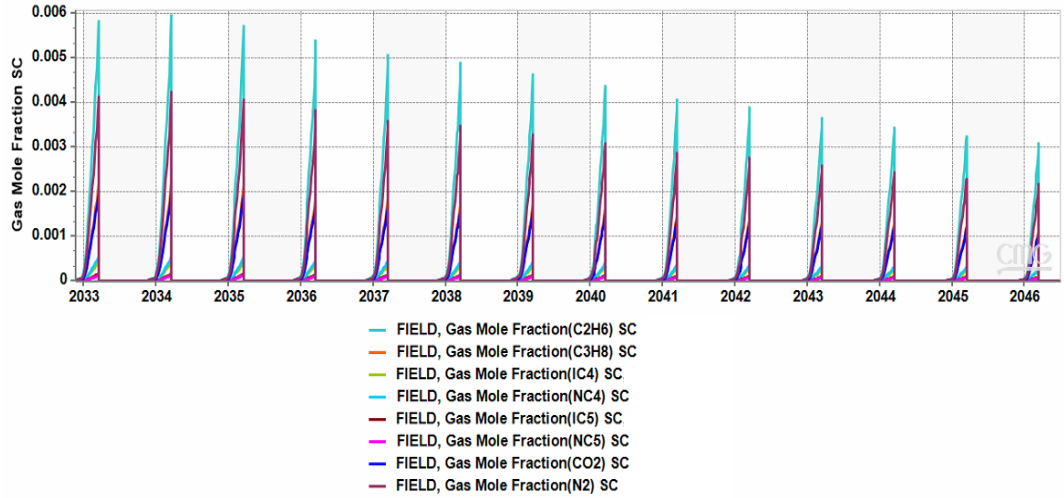

Figure 7.7. Mole fraction of other gases present in the stream

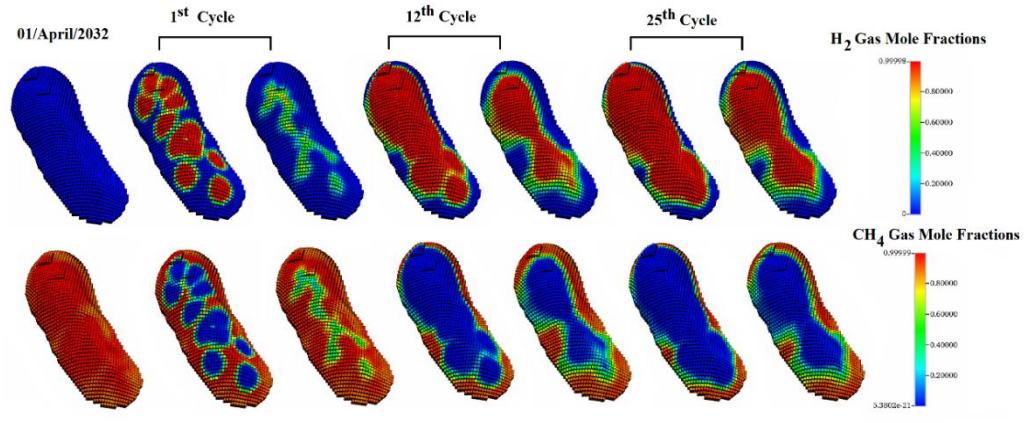

Figure 7.8. Hydrogen and methane mole fractions during the hydrogen storage period

As shown in Figure 7.9., it was possible to retrieve the 2.61% hydrogen that was left behind in the reservoir within a year. Depletion down to 6000 kPa was already enough to withdraw up to 99.5% of the injected hydrogen.

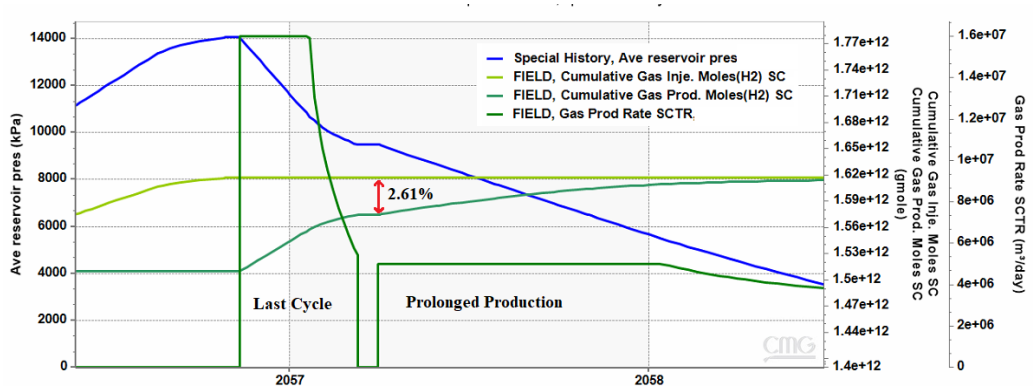

Figure 7.9. Extended production period showing depletion of the field.

Perhaps the most important finding was the difference in individual well performances shown in Figures 7.10, 7.11, and 7.12. At each well, methane breakthrough is observed after a certain time in the production period. However, the time and the amount of this breakthrough varied significantly. Some wells managed to produce up to 100% purity for a long time, whereas some others performed more poorly. Although, all wells' performances in terms of purity improved over time, the difference in the purity of the streams remained.

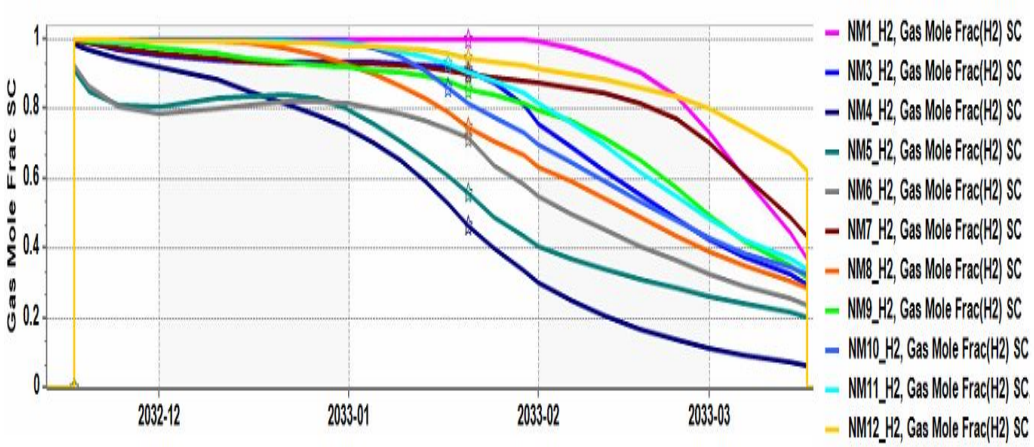

Figure 7.10. H_2 purity of streams from separate wells within the first cycle

The findings mean that large scale fields can potentially produce almost pure hydrogen. With meticulous monitoring and separate treatment of the streams, the purity problem seems to be surmountable.

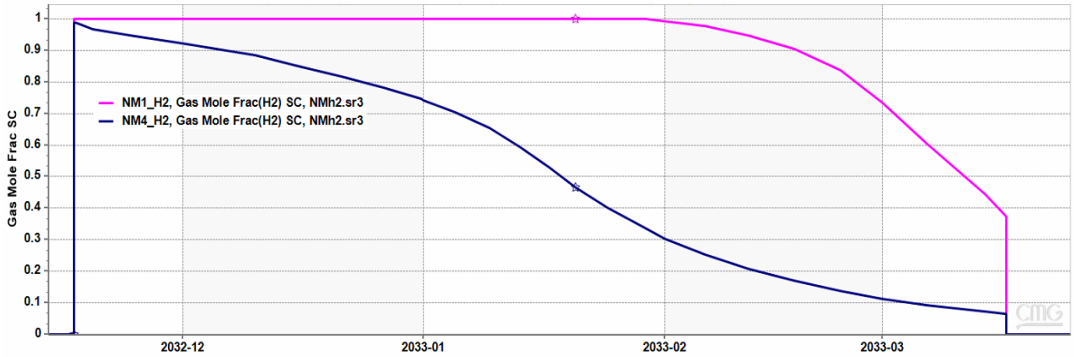

Figure 7.11. Best and worst performing wells in terms of purity for the first cycle

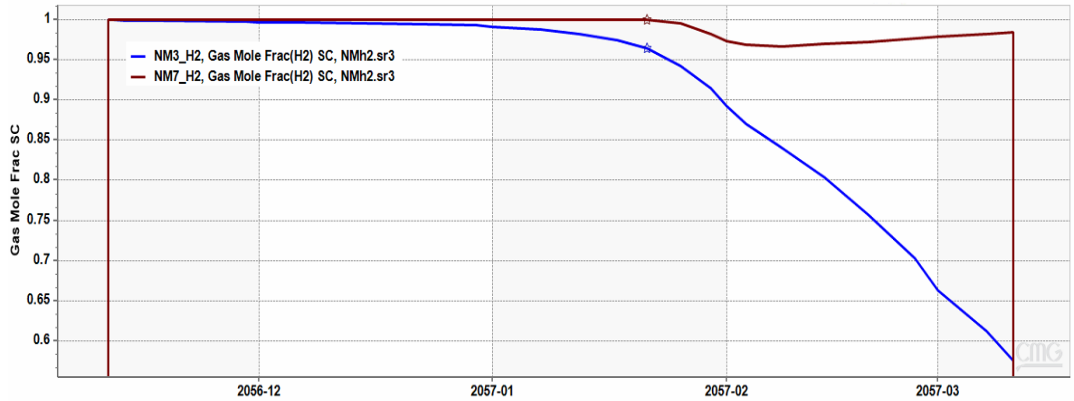

Figure 7.12. Best and worst performing wells in terms of purity for the last cycle

The simulation was also run without the extended production period to see the gas mixing without dispersion. Since the Northern Marmara has an anticlinal structure, the effect of gravitational segregation was clearly visible throughout the whole simulations. It caused the hydrogen to accumulate towards the middle dome shaped part while pushing the methane to the periphery. This could eventually cause the spilling point to be passed for the heavier fractions. As seen in Figure 7.13, it took more than a century before the diffusion effects became considerable.

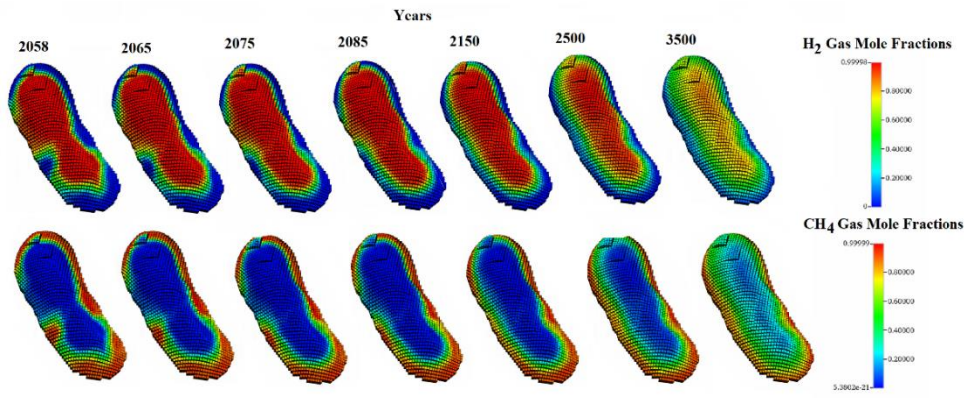

Figure 7.13. Reservoir let be between 2058-3500 showing the gas mixing due to diffusion

To summarize, this study agreed with the previous ones that, dispersion is the dominant factor for gas mixing in the reservoir. In porous media cyclic storage, some portion of the injected gas always remains in the reservoir due to the process being irreversible. However, the remaining portion can be withdrawn with an extended production period before the abandonment. It was shown that hydrogen tends to spread more into the reservoir while pushing the host gas. This could potentially end up with passing of the spill point. The composition of produced gas stream showed a significant difference between the wells. In the earlier production period, serious amounts of methane production was observed. Although, the purity has gotten better in the later cycles, it changed significantly even within the same cycle. This situation might call for on-site optimisation of production and purification methods for specific purity targets.

CHAPTER 8

CONCLUSIONS

Even though, the demand for hydrogen is at fairly low values for the time being, it is expected to increase with the diversification of the end-uses. Although, the price competition is tough, given the external benefits of energy security and climate change mitigation, hydrogen can become a much more ubiquitous option as an energy carrier.

When bulk storage of hydrogen is needed, for instance for seasonal storage, depleted gas fields are prominent candidates among the other options as they already have some data and infrastructure available, and they offer large volumes of storage capacity.

The Northern Marmara Field can be an exemplary field for seasonal storage of hydrogen as it currently serves the same purpose with natural gas. Even though, much preliminary work is still needed for a decision, an evaluation of the field showed no insurmountable problem associated with UHS.

After a model based on the past performance of the field was created, forward simulations were run to compare 25 years of storage cycles for methane and hydrogen. During the methane cycles, on average 14.8 TWhs of energy was withdrawn annually, corresponding to 371 TWhs in total. During the hydrogen cycles, due to methane also being produced in differing amounts, the energy withdrawn varied significantly over time. As earlier cycles produced more methane compared to the later ones, their energy content was higher. A total of 119 TWhs was produced during the hydrogen cycles.

In comparison, the first methane cycle produced 2.6 times more energy than the first cycle of hydrogen storage. This number has increased up to 6.2 times for the last cycles. As a result of 25 years, 3.1 times more energy was withdrawn from the

methane cycles. When hydrogen's externalities are not considered and assuming there is limited space for storage, this difference in energy content could mean that storing natural gas is more sensible. However, if enough storage structures are characterised, and hydrogen is prioritised for energy security and climate change mitigation, this comparison can become futile.

Since each well produced with varying purity even within the same cycle, managing the production and optimisation of the surface treatment is an issue that needs to be addressed in future work. Also, the change in the withdrawn energy per annum for hydrogen cycles adds complexity to the long term project planning. However, by exclusive treatment of the different streams, this could be turned into an advantage to produce different products tailored for the demand as done by the refineries.

Some possible microbial and geochemical reactions that could result in conversion of the injected hydrogen have been addressed. But since the required data to model them was not available, they were left outside the scope of this study for future studies. No leakage was assumed for this study, but cap rock integrity is also another issue that needs assurance by future studies.

It was shown by the simulations until the year 3500 that diffusion and dissolution into the brine are not significant compared to dispersion. However, since hydrogen solubility in brine might change significantly depending on brine composition, formation water needs to be tested for an accurate measurement.

Furthermore, as the use of numerical methods causes truncation errors, the usage of any simulator causes an issue of numerical dispersion. This problem was tried to be avoided by applying numerical controls available in the software and using the remainder part of the numerical errors as a substitution for physical dispersion. However, how well these two dispersions match each other is questionable. A thorough, site-specific sensitivity analysis should be carried out to see the effect of grid size and time step length on numerical dispersion.

REFERENCES

Abravcı, S. (2017). Silivri Doğalgaz Depolama Tesisi ve Güncel Durum. *22nd World Petroleum Congress (2017)*.

Abravcı, S. (2022). *Dünya'da ve Türkiye'de Doğal Gaz Depolamaya Geneş Bakış*. SPE Batman Student Chapter.

Acar, C. (2018). A comprehensive evaluation of energy storage options for better sustainability. *International Journal of Energy Research*, *42*(12), 3732–3746. https://doi.org/10.1002/er.4102

Advanced Energy Technologies. (2020). *World Map of Hydrogen Energy Infrastructure*. https://aenert.com/technologies/renewable-energy/hydrogen-energy/world-map-of-hydrogen-energy-infrastructure-2020/

Åhman, M. (n.d.). *Unlocking the "Hard to Abate" Sectors*. https://www.wri.org/climate/expert-perspective/unlocking-hard-abate-sectors

AIChE Academy. (2020). *Hydrogen Safety: Hydrogen Flame Prop Demonstration*. https://www.youtube.com/watch?v=r-8H5u4YzuY&t=64s&ab_channel=AIChEAcademy

Ali Kasraian. (2020). *Underground Hydrogen Storage Simulation Using CMG*. CMG.

Altıner, D., Batı, Z., Şenel, M., & Ekmekçi, E. (2006). Trakya Bölgesi Litostratigrafi Birimleri. In *Litostratigrafi Birimleri Serisi* (Vol. 2, pp. 54–56). Maden Tetkik ve Arama Genel Müdürlüğü (MTA).

Amber Grid, Bulgartransgaz, Conexus, CREOS, DESFA, Elering, Enagas, Energinet, Eustream, FGSZ, FluxSwiss, Fluxys Belgium, Gas Connect Austria, Gasgrid Finland, Gassco, Gasunie, Gas Networks Ireland, GAZ-SYSTEM, GRTgaz, … Transgaz. (2022). *European Hydrogen Backbone: A European Hydrogen Infrastructure Vision Covering 28 Countries*. https://www.ehb.eu/maps

Asante, D., He, Z., Adjei, N. O., & Asante, B. (2020). Exploring the barriers to renewable energy adoption utilising MULTIMOORA- EDAS method. *Energy Policy*, *142*. https://doi.org/10.1016/j.enpol.2020.111479

Bagci, A. S., & Öztürk, B. (2007, September). Performance Analysis of Horizontal Wells for Underground Gas Storage in Depleted Gas Fields. *SPE Eastern Regional Meeting*.

Baladão, L. F., Soares, R. P., & B Fernandes, P. R. (2018). Comparison of the GERG-2008 and Peng-Robinson Equations of State for Natural Gas Mixtures. *Baladão Journal of Engineering Research and Application Www.Ijera.Com*, *8*, 25–34. https://doi.org/10.9790/9622-0808032534

Beswick, R. R., Oliveira, A. M., & Yan, Y. (2021). Does the Green Hydrogen Economy Have a Water Problem? In *ACS Energy Letters* (Vol. 6, Issue 9, pp. 3167–3169). American Chemical Society. https://doi.org/10.1021/acsenergylett.1c01375

Bolin, B. (2007). *A History of the Science and Politics of Climate Change*.

BOTAS. (n.d.). *Hassas Alanlar*. Retrieved May 19, 2022, from https://www.botas.gov.tr/Sayfa/hassas-alanlar/133

BOTAŞ. (2022). *Silivri Underground Natural Gas Storage Facility*. BOTAŞ. https://www.botas.gov.tr/pages/silivri-underground-natural-gas-storage-facility/374

Boyce, M. P. (2012). Combined cycle power plants. In *Combined Cycle Systems for Near-Zero Emission Power Generation*. Woodhead Publishing.

British Geological Survey. (2008). *Underground Storage Mineral Planning Factsheet*. https://www2.bgs.ac.uk/mineralsuk/download/planning_factsheets/mpf_storage.pdf

Caglayan, D. G., Weber, N., Heinrichs, H. U., Linßen, J., Robinius, M., Kukla, P. A., & Stolten, D. (2020). Technical potential of salt caverns for hydrogen storage in Europe. *International Journal of Hydrogen Energy*, *45*(11), 6793–6805. https://doi.org/10.1016/j.ijhydene.2019.12.161

Çalışgan, H. (2005). *Comprehensive Modelling of Gas Condensate Relative Permeability and Its Influence on Field Performance* [PhD]. Middle East Technical University.

Cavanagh, A., Yousefi, H., Wilkinson, M., & Groenenberg, R. (2022). *Hydrogen storage potential of existing European gas storage sites in depleted gas fields and aquifers*. www.hyuspre.eu

Cembalest, M. (2020). Cost declines required to make the hydrogen economy a reality. *J.P. Morgan Annual Energy Paper, May 2021*.

Clerjon, A., & Perdu, F. (2019). Matching intermittency and electricity storage characteristics through time scale analysis: An energy return on investment comparison. *Energy and Environmental Science*, *12*(2), 693–705. https://doi.org/10.1039/c8ee01940a

Computer Modelling Group. (n.d.). *GEM User Guide (2020.10)*.

Dawood, F., Anda, M., & Shafiullah, G. M. (2020). Hydrogen production for energy: An overview. In *International Journal of Hydrogen Energy* (Vol. 45, Issue 7, pp. 3847–3869). Elsevier Ltd. https://doi.org/10.1016/j.ijhydene.2019.12.059

Demir, M. E., & Dincer, I. (2018). Cost assessment and evaluation of various hydrogen delivery scenarios. *International Journal of Hydrogen Energy*, *43*(22), 10420–10430. https://doi.org/10.1016/j.ijhydene.2017.08.002

Denholm, P. (2015). The Role of Storage and Demand Response. In *National Renewable Energy Laboratory (NREL)*. Greening the Grid.

Dentz, M. (2022). Mixing Relevant to UHS. In *1st International Summer School on UHS*. TU Delft. https://www.tudelft.nl/citg/UHS-SummerSchool

Dincer, I., & Acar, C. (2014). Review and evaluation of hydrogen production methods for better sustainability. *International Journal of Hydrogen Energy*, *40*(34), 11094–11111. https://doi.org/10.1016/j.ijhydene.2014.12.035

Dinçer, İ., Javani, N., Sorgulu, F., Öztürk, M., Ali Akman, M., Kürşad Marancı, M., Sarıkaya, Ş., Gölbaşı, Ş., Serhat Ertürk, A., Güney, İ., & Demirhan, A. (2021). *Temiz Hidrojen Enjeksiyonu ile Doğal Gaz Sistemlerinin Performansının İyileştirilmesi Proje Ekibi Türkiye'de Yeşil Hidrojenin Üretilip Doğal Gaza Karıştırılması Çalışmaları*.

Doke, J. (2022). *Grabit*. Mathworks. https://www.mathworks.com/matlabcentral/fileexchange/7173-grabit

Dopffel, N., Jansen, S., & Gerritse, J. (2021). Microbial side effects of underground hydrogen storage – Knowledge gaps, risks and opportunities for successful implementation. In *International Journal of Hydrogen Energy* (Vol. 46, Issue 12, pp. 8594–8606). Elsevier Ltd. https://doi.org/10.1016/j.ijhydene.2020.12.058

Du, Z., Liu, C., Zhai, J., Guo, X., Xiong, Y., Su, W., & He, G. (2021). A review of hydrogen purification technologies for fuel cell vehicles. In *Catalysts* (Vol. 11, Issue 3, pp. 1–19). MDPI. https://doi.org/10.3390/catal11030393

Edlmann, K. (2022). Geological Characterization. In *1st International Summer School on UHS*. TU Delft. https://www.tudelft.nl/citg/UHS-SummerSchool

EIA. (n.d.). *Hydrogen explained*. Retrieved December 7, 2021, from https://www.eia.gov/energyexplained/hydrogen/

Eller, J., Sauerborn, T., Becker, B., Buntic, I., Gross, J., & Helmig, R. (2022). Modeling Subsurface Hydrogen Storage With Transport Properties From Entropy Scaling Using the PC-SAFT Equation of State. *Water Resources Research*, *58*(4). https://doi.org/10.1029/2021WR030885

Ennis-King, J., Michael, K., Strand, J., Sander, R., & Green, C. (2021). *Underground storage of hydrogen: mapping out the options for Australia*.

ENTSOG. (2022). *Hydrogen Project Visualisation Platform*. https://h2-project-visualisation-platform.entsog.eu/

Fanchi, J. R. (2018). *Principles of applied reservoir simulation* (Fourth Edition). Gulf Professional Publishing.

Faraj Zarei. (2021). Underground hydrogen storage simulation using CMG suite. In *Energi Simulation Summit 2021*. Energi Simulation. https://www.youtube.com/watch?v=V0H4fC1dvao&t=1611s&ab_channel=EnergiSimuation

Farajzadeh, R., Lomans, B. P., Hajibeygi, H., & Bruining, J. (2022). Exergy Return on Exergy Investment and CO2 Intensity of the Underground Biomethanation Process. *ACS Sustainable Chemistry & Engineering*. https://doi.org/10.1021/acssuschemeng.2c02931

FCH2JU. (2019). *Hydrogen Roadmap Europe: A Sustainable Pathway for the European Energy Transition*. https://doi.org/10.2843/249013

Fekete, H., Kuramochi, T., Roelfsema, M., Elzen, M. den, Forsell, N., Höhne, N., Luna, L., Hans, F., Sterl, S., Olivier, J., van Soest, H., Frank, S., & Gusti, M. (2021). A review of successful climate change mitigation policies in major emitting economies and the potential of global replication. *Renewable and Sustainable Energy Reviews*, *137*. https://doi.org/10.1016/j.rser.2020.110602

Feldmann, F., Hagemann, B., Ganzer, L., & Panfilov, M. (2016). Numerical simulation of hydrodynamic and gas mixing processes in underground hydrogen storages. *Environmental Earth Sciences*, *75*(16). https://doi.org/10.1007/s12665-016-5948-z

Foh, S., Novil, M., Rockar, E., & Randolph, P. (1979). *Underground Hydrogen Storage Final Report*.

Gholami, R. (2022). Viscous Flow and Operational Difficulties in Salt Caverns. *2nd International Seminar "Living on Hydrogen" - II Microbial Influence on Hydrogen*.

Glanville, P., Fridlyand, A., Sutherland, B., Liszka, M., Zhao, Y., Bingham, L., & Jorgensen, K. (2022). Impact of Hydrogen/Natural Gas Blends on Partially Premixed Combustion Equipment: NOx Emission and Operational Performance. *Energies*, *15*(5). https://doi.org/10.3390/en15051706

Glenk, G., & Reichelstein, S. (2019). Economics of converting renewable power to hydrogen. *Nature Energy*, *4*(3), 216–222. https://doi.org/10.1038/s41560-019-0326-1

Golden Software. (2020, July 16). *Create Dynamic Models from Scanned Maps with Surfer*. Golden Software Youtube Channel. Create Dynamic Models from Scanned Maps with Surfer

Gumrah, F., Izgec, Ö., Gokcesu, U., & Bagci, S. (2005). Modeling of Underground Gas Storage in a Depleted Gas Field. *Energy Sources*, *27*(10), 913–920. https://doi.org/10.1080/00908310490449009

Guo, Y., Li, G., Zhou, J., & Liu, Y. (2019). Comparison between hydrogen production by alkaline water electrolysis and hydrogen production by PEM electrolysis. *IOP Conference Series: Earth and Environmental Science*, *371*(4). https://doi.org/10.1088/1755-1315/371/4/042022

Gupta, R., Basile, A., & Veziroglu, N. (2016). *Compendium of Hydrogen Energy Volume 2: Hydrogen Storage, Distribution and Infrastructure*. Elsevier. https://doi.org/10.1016/b978-1-78242-362-1.00001-8

Gupta Ram B. (2009). *HYDROGEN FUEL - Production, Transport, and Storage*.

Habibi, R. (2019). *An investigation into design concepts, design methods and stability criteria of salt caverns*. *74*. https://doi.org/10.2516/ogst/2018066ï

Hagemann, B. (2018). *Numerical and Analytical Modeling of Gas Mixing and Bio-Reactive Transport during Underground Hydrogen Storage* [Doctoral Thesis, Clausthal University of Technology]. https://tel.archives-ouvertes.fr/tel-01735019

Hagemann, B., Rasoulzadeh, M., Panfilov, M., Ganzer, L., & Reitenbach, V. (2015). Mathematical modeling of unstable transport in underground hydrogen storage. *Environmental Earth Sciences*, *73*(11), 6891–6898. https://doi.org/10.1007/s12665-015-4414-7

Han, G., Bruno, M., Lao, K., Young, J., & Dorfmann, L. (2006). Gas Storage and Operations in Single Bedded Salt Caverns: Stability Analyses. *41st U.S. Symposium on Rock Mechanics (USRMS)*.

Hangx, S. (2022). H2 Containment. In *1st International Summer School on UHS*. TU Delft.

Hashemi, L., Blunt, M., & Hajibeygi, H. (2021). Pore-scale modelling and sensitivity analyses of hydrogen-brine multiphase flow in geological porous media. *Scientific Reports*, *11*(1). https://doi.org/10.1038/s41598-021-87490-7

Hassan, I. A., Ramadan, H. S., Saleh, M. A., & Hissel, D. (2021). Hydrogen storage technologies for stationary and mobile applications: Review, analysis and perspectives. In *Renewable and Sustainable Energy Reviews* (Vol. 149). Elsevier Ltd. https://doi.org/10.1016/j.rser.2021.111311

Hassannayebi, N., Azizmohammadi, S., de Lucia, M., & Ott, H. (2019). Underground hydrogen storage: application of geochemical modelling in a case study in the Molasse Basin, Upper Austria. *Environmental Earth Sciences*, *78*(5). https://doi.org/10.1007/s12665-019-8184-5

Hassanpouryouzband, A., Joonaki, E., Edlmann, K., Heinemann, N., & Yang, J. (2020). Thermodynamic and transport properties of hydrogen containing streams. *Scientific Data*, *7*(1). https://doi.org/10.1038/s41597-020-0568-6

Heinemann, N. (2021). *Enabling large-scale hydrogen storage in porous media – the scientific challenges*. Società Geologica Italiana.

Heinemann, N., Alcalde, J., Miocic, J. M., Hangx, S. J. T., Kallmeyer, J., Ostertag-Henning, C., Hassanpouryouzband, A., Thaysen, E. M., Strobel, G. J., Schmidt-Hattenberger, C., Edlmann, K., Wilkinson, M., Bentham, M., Stuart Haszeldine, R., Carbonell, R., & Rudloff, A. (2021). Enabling large-scale hydrogen storage in porous media-the scientific challenges. In *Energy and Environmental Science* (Vol. 14, Issue 2, pp. 853–864). Royal Society of Chemistry. https://doi.org/10.1039/d0ee03536j

Hemme, C., & van Berk, W. (2018). Hydrogeochemical modeling to identify potential risks of underground hydrogen storage in depleted gas fields. *Applied Sciences (Switzerland)*, *8*(11). https://doi.org/10.3390/app8112282

Hévin, G. (2019). Underground storage of Hydrogen in salt caverns. In *European Workshop on Underground Energy Storage*. Storengy.

Hoff, K. (2020). *Expert Know-how with Hydrogen Compressors*. https://www.youtube.com/watch?v=UvcQXFGm6lE&ab_channel=InIPED

Housecroft. (n.d.). Isotopes of Hydrogen. In *Inorganic Chemistry*. Libretexts. Retrieved October 9, 2022, from https://chem.libretexts.org/Bookshelves/Inorganic_Chemistry/Map%3A_Inorganic_Chemistry_(Housecroft)/10%3A_Hydrogen/10.3%3A_Isotopes_of_Hydrogen

Hughes, L. (2009). The four 'R's of energy security. *Energy Policy*, *37*(6), 2459–2461. https://doi.org/10.1016/j.enpol.2009.02.038

Hydrogen Analysis Resource Center. (2022). *Hydrogen Compressibility Factor at Different Temperatures and Pressures*. H2tools.Org. https://h2tools.org/hyarc/hydrogen-data/hydrogen-compressibility-different-temperatures-and-pressures

IEA. (2019). *The Future of Hydrogen*.

IEA. (2021). *Global Hydrogen Review*.

IEA. (2022a). *Policies Database*. https://www.iea.org/policies

IEA. (2022b). *World*. https://www.iea.org/world

Iglauer, S. (2022). Optimum geological storage depths for structural H2 geo-storage. *Journal of Petroleum Science and Engineering*, *212*. https://doi.org/10.1016/j.petrol.2021.109498

Kabel, T. S., & Bassim, M. (2020). Reasons for Shifting and Barriers to Renewable Energy: A Literature Review. *International Journal of Energy Economics and Policy*. https://doi.org/10.32479/ijeep.8710

Kanaani, M., Sedaee, B., & Asadian-Pakfar, M. (2022). Role of Cushion Gas on Underground Hydrogen Storage in Depleted Oil Reservoirs. *Journal of Energy Storage*, *45*. https://doi.org/10.1016/j.est.2021.103783

Kaptanoğlu, A. A., Atalay, R., & Yoruk R. (1998, May). Development of a North Marmara Field Offshore Turkiye: A Case Study. *International Offshore and Polar Engineering Conference* .

Karaalioğlu, H. (1997). *Türkiye'de Yeraltı Gaz Depolaması Gereksinimi ve Kuzey Marmara Gaz Sahasının Depo Olarak Modellenmesi* [MSc. Thesis]. Istanbul Technical University .

Karlsson, A. (2021). *Hydrogen storage on islands-The possibility for Gotland and Åland to become self-sufficient with renewable electricity and energy storage in form of hydrogen*. http://stud.epsilon.slu.se

Kelly, N. A. (2014). Hydrogen production by water electrolysis. In *Advances in Hydrogen Production, Storage and Distribution* (pp. 159–185). Elsevier Inc. https://doi.org/10.1533/9780857097736.2.159

Kennedy, E., Botero, J. M., & Zonneveld, J. (2019). *Hychain 3: Analysis of the current state and outlook of technologies for production - Technology Assessment* (Vol. 37). www.ispt.eu/projects/hychain.

Knoors, B., Katakwar, P., Wirtz, A., Berkhout, J., Detz, R., & Weeda, M. (2019). *HyChain 1 Energy carriers and Hydrogen Supply Chain: Assessment of future trends in industrial hydrogen demand and infrastructure* (Vol. 37). www.ispt.eu/projects/hychain.

Kolin. (2022). *Kuzey Marmara Doğalgaz Depolama Tevsi (Faz-iii) Projesi*. https://www.kolin.com.tr/tr/projeler/devam-eden-projeler/bina-konut-ve-endustriyel-tesis-projeleri/kuzey-marmara-dogalgaz-depolama-tevsi-faz-iii-projesi#

Kruck, O., Crotogino, F., Prelicz, R., & Rudolph, T. (2013). *HyUnder Deliverable No 3.1: Overview on all Known Underground Storage Technologies for Hydrogen*.

Kumar, R. K., Makhmutov, A., Spiers, C. J., & Hajibeygi, H. (2021). Geomechanical simulation of energy storage in salt formations. *Scientific Reports*, *11*(1). https://doi.org/10.1038/s41598-021-99161-8

Laban, M. P. (2020). *Hydrogen storage in salt caverns Chemical modelling and analysis of large-scale hydrogen storage in underground salt caverns*. http://repository.tudelft.nl/.

le Duigou, A., Bader, A. G., Lanoix, J. C., & Nadau, L. (2017). Relevance and costs of large scale underground hydrogen storage in France. *International Journal of Hydrogen Energy*, *42*(36), 22987–23003. https://doi.org/10.1016/j.ijhydene.2017.06.239

Li, X., Ma, X., Zhang, J., Akiyama, E., Wang, Y., & Song, X. (2020). Review of Hydrogen Embrittlement in Metals: Hydrogen Diffusion, Hydrogen Characterization, Hydrogen Embrittlement Mechanism and Prevention. In *Acta Metallurgica Sinica (English Letters)* (Vol. 33, Issue 6, pp. 759–773). Chinese Society for Metals. https://doi.org/10.1007/s40195-020-01039-7

Londe, L. F. (2021). Four Ways to Store Large Quantities of Hydrogen. *Abu Dhabi International Petroleum Exhibition & Conference*.

http://onepetro.org/SPEADIP/proceedings-pdf/21ADIP/2-21ADIP/D022S189R001/2536636/spe-208178-ms.pdf/1

Lord, A. S., Kobos, P. H., Klise, G. T., & Borns, D. J. (2011). *A Life Cycle Cost Analysis Framework for Geologic Storage of Hydrogen: A User's Tool*. http://www.ntis.gov/help/ordermethods.asp?loc=7-4-0#online

Luna, M. J. L. (2019). *Hydrogen as a Potential Renewable and Secure Source for Energy Supply* [MSc, TU Wien]. https://doi.org/10.13140/RG.2.2.26607.38563

Mandal, K. (2021). Refinery/Petrochemicals. In *Petroleum Engineers Association (PEA)*. Petroleum Engineers Association.

Martino, M., Ruocco, C., Meloni, E., Pullumbi, P., & Palma, V. (2021). Main hydrogen production processes: An overview. In *Catalysts* (Vol. 11, Issue 5). MDPI AG. https://doi.org/10.3390/catal11050547

Masson-Delmotte, V., P. Zhai, A., Pirani, S. L., Connors, C., Péan, S., Berger, N., Caud, Y., Chen, L., Goldfarb, M. I., Gomis, M., Huang, K., Leitzell, E., Lonnoy, J. B. R., Matthews, T. K., Maycock, T., T. Waterfield, O., Yelekçi, R., Yu, R., Zhou, B., & (eds.). (2021). *IPCC, 2021: Summary for Policymakers. In: Climate Change 2021: The Physical Science Basis. Contribution of Working Group I to the Sixth Assessment Report of the Intergovernmental Panel on Climate Change*.

Mathworks. (2022). *Mathworks*. https://www.mathworks.com/company.html

Matos, C. R., Carneiro, J. F., & Silva, P. P. (2019). Overview of Large-Scale Underground Energy Storage Technologies for Integration of Renewable Energies and Criteria for Reservoir Identification. In *Journal of Energy Storage* (Vol. 21, pp. 241–258). Elsevier Ltd. https://doi.org/10.1016/j.est.2018.11.023

Mccain, W. D. (1991). *Reservoir·Fluid Property Correlations-State of the Art*.

Mcdonald, Z. L. (2018). *Hydrogen Energy Storage for Renewable-Intensive Electricity Grids: A WECC Case Study* [MSc.]. University of California Davis.

Melaina, M. W., Antonia, O., & Penev, M. (2013). *Blending Hydrogen into Natural Gas Pipeline Networks: A Review of Key Issues*. http://www.osti.gov/bridge

Minke, C., Suermann, M., Bensmann, B., & Hanke-Rauschenbach, R. (2021). Is iridium demand a potential bottleneck in the realization of large-scale PEM water electrolysis? *International Journal of Hydrogen Energy*, *46*(46), 23581–23590. https://doi.org/10.1016/j.ijhydene.2021.04.174

Møller, K. T., Jensen, T. R., Akiba, E., & Li, H. wen. (2017). Hydrogen - A sustainable energy carrier. *Progress in Natural Science: Materials International*, *27*(1), 34–40. https://doi.org/10.1016/j.pnsc.2016.12.014

Mondial L, C. de. (2016). *WORLD ENERGY COUNCIL World Energy Resources*. www.worldenergy.org'

Mouli-Castillo, J., Bartlett, S., Murugan, A., Badham, P., Wrynne, A., Haszeldine, S., Wheeldon, M., & McIntosh, A. (2020). Olfactory appraisal of odorants for 100% hydrogen networks. *International Journal of Hydrogen Energy*, *45*(20), 11875–11884. https://doi.org/10.1016/j.ijhydene.2020.02.095

Mouli-Castillo, J., Heinemann, N., & Edlmann, K. (2021). Mapping geological hydrogen storage capacity and regional heating demands: An applied UK case study. *Applied Energy*, *283*. https://doi.org/10.1016/j.apenergy.2020.116348

Muhammed, N. S., Haq, B., al Shehri, D., Al-Ahmed, A., Rahman, M. M., & Zaman, E. (2022). A review on underground hydrogen storage: Insight into geological sites, influencing factors and future outlook. In *Energy Reports* (Vol. 8, pp. 461–499). Elsevier Ltd. https://doi.org/10.1016/j.egyr.2021.12.002

Nasr, A. K., Kashan, M. K., Maleki, A., Jafari, N., & Hashemi, H. (2020). Assessment of barriers to renewable energy development using stakeholders approach. *Entrepreneurship and Sustainability Issues*, *7*(3), 2526–2541. https://doi.org/10.9770/jesi.2020.7.3(71)

Nasrifar, K. (2010). Comparative study of eleven equations of state in predicting the thermodynamic properties of hydrogen. *International Journal of Hydrogen Energy*, *35*(8), 3802–3811. https://doi.org/10.1016/j.ijhydene.2010.01.032

NIST Chemistry WebBook, S. (2022). *Thermophysical Properties of Fluid Systems*. https://webbook.nist.gov/chemistry/fluid/

Oldenburg, C. M. (2003). Carbon dioxide as cushion gas for natural gas storage. *Energy and Fuels*, *17*(1), 240–246. https://doi.org/10.1021/ef020162b

Oxford Learner's Dictionaries. (n.d.). *Hydrogen* . Retrieved February 11, 2022, from https://www.oxfordlearnersdictionaries.com/definition/english/hydrogen

Özkiliç, Ö. İ. (2005). *Simulating CO2 Sequestration in a Depleted Gas Reservoir* [MSc. Thesis]. Middle East Technical University.

Öztürk, B. (2004). *Simulation of Depleted Gas Reservoir for Underground Gas Storage* [MSc. Thesis]. Middle East Technical University.

Passaris, E. (2022). Experience with Salt Caverns. In *1st International Summer School on UHS*. TU Delft. https://www.tudelft.nl/citg/UHS-SummerSchool

Pellow, M. A., Emmott, C. J. M., Barnhart, C. J., & Benson, S. M. (2015). Hydrogen or batteries for grid storage? A net energy analysis. *Energy and Environmental Science*, *8*(7), 1938–1952. https://doi.org/10.1039/c4ee04041d

Perez, A. (2022). Implementing UHS in Porous Rocks. In *1st International Summer School on UHS*. TU Delft. https://www.tudelft.nl/citg/UHS-SummerSchool

Pérez, A., Pérez, E., Dupraz, S., & Bolcich, J. (2016). *Patagonia Wind-Hydrogen Project: Underground Storage and Methanation*.

Peters, C. (2022). Geo-chemistry of UHS. In *1st International Summer School on UHS*. TU Delft. https://www.tudelft.nl/citg/UHS-SummerSchool

Pichler, M. (2013). *Assesment of Hydrogen-Rock Interactions During Geological Storage of CH4-H2 Mixtures* [MSc.]. Montanuniversität Leoben.

Pichler, M. (2022). *Underground Hydrogen Storage*. Mission Hydrogen GmbH.

Pivovar, B. (2021). *Hydrogen Shot Summit: Current Status of (Low Temperature) Electrolyzer Technology and Needs for Successful Widespread Commercialization and Meeting Hydrogen Shot Targets*. U.S. Department of Energy. https://www.energy.gov/sites/default/files/2021-09/h2-shot-summit-panel1-lte-status.pdf

Poljak, J. (2022). *Levelised Cost of Green Hydrogen*. Mission Hydrogen GmbH. mission-hydrogen.de

Quintino, F. M., Nascimento, N., & Fernandes, E. C. (2021). Aspects of Hydrogen and Biomethane Introduction in Natural Gas Infrastructure and Equipment. *Hydrogen*, *2*(3), 301–318. https://doi.org/10.3390/hydrogen2030016

RAG, A. AG., AXIOM, angewandte P. G., Verbund, A., MONTANUNIVERSITÄT LEOBEN, UNIVERSITÄT für Bodenkultur Wien, & ENERGIEINSTITUT an der Johannes Kepler Universität Linz. (2017). *Underground Sun Storage Publishable Final Report*. www.underground-sun-storage.at

Reitenbach, V., Ganzer, L., Albrecht, D., & Hagemann, B. (2015). Influence of added hydrogen on underground gas storage: a review of key issues. *Environmental Earth Sciences*, *73*(11), 6927–6937. https://doi.org/10.1007/s12665-015-4176-2

Riaz, A., & Cinar, Y. (2014). Carbon dioxide sequestration in saline formations: Part I-Review of the modeling of solubility trapping. In *Journal of Petroleum Science and Engineering* (Vol. 124, pp. 367–380). Elsevier. https://doi.org/10.1016/j.petrol.2014.07.024

RISC. (2021). *Hydrogen storage potential of depleted oil and gas fields in Western Australia : literature review and scoping study*. Geological Survey of Western Australia.

Rivard, E., Trudeau, M., & Zaghib, K. (2019). Hydrogen storage for mobility: A review. In *Materials* (Vol. 12, Issue 12). MDPI AG. https://doi.org/10.3390/ma12121973

Royal Society of Chemistry. (n.d.). *Periodic Table - Hydrogen*. Retrieved October 10, 2021, from https://www.rsc.org/periodic-table/element/1/hydrogen

Sabine Hossenfelder. (2022). *Renewable Energy Storage: No Wind, No Sun, Now What?* https://www.youtube.com/watch?v=Q8xsg9iK5yo&ab_channel=SabineHossenfelder

Sahin, S., Abravci, S., & Tirek, A. (2012). Design and Status of the only Underground Gas Storage Project in Turkey after Three Years of Operation. *SPE Russian Oil & Gas Exploration & Production Technical Conference and Exhibition*, 16–18. http://onepetro.org/SPERPTC/proceedings-pdf/12ROGC/All-12ROGC/SPE-158074-MS/1645656/spe-158074-ms.pdf/1

Samura, L., Ginting, M., & Fattahanisa, A. (2021). The Application of P/Z Methods in Evaluation of Initial Gas in Place of X Reservoir. *Jurnal Petro*. http://trijurnal.lemlit.trisakti.ac.id/index.php/petro

Sarah Gasda. (2022). From CCS/UGS to UHS. In *1st International Summer School on UHS*. TU Delft. https://www.tudelft.nl/citg/over-faculteit/afdelingen/geoscience-engineering/research/subsurface/1st-international-summer-school-on-underground-hydrogen-storage

Schmidt, O., Gambhir, A., Staffell, I., Hawkes, A., Nelson, J., & Few, S. (2017). Future cost and performance of water electrolysis: An expert elicitation study. *International Journal of Hydrogen Energy*, *42*(52), 30470–30492. https://doi.org/10.1016/j.ijhydene.2017.10.045

Scott, R. (2004). *The History of the International Energy Agency - The First 20 Years: Origins and Structure Volume 1*. OECD Publishing.

Sheffield, J. W. (2007). Energy Security Through Hydrogen. *Proceedings of the NATO Advanced Study Institute on Assessment of Hydrogen Energy for Sustainable Development: Energy & Environment Security*, 1–8. http://www.nato.int/science

Shrivastava, V. K. (2003). *Physical Dispersion in Compositional Reservoir Simulation* [Doctoral Thesis, University of Calgary]. http://archives.ucalgary.ca

Shukla, P. R., Skea, J., Slade, R., al Khourdajie, A., van Diemen, R., McCollum, D., Pathak, M., Some, S., Vyas, P., Fradera, R., Belkacemi, M., Hasija, A., Lisboa, G., Luz, S., Malley, J., & (eds.). (2022). *IPCC, 2022: Summary for Policymakers. In: Climate Change 2022: Mitigation of Climate Change. Contribution of Working Group III to the Sixth Assessment Report of the Intergovernmental Panel on Climate Change*. https://doi.org/doi: 10.1017/9781009157926.001

Song, S., Lin, H., Sherman, P., Yang, X., Nielsen, C. P., Chen, X., & McElroy, M. B. (2021). Production of hydrogen from offshore wind in China and cost-competitive supply to Japan. *Nature Communications*, *12*(1). https://doi.org/10.1038/s41467-021-27214-7

Strobel, G., Hagemann, B., Huppertz, T. M., & Ganzer, L. (2020). Underground bio-methanation: Concept and potential. In *Renewable and Sustainable Energy Reviews* (Vol. 123). Elsevier Ltd. https://doi.org/10.1016/j.rser.2020.109747

Subramani, V., Basile, A., & Veziroğlu, N. T. (2012). *Compendium of Hydrogen Energy Volume 1: Hydrogen Production and Purification*. Woodhead Pub.

Taibi, E., Blanco, H., Miranda, R., & Carmo, M. (2020). *Green Hydrogen Cost Reduction: Scaling up Electrolysers to Meet the 1.5 ^{0}C Climate Goal* (J.

Gorvett, Ed.). International Renewable Energy Agency. www.irena.org/publications

Taibi, E., Miranda, R., Vanhoudt, W., Winkel, T., Lanoix, J.-C., & Barth, F. (2018). *Hydrogen from renewable power: Technology outlook for the energy transition*. IRENA. www.irena.org

Tarkowski, R., & Uliasz-Misiak, B. (2022). Towards underground hydrogen storage: A review of barriers. *Renewable and Sustainable Energy Reviews*, *162*, 112451. https://doi.org/10.1016/j.rser.2022.112451

Terstappen, R. J. (2021). *Analysis of Mixing During Hydrogen Storage in Gas Reservoirs* [MSc., TU Delft]. http://repository.tudelft.nl/.

Terwel, R., & Kerkhoven, J. (2019). *HyChain 2 Cost implications of importing renewable electricity, hydrogen and hydrogen carriers into the Netherlands from a 2050 perspective: Model User Guide, Technical Documentation, First Results and Country Profiles* (Vol. 37). www.ispt.eu/projects/hychain.

Thaysen, E. M., McMahon, S., Strobel, G. J., Butler, I. B., Ngwenya, B. T., Heinemann, N., Wilkinson, M., Hassanpouryouzband, A., McDermott, C. I., & Edlmann, K. (2021). Estimating microbial growth and hydrogen consumption in hydrogen storage in porous media. In *Renewable and Sustainable Energy Reviews* (Vol. 151). Elsevier Ltd. https://doi.org/10.1016/j.rser.2021.111481

The Engineering Toolbox. (n.d.). *Critical Temperatures and Pressures for some Common Substances*. Retrieved July 28, 2022, from https://www.engineeringtoolbox.com/gas-critical-temperature-pressure-d_161.html

Thiyagarajan, S. R., Emadi, H., Hussain, A., Patange, P., & Watson, M. (2022). A comprehensive review of the mechanisms and efficiency of underground hydrogen storage. In *Journal of Energy Storage* (Vol. 51). Elsevier Ltd. https://doi.org/10.1016/j.est.2022.104490

Tong, D., Farnham, D. J., Duan, L., Zhang, Q., Lewis, N. S., Caldeira, K., & Davis, S. J. (2021). Geophysical constraints on the reliability of solar and wind power worldwide. *Nature Communications*, *12*(1). https://doi.org/10.1038/s41467-021-26355-z

TPAO. (2022). *Deniz*. https://www.tpao.gov.tr/deniz

Treese, S. A., Pujadó, P. R., & Jones, D. S. J. (2015). *Handbook of Petroleum Processing* (2nd ed.). Springer International Publishing. https://doi.org/10.1007/978-3-319-14529-7_12

Turkiewicz, A., Brzeszcz, J., & Kapusta, P. (2013). The application of biocides in the oil and gas industry. *NAFTA-GAZ*.

UKCDR. (2021). *Hydrogen Production Costs 2021*.

UN. (2016). *The 2030 Agenda for Sustainable Development*.

UNDRR. (2015). *Sendai Framework for Disaster Risk Reduction 2015 - 2030*.

UNECE Task Force on Hydrogen. (2022). Technology Brief: Hydrogen. In *UNECE webinar: How to jumpstart hydrogen production and export potential of CIS countries?*

USDOE. (2022). Hydrogen Storage. In *US Department of Energy Hydrogen and Fuel Cell Technologies Office*. https://www.energy.gov/eere/fuelcells/hydrogen-storage

van Gessel, S., Jaarsma, B., Gronenenberg, R., Kleijweg, D., Judge-Larre, J., van Klaveren, S., Eikelenboom, W., Remmelts, G., van Slooten, R., Butter, E., Huijskes, T., & Koning, M. (2022). *Haalbaarheidsstudie: Offshore Ondergrondse Waterstofopslag*. www.ebn.nl

Viktorsson, L., Heinonen, J. T., Skulason, J. B., & Unnthorsson, R. (2017). A step towards the hydrogen economy - A life cycle cost analysis of a hydrogen refueling station. *Energies*, *10*(6). https://doi.org/10.3390/en10060763

Visser, T. M. R. B. (2020). *Seasonal Hydrogen Storage in Depleted Gas Reservoirs A Feasibility Study for The Netherlands*. http://repository.tudelft.nl/.Acknowledgement

Wallace, R. L., Cai, Z., Zhang, H., Zhang, K., & Guo, C. (2021). Utility-scale subsurface hydrogen storage: UK perspectives and technology. In *International Journal of Hydrogen Energy* (Vol. 46, Issue 49, pp. 25137–25159). Elsevier Ltd. https://doi.org/10.1016/j.ijhydene.2021.05.034

Wanner, M. (2021). Transformation of electrical energy into hydrogen and its storage. *European Physical Journal Plus*, *136*(5). https://doi.org/10.1140/epjp/s13360-021-01585-8

Warren, J. K. (2017). Salt usually seals, but sometimes leaks: Implications for mine and cavern stabilities in the short and long term. In *Earth-Science Reviews* (Vol. 165, pp. 302–341). Elsevier B.V. https://doi.org/10.1016/j.earscirev.2016.11.008

WEF. (2022). *The Global Risks Report 2022 17th Edition*. World Economic Forum.

Wu, X., Zhang, H., Yang, M., Jia, W., Qiu, Y., & Lan, L. (2022). From the perspective of new technology of blending hydrogen into natural gas pipelines transmission: Mechanism, experimental study, and suggestions for further work of hydrogen embrittlement in high-strength pipeline steels. In *International Journal of Hydrogen Energy*. Elsevier Ltd. https://doi.org/10.1016/j.ijhydene.2021.12.108

Yang, C., Jing, W., Daemen, J. J. K., Zhang, G., & Du, C. (2013). Analysis of major risks associated with hydrocarbon storage caverns in bedded salt rock. *Reliability Engineering and System Safety*, *113*(1), 94–111. https://doi.org/10.1016/j.ress.2012.12.017

Yildirim, D., Volkan, V. v., Yilmaz, M., & Akin, S. (2009). Performance Prediction for Kuzey Marmara Gas Storage Field by Using a Compositional Simulator. *IPETGAS*.

Zamehrian, M., & Sedaee, B. (2022). Underground hydrogen storage in a partially depleted gas condensate reservoir: Influence of cushion gas. *Journal of Petroleum Science and Engineering*, *212*. https://doi.org/10.1016/j.petrol.2022.110304

Zauner, A., Fazeni-Fraisl, K., Wolf-Zoellner, P., Veseli, A., Holzleitner, M. T., Lehner, M., Bauer, S., & Pichler, M. (2022). Multidisciplinary Assessment of a Novel Carbon Capture and Utilization Concept including Underground Sun Conversion. *Energies*, *15*(3). https://doi.org/10.3390/en15031021

Zgonnik, V. (2020). The occurrence and geoscience of natural hydrogen: A comprehensive review. In *Earth-Science Reviews* (Vol. 203). Elsevier B.V. https://doi.org/10.1016/j.earscirev.2020.103140

Zhao, G., Nielsen, E. R., Troncoso, E., Hyde, K., Romeo, J. S., & Diderich, M. (2019). Life cycle cost analysis: A case study of hydrogen energy application on the Orkney Islands. *International Journal of Hydrogen Energy*, 9517–9528. https://doi.org/10.1016/j.ijhydene.2018.08.015

Zivar, D., Kumar, S., & Foroozesh, J. (2021). Underground hydrogen storage: A comprehensive review. *International Journal of Hydrogen Energy*, *46*(45), 23436–23462. https://doi.org/10.1016/j.ijhydene.2020.08.138

Zoback, M. (2022). Geomechanics of UHS. In *1st International Summer School on UHS*. TU Delft. https://www.tudelft.nl/citg/UHS-SummerSchool

APPENDICES

A. Golden Software – Surfer

Golden Software is a US based company that provide computer applications for fields that require geographical input. In order to define grid top at the Builder, contour maps needed to be created. For this purpose, trial version of the Surfer software was used. The map was digitized by drawing the contours by hand and georeferencing based on the well locations data from Kaptanoglu et al. (1998). Reformatting of the resulting .bna file was necessary before it could be used by the Builder, which was done using the guide at the Golden Software's website (Golden Software, n.d., 2020, 2022).

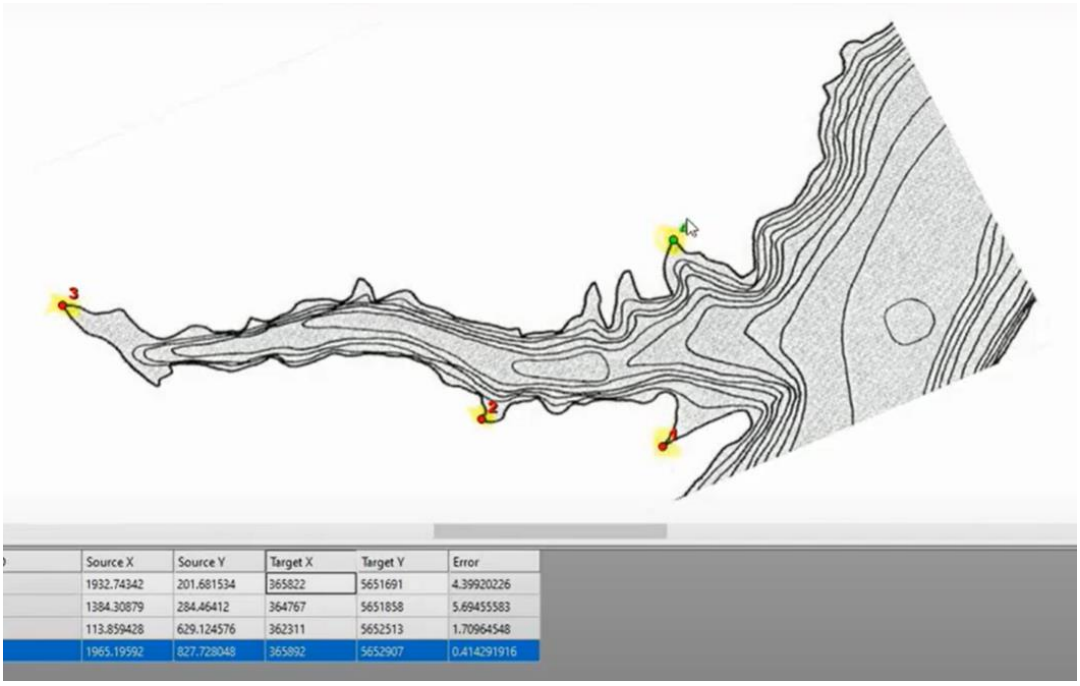

Figure 8.1. Georeference example for Surfer (Golden Software, 2020)

B. Mathworks – MATLAB Grabit

Mathworks is a company which was founded in 1984 with the purpose of supplying engineers and scientists with computational software. Their best known products are MATLAB and SIMULINK. Grabit is a program with graphic user interface that enables extracting data points from images (Doke, 2022; Mathworks, 2022).

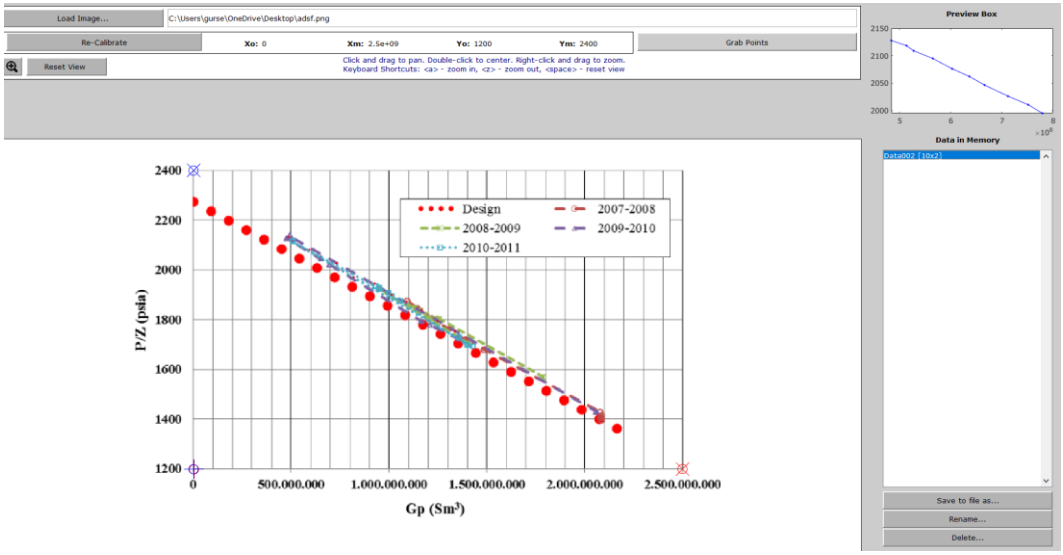

Figure 8.2. Screenshot from Grabit of the extraction from Şahin et al. (2012)

C. Computer Modelling Group – Builder, WinProp, GEM, CMOST

Computer Modelling Group (CMG) is a Canada based company founded in 1978. It provides R&D based reservoir simulation tools with full-functionality and customer support with response time less than 24 hours (CMG, n.d.).

The reservoir simulation tools can be accessed via “Launcher” which is the project management tool that enables user to create projects through different software to run in the desired order. These jobs can either be submitted to cloud servers (Microsoft HPC/IBM Platform LSF) or can be run using the local machines (Computer Modelling Group, n.d.-d).

Simulations work based on .dat format files which can be created by the Builder pre-processor reservoir modelling tool. Builder is a Windows based tool which can create the model for the grid, wells, production/injection and rock-fluid interactions. Builder also enables the user to adjust the numerical settings and outputs which will later on be used by the reservoir simulator (Computer Modelling Group, n.d.-a).

Three reservoir simulators offered by CMG are the IMEX (Black Oil and Unconventional), GEM (Compositional and Unconventional) and STARS (Thermal and Advanced Processes). Since the project was about hydrogen storage IMEX couldn not have been used. The main difference between GEM and STARS is that GEM is based on EOS while STARS uses K-value based PVT. STARS is able to simulate pretty much everything that GEM can, yet at the same time it requires more descriptive inputs. For a more advanced simulation, involving reactions dependent on other parameters like microbial growth or reactions in the gaseous phase, STARS might be used since GEM might be unable to capture some of those reactions (Faraj Zarei, 2021). Even though the reservoir in this study was prone to such reactions, they were left outside the scope for the time being, and therefore, GEM simulator was used.

For solving the equations in each grid block, GEM uses variations of adaptive implicit method which was first introduced by Thomas and Thurnau (1983) and later on developed by the CMG scientists. The adaptive implicit method enables only a small number of blocks to be solved implicitly while the others are solved explicitly. Also by decoupling the thermodynamic phase equilibrium equations and then solving them seperately for every Newtonian iteration, the decoupled flash calculation approach lowers the calculational complexity. In comparison with fully implicit methods and explicit-transmissability methods, adaptive implicit method was shown to be far more efficient by lowering the execution time greatly (Computer Modelling Group, n.d.-c; Thomas & Thurnau, 1983).

CMOST AI is the CMG application that enables user to perform sensitivity analysis, history matching, optimization and uncertainty assessment operations. For history matching, after the data to be matched is converted into .fhf format, it is imported to CMOST. The parameters subject to change are defined through cEDIT which is the user friendly tool for viewing and editing .dat files. Following that, the range and probability distribution for parameters are entered. Objective functions of interest are chosen and history matching values are selected by the drop down menu. The by changing the values for the chosen parameters depending on the optimizers' preference, CMOST tries to minimize the error between the data and the simulation (Computer Modelling Group, n.d.-b).

CMG Designed Exploration and Controlled Evolution (DECE) was chosen to be used as the optimizer in this study since it has demonstrated its success in real-world applications. CMG DECE uses an approach similar to a reservoir engineer by changing the parameters in the given range in a manner that would give the most information about the change in the objective function. By evaluating the results it then rejects some values for the parameters, iteratively trying to minimize the error. The rejected parameter values are reconsidered from time to time when the results show their effect could have been misjudged (Computer Modelling Group Ltd., 2017).

D. Field History Files (.fhf)

The files are available at https://github.com/3hasangursel/NMH2

Field Cumulative Productions and Bottom Hole Pressure

2022-01-01
'Field Data'
1997 09 01
'YYYY/MM/DD'
3
'Bottom Hole Pressure' 'Cumulative Water SC' 'Cumulative Gas SC'
'kPa' 'bbl' 'MSCF'
1
'FIELD' *SECTOR

1997/09/01	13375.51829	0	16564
1997/10/01	13371.33122	0	441988
1997/11/01	13262.06517	38	1022492
1997/12/01	13222.85566	199	1793724
1998/01/01	13152.98583	353	2582745
1998/02/01	13089.69129	433	3204030
1998/03/01	13037.34873	485	3825728
1998/04/01	12977.87687	526	4414295
1998/05/01	12934.27315	548	4996599
1998/06/01	12890.68985	922	6107228
1998/07/01	12797.62075	1354	7335650
1998/08/01	12709.81352	1781	8546879
1998/09/01	12605.51999	2179	9685019
1998/10/01	12530.60597	2605	10881525
1998/11/01	12415.05378	3138	12260273
1998/12/01	12322.60277	3820	13863407
1999/01/01	12178.15289	4490	15397163

1999/02/01	12065.66783	5110	16806263
1999/03/01	11946.63859	5784	18352047
1999/04/01	11836.80493	6416	19802247
1999/05/01	11708.65343	7070	21302645
1999/06/01	11571.2697	7694	22707735
1999/07/01	11470.57051	8342	24178876
1999/08/01	11369.89576	8883	25410258
1999/09/01	11221.08171	9519	26830608
1999/10/01	11166.2382	10181	28299016
1999/11/01	10992.24325	10599	29722276
1999/12/01	10946.54642	11282	31201410
2000/01/01	10781.72261	11971	32721774
2000/02/01	10644.41219	12638	34176298
2000/03/01	10589.4587	13346	35695980
2000/04/01	10442.97716	13985	37110690
2000/05/01	10333.10683	14593	38388810
2000/06/01	10241.59099	15167	39663622
2000/07/01	10122.62285	15810	41074897
2000/08/01	9976.116863	16442	42475074
2000/09/01	9902.918857	17001	43698963
2000/10/01	9811.403019	17406	44570350
2000/11/01	9683.214864	17836	45449334
2000/12/01	9665.019225	18257	46387084
2001/01/01	9527.757688	18617	47100293
2001/02/01	9482.219713	18942	47700136
2001/03/01	9436.474014	19205	48260896
2001/04/01	9390.838286	19487	48848034
2001/05/01	9354.263721	19733	49361073
2001/06/01	9308.640212	19900	49768038
2001/07/01	9262.992265	20137	50256737

2001/08/01 9244.833283 20425 50778975

2001/09/01 9199.221994 20700 51329113

2001/10/01 9123.777025 20998 51915651

2001/11/01 9096.42247 21289 52517932

2001/12/01 9050.786743 21559 53127939

2002/01/01 9023.468845 21712 53485330

Average Reservoir Pressure

2022-01-01

"

1997 09 01

'YYYY/MM/DD'

1

'Ave reservoir pres'

'kPa'

1

'PAVG' *SPECIAL 1998/11/01 13859 2000/02/01 12626

1997/09/01 13669 1998/12/01 13872 2000/03/01 12346

1997/10/01 13873 1999/01/01 13821 2000/04/01 12486

1997/11/01 13796 1999/02/01 13719 2000/05/01 12219

1997/12/01 13784 1999/03/01 13655 2000/06/01 12219

1998/01/01 13796 1999/04/01 13592 2000/07/01 12219

1998/02/01 13860 1999/05/01 13516 2000/08/01 12143

1998/03/01 13860 1999/06/01 13439 2000/09/01 11800

1998/04/01 13859 1999/07/01 13388 2000/10/01 11533

1998/05/01 13859 1999/08/01 13388 2000/11/01 11520

1998/06/01 13936 1999/09/01 13109 2000/12/01 11317

1998/07/01 13859 1999/10/01 13122 2001/01/01 11164

1998/08/01 13834 1999/11/01 12969 2001/02/01 11037

1998/09/01 13872 1999/12/01 12880 2001/03/01 11723

1998/10/01 13872 2000/01/01 12626 2001/04/01 11253

2001/05/01	11177	2001/08/01	10961	2001/11/01	10910
2001/06/01	11317	2001/09/01	10999	2001/12/01	10618
2001/07/01	11101	2001/10/01	11024	2002/01/01	10554

Wellhead Pressures between 1997-2002

20022-01-01

'NM Wells Wellhead Pressure'

1997 09 01

'YYYY/MM/DD'

1

'Well Head Pressure'

'kPa'

5

'NM1_Producer'

1997/09/01	1998/05/01	1999/01/01
11858.98254	11652.13982	10204.24079
1997/10/01	1998/06/01	1999/02/01
11652.13982	11238.45438	9928.450498
1997/11/01	1998/07/01	1999/03/01
11858.98254	11100.55924	9928.450498
1997/12/01	1998/08/01	1999/04/01
11790.03497	11307.40196	9928.450498
1998/01/01	1998/09/01	1999/05/01
12272.66798	10480.03108	9859.502925
1998/02/01	1998/10/01	1999/06/01
11790.03497	10480.03108	9790.555352
1998/03/01	1998/11/01	1999/07/01
11583.19225	10204.24079	9583.712633
1998/04/01	1998/12/01	1999/08/01
11583.19225	10066.34564	9790.555352

1999/09/01 9514.76506
1999/10/01 9445.817487
1999/11/01 9238.974769
1999/12/01 9101.079623
2000/01/01 8549.49904
2000/02/01 8618.446613
2000/03/01 8273.708748
2000/04/01 8756.341758
2000/05/01 8825.289331
2000/06/01 8894.236904
2000/07/01 8756.341758
2000/08/01 8618.446613
2000/09/01 8618.446613
2000/10/01 9032.13205
2000/11/01 9032.13205
2000/12/01 8963.184477
2001/01/01 8928.710691
2001/02/01 8308.182534
2001/03/01 8480.551467
2001/04/01 8549.49904
2001/05/01 8618.446613
2001/06/01 8825.289331
2001/07/01 8894.236904
2001/08/01 8963.184477
2001/09/01 8859.763118
2001/10/01 8963.184477
2001/11/01 8721.867972
2001/12/01 8859.763118
2002/01/01 8894.236904
'NM3_Producer'
1997/09/01 0
1997/10/01 10686.8738
1997/11/01 10755.82137
1997/12/01 10755.82137
1998/01/01 10893.71652
1998/02/01 10879.927
1998/03/01 10300.76739
1998/04/01 10824.76895
1998/05/01 10893.71652
1998/06/01 10686.8738
1998/07/01 10480.03108
1998/08/01 10617.92623
1998/09/01 9997.398071
1998/10/01 9790.555352
1998/11/01 9721.607779
1998/12/01 9652.660206

1999/01/01
9790.555352
1999/02/01
9514.76506
1999/03/01
9583.712633
1999/04/01
9583.712633
1999/05/01
9514.76506
1999/06/01
9445.817487
1999/07/01
9307.922342
1999/08/01
9445.817487
1999/09/01
9170.027196
1999/10/01
9101.079623
1999/11/01
8963.184477
1999/12/01
8963.184477
2000/01/01
8687.394185
2000/02/01
8273.708748
2000/03/01
8273.708748
2000/04/01
8480.551467
2000/05/01
8549.49904
2000/06/01
8618.446613
2000/07/01
8342.656321
2000/08/01
8273.708748
2000/09/01
8342.656321
2000/10/01
8825.289331
2000/11/01
8825.289331
2000/12/01
8756.341758
2001/01/01
8859.763118
2001/02/01
8721.867972
2001/03/01
8687.394185
2001/04/01
8411.603894
2001/05/01
8101.339816
2001/06/01
8618.446613
2001/07/01
8549.49904
2001/08/01
8618.446613
2001/09/01
8618.446613
2001/10/01
8480.551467
2001/11/01
8411.603894
2001/12/01
8411.603894
2002/01/01
8342.656321
'NM4_Producer'
1997/09/01
11721.08739
1997/10/01
11514.24467
1997/11/01
11652.13982
1997/12/01
11721.08739
1998/01/01
11721.08739
1998/02/01
11445.2971
1998/03/01
11376.34953

1998/04/01 10824.76895
1998/05/01 11583.19225
1998/06/01 11307.40196
1998/07/01 11100.55924
1998/08/01 10411.08351
1998/09/01 10411.08351
1998/10/01 10342.13594
1998/11/01 10342.13594
1998/12/01 10204.24079
1999/01/01 10273.18836
1999/02/01 10066.34564
1999/03/01 9997.398071
1999/04/01 9997.398071
1999/05/01 9859.502925
1999/06/01 9790.555352
1999/07/01 9652.660206
1999/08/01 9790.555352
1999/09/01 9583.712633
1999/10/01 9445.817487
1999/11/01 9376.869914
1999/12/01 9238.974769
2000/01/01 8963.184477
2000/02/01 8756.341758
2000/03/01 8756.341758
2000/04/01 8825.289331
2000/05/01 8894.236904
2000/06/01 8825.289331
2000/07/01 8687.394185
2000/08/01 8549.49904
2000/09/01 8618.446613
2000/10/01 8894.236904
2000/11/01 8756.341758
2000/12/01 8756.341758
2001/01/01 8790.815545
2001/02/01 7928.970884
2001/03/01 7928.970884
2001/04/01 8549.49904
2001/05/01 8687.394185
2001/06/01 8756.341758
2001/07/01 8790.815545
2001/08/01 8687.394185
2001/09/01 0
2001/10/01 0
2001/11/01 8446.07768
2001/12/01 8273.708748
2002/01/01 8480.551467

'NM5_Producer'
1997/09/01 0
1997/10/01 0
1997/11/01 11996.87768
1997/12/01 11996.87768
1998/01/01 11652.13982
1998/02/01 11376.34953
1998/03/01 11238.45438
1998/04/01 11238.45438
1998/05/01 12548.45827
1998/06/01 11238.45438
1998/07/01 10480.03108
1998/08/01 10824.76895
1998/09/01 12272.66798
1998/10/01 10755.82137
1998/11/01 10411.08351
1998/12/01 9997.398071
1999/01/01 10066.34564
1999/02/01 9859.502925
1999/03/01 9859.502925
1999/04/01 9859.502925
1999/05/01 9790.555352
1999/06/01 9790.555352
1999/07/01 9583.712633
1999/08/01 9652.660206
1999/09/01 9445.817487
1999/10/01 9376.869914
1999/11/01 9238.974769
1999/12/01 9238.974769
2000/01/01 8894.236904
2000/02/01 8756.341758
2000/03/01 8687.394185
2000/04/01 8756.341758
2000/05/01 8825.289331
2000/06/01 8825.289331
2000/07/01 8687.394185
2000/08/01 8549.49904
2000/09/01 8549.49904
2000/10/01 8756.341758
2000/11/01 8480.551467
2000/12/01 8618.446613
2001/01/01 8687.394185
2001/02/01 8411.603894
2001/03/01 8342.656321
2001/04/01 8411.603894
2001/05/01 8756.341758

2001/06/01 8825.289331
2001/07/01 8411.603894
2001/08/01 0
2001/09/01 8721.867972
2001/10/01 8687.394185
2001/11/01 8273.708748
2001/12/01 0
2002/01/01 0
'NM6_Producer'
1997/09/01 0
1997/10/01 0
1997/11/01 12272.66798
1997/12/01 12272.66798
1998/01/01 12203.7204
1998/02/01 12134.77283
1998/03/01 11790.03497
1998/04/01 12548.45827
1998/05/01 12548.45827
1998/06/01 11376.34953
1998/07/01 11721.08739
1998/08/01 11583.19225
1998/09/01 11583.19225
1998/10/01 11514.24467
1998/11/01 10342.13594
1998/12/01 10342.13594
1999/01/01 10342.13594
1999/02/01 9997.398071
1999/03/01 9997.398071
1999/04/01 9997.398071
1999/05/01 9859.502925
1999/06/01 9859.502925
1999/07/01 9859.502925
1999/08/01 0
1999/09/01 9652.660206
1999/10/01 9445.817487
1999/11/01 9307.922342
1999/12/01 9238.974769
2000/01/01 8963.184477
2000/02/01 8756.341758
2000/03/01 8687.394185
2000/04/01 8825.289331
2000/05/01 8825.289331
2000/06/01 8894.236904
2000/07/01 8756.341758
2000/08/01 8549.49904
2000/09/01 8618.446613
2000/10/01 8756.341758
2000/11/01 8273.708748

2000/12/01 2001/05/01 2001/10/01
8549.49904 7963.44467 8963.184477
2001/01/01 2001/06/01 2001/11/01
8618.446613 8963.184477 8790.815545
2001/02/01 2001/07/01 2001/12/01
7308.442727 8963.184477 8756.341758
2001/03/01 2001/08/01 2002/01/01
9652.660206 8928.710691 8687.394185
2001/04/01 2001/09/01
8377.130107 8963.184477

Cumulative Productions for Wells between 1997-2002

20022-01-01 1
'NM Wells Production' 'Cumulative Gas SC'
1997 09 01 'MSCF'
'YYYY/MM/DD'
5
'NM1_Producer' 1998/06/01 1999/01/01
1997/09/01 8116 1790842 4060077
1997/10/01 165028 1998/07/01 1999/02/01
1997/11/01 340978 2097959 4382665
1997/12/01 533488 1998/08/01 1999/03/01
1998/01/01 723921 2344874 4736840
1998/02/01 894301 1998/09/01 1999/04/01
1998/03/01 2668904 5062610
1069453 1998/10/01 1999/05/01
1998/04/01 3006580 5404974
1289186 1998/11/01 1999/06/01
1998/05/01 3347170 5730144
1509472 1998/12/01 1999/07/01
3713652 6055494

1999/08/01 6370175
1999/09/01 6688535
1999/10/01 7015213
1999/11/01 7335523
1999/12/01 7673702
2000/01/01 8025862
2000/02/01 8363219
2000/03/01 8717456
2000/04/01 9043856
2000/05/01 9339416
2000/06/01 9628106
2000/07/01 9947127
2000/08/01 10264381
2000/09/01 10533820
2000/10/01 10758446
2000/11/01 10982576
2000/12/01 11188292
2001/01/01 11375462
2001/02/01 11553962
2001/03/01 11735906
2001/04/01 11866636
2001/05/01 11974588
2001/06/01 12096577
2001/07/01 12187243
2001/08/01 12341809
2001/09/01 12522559
2001/10/01 12703227
2001/11/01 12874707
2001/12/01 12987743
2002/01/01 13050095

'NM3_Producer'

1997/09/01 0
1997/10/01 10584
1997/11/01 23511
1997/12/01 374579
1998/01/01 502454
1998/02/01 535070
1998/03/01 584300
1998/04/01 707000
1998/05/01 829233
1998/06/01 974613
1998/07/01 1125552
1998/08/01 1269423
1998/09/01 1433013
1998/10/01 1599357
1998/11/01 1776837
1998/12/01 1971424
1999/01/01 2159315
1999/02/01 2328687
1999/03/01 2515431

1999/04/01 2686791
1999/05/01 2862716
1999/06/01 3028646
1999/07/01 3198061
1999/08/01 3362485
1999/09/01 3524185
1999/10/01 3696173
1999/11/01 3854663
1999/12/01 4015305
2000/01/01 4174025
2000/02/01 4321896
2000/03/01 4473982
2000/04/01 4613422
2000/05/01 4733602
2000/06/01 4860562
2000/07/01 4998233
2000/08/01 5135811
2000/09/01 5255494
2000/10/01 5306632
2000/11/01 5375862
2000/12/01 5462042
2001/01/01 5514735
2001/02/01 5532480
2001/03/01 5625954
2001/04/01 5718684
2001/05/01 5768132
2001/06/01 5831405
2001/07/01 5870871
2001/08/01 5897579
2001/09/01 5975339
2001/10/01 6030971
2001/11/01 6068587
2001/12/01 6133170
2002/01/01 6173730
'NM4_Producer'
1997/09/01 8448
1997/10/01 17112
1997/11/01 39225
1997/12/01 640963
1998/01/01 857839
1998/02/01 1055074
1998/03/01 1224514
1998/04/01 1465534
1998/05/01 1705319
1998/06/01 2016629
1998/07/01 2353537
1998/08/01 2780345
1998/09/01 3172265

1998/10/01 3574335
1998/11/01 3930948
1998/12/01 4330166
1999/01/01 4696772
1999/02/01 5046408
1999/03/01 5422376
1999/04/01 5770286
1999/05/01 6135931
1999/06/01 6485881
1999/07/01 6851278
1999/08/01 7191565
1999/09/01 7537705
1999/10/01 7893058
1999/11/01 8239048
1999/12/01 8599051
2000/01/01 8971361
2000/02/01 9330004
2000/03/01 9699245
2000/04/01 10047755
2000/05/01 10366145
2000/06/01 10687325
2000/07/01 11039423
2000/08/01 11388824
2000/09/01 11688481
2000/10/01 11931211
2000/11/01 12055915
2000/12/01 12284726
2001/01/01 12446102
2001/02/01 12654466
2001/03/01 12810338
2001/04/01 13016830
2001/05/01 13232452
2001/06/01 13335124
2001/07/01 13399300
2001/08/01 13533742
2001/09/01 13533742
2001/10/01 13533742
2001/11/01 13653406
2001/12/01 13882992
2002/01/01 13986880
'NM5_Producer'
1997/09/01 0
1997/10/01 0
1997/11/01 23776
1997/12/01 103722
1998/01/01 206992
1998/02/01 304338
1998/03/01 407930
1998/04/01 413044
1998/05/01 413044

1998/06/01 553238
1998/07/01 737084
1998/08/01 865235
1998/09/01 865235
1998/10/01 889950
1998/11/01 1102229
1998/12/01 1321771
1999/01/01 1543886
1999/02/01 1738934
1999/03/01 1956554
1999/04/01 2151434
1999/05/01 2338455
1999/06/01 2490205
1999/07/01 2684544
1999/08/01 3096534
1999/09/01 3278214
1999/10/01 3465361
1999/11/01 3645601
1999/12/01 3832903
2000/01/01 4026250
2000/02/01 4210139
2000/03/01 4403176
2000/04/01 4584136
2000/05/01 4742836
2000/06/01 4896188
2000/07/01 5077104
2000/08/01 5257927
2000/09/01 5423347
2000/10/01 5538667
2000/11/01 5671267
2000/12/01 5787455
2001/01/01 5855615
2001/02/01 5885711
2001/03/01 6015181
2001/04/01 6050765
2001/05/01 6147017
2001/06/01 6191842
2001/07/01 6246572
2001/08/01 6246572
2001/09/01 6311400
2001/10/01 6421884
2001/11/01 6480605
2001/12/01 6480606
2002/01/01 6480607
'NM6_Producer'
1997/09/01 0
1997/10/01 0
1997/11/01 30378
1997/12/01 140972
1998/01/01 291539

1998/02/01 415247
1998/03/01 539531
1998/04/01 539531
1998/05/01 539531
1998/06/01 771906
1998/07/01 1021518
1998/08/01 1287002
1998/09/01 1545602
1998/10/01 1811303
1998/11/01 2103089
1998/12/01 2526394
1999/01/01 2937113
1999/02/01 3309569
1999/03/01 3720846
1999/04/01 4131126
1999/05/01 4560569
1999/06/01 4972859
1999/07/01 5389499
1999/08/01 5389499
1999/09/01 5801969
1999/10/01 6229211
1999/11/01 6647441
1999/12/01 7080449
2000/01/01 7524276
2000/02/01 7951040
2000/03/01 8402121
2000/04/01 8821521
2000/05/01 9206811
2000/06/01 9591441
2000/07/01 10013010
2000/08/01 10428131
2000/09/01 10797821
2000/10/01 11035394
2000/11/01 11363714
2000/12/01 11664569
2001/01/01 11908379
2001/02/01 12073517
2001/03/01 12073517
2001/04/01 12195119
2001/05/01 12238884
2001/06/01 12313090
2001/07/01 12552751
2001/08/01 12759273
2001/09/01 12986073
2001/10/01 13225827
2001/11/01 13440627
2001/12/01 13643429

2002/01/01 137940

E. Exemplary .dat file for GEM

**This is a base model other models are also available at
**https://github.com/3hasangursel/NMH2

**After the time steps (dates) are defined Field History files can be imported to history match

**A different fluid model can be defined and imported instead of the one used here

**Please note that the well trajectories used in this model are not necessarily the real locations

RESULTS SIMULATOR GEM 202021

SRFORMAT SR3

INUNIT SI

WSRF WELL 1

WSRF GRID TIME

OUTSRF GRID COMPRG COMPRT PRES SG SO SW YALL ZFACG

OUTSRF RES ALL

OUTSRF SPECIAL PAVG

OUTSRF *FLUX_SECTOR *ALL *RC *SUM *MASS *MOLE

WPRN GRID 0

OUTPRN GRID NONE

OUTPRN RES NONE

** Distance units: m

RESULTS XOFFSET -1815.1533

RESULTS YOFFSET 2540.7472

RESULTS ROTATION 0.0000 ** (DEGREES)

RESULTS AXES-DIRECTIONS 1.0 -1.0 1.0

**
****
****

** Definition of fundamental cartesian grid

**
****
****

GRID VARI 51 61 4

KDIR DOWN

DI IVAR

51*65

DJ JVAR

61*65

DK ALl

12444*8.5

DTOP

2*1200 1208.598 1207.855 1206.265 1204.76 1204.059 1203.212 1202.441

1201.776 1201.044 1200.211 1200.296 1200.693 1201.14 1202.2 1203.572

1205.002 1207.79 1210.68 1214.226 1216.544 1215.996 1215.291 1214.693

1213.943 1213.254 1212.63 1212.097 1211.752 1211.46 1211.364 1211.197

1211.204 1211.275 1211.273 1211.28 1211.3 1211.279 1211.114 1211.092

1211.058 1211.048 1211.105 1211.132 1211.153 1211.173 6*1200 1206.42

1205.556 1204.074 1202.635 1201.791 1200.785 1199.852 1197.717 1195.711

1194.033 1193.86 1194.621 1195.804 1198.08 1200.449 1201.703 1203.856

1206.272 1209.232 1211.994 1213.986 1213.363 1212.866 1212.193 1211.59

1211.056 1210.613 1210.358 1210.147 1210.128 1210.029 1210.097 1210.225

1210.274 1210.327 1210.39 1210.408 1210.277 1210.287 1210.284 1210.302

1210.387 1210.438 1210.483 1210.524 6*1200 1204.664 1203.661 1202.235

1200.823 1199.457 1195.99 1193.098 1190.708 1188.653 1187.397 1187.027

1187.76 1188.969 1191.099 1193.984 1197.184 1200.895 1203.072 1205.714
1208.38 1210.616 1211.435 1212.091 1211.438 1210.868 1210.373 1209.97
1209.758 1209.587 1209.607 1209.54 1209.64 1209.798 1209.872 1209.948
1210.031 1210.067 1209.949 1209.974 1209.983 1210.014 1210.111 1210.174
1210.229 1210.28 6*1200 1203.274 1202.126 1200.711 1197.14 1193.184
1189.803 1186.55 1183.927 1181.429 1180.614 1180.171 1180.894 1181.92
1183.901 1186.472 1190.059 1195.068 1200.427 1202.83 1205.446 1207.808
1209.06 1210.712 1211.048 1210.475 1209.989 1209.603 1209.417 1209.267
1209.314 1209.266 1209.388 1209.567 1209.657 1209.747 1209.844 1209.89
1209.778 1209.811 1209.828 1209.866 1209.972 1210.041 1210.103 1210.159
4*1200 1205.072 1203.441 1204.344 1201.777 1198.155 1192.377 1186.966
1183.49 1180.326 1177.357 1173.97 1172.898 1172.206 1173.259 1174.433
1176.447 1178.73 1182.11 1186.465 1192.486 1199.987 1203.629 1207.244
1210.224 1213.364 1216.917 1217.928 1219.076 1220.337 1221.705 1223.104
1224.531 15*1225 1214.902 1214.855 1214.917 1225 1205.234 1203.197
1202.729 1199.314 1193.106 1187.29 1181.833 1177.048 1173.201 1168.02
1164.015 1161.883 1160.905 1161.421 1162.752 1165.991 1169.187 1173.012
1176.594 1183.026 1190.277 1199.473 1204.221 1208.419 1212.549 1217.284
1220.608 1222.786 19*1225 1214.985 1214.935 1214.995 1225 1205.083
1202.656 1200.995 1194.667 1187.69 1181.846 1176.375 1168.687 1162.155
1156.385 1153.375 1151.049 1149.875 1149.871 1151.542 1154.984 1158.99
1163.384 1167.984 1173.247 1179.803 1189.313 1200.022 1205.23 1210.164
1215.654 1221.013 1224.125 19*1225 1215.051 1214.997 1215.055 1225
1204.506 1201.745 1197.774 1190.019 1182.675 1176.018 1166.598 1158.269
1151.479 1146.459 1147.959 1147.275 1146.723 1146.62 1147.196 1148.155
1149.796 1154.299 1159.882 1165.316 1171.085 1178.568 1190.242 1201.716
1207.594 1214.027 1220.379 20*1225 1215.063 1215.008 1215.067 1225

1203.539 1200.539 1192.922 1184.972 1177.461 1167.614 1155.873 1147.207
1142.236 1137.563 1145.096 1144.306 1143.605 1143.392 1143.904 1144.889
1146.44 1148.458 1152.086 1158.636 1164.91 1170.813 1178.984 1194.015
1203.955 1211.342 1218.705 1224.407 19*1225 1215.075 1215.017 1215.077
1225 1202.626 1197.681 1188.121 1179.551 1170.606 1159.792 1148.726
1141.901 1137.233 1133.005 1130.936 1141.422 1140.54 1140.208 1140.575
1141.582 1143.021 1145.1 1148.084 1152.864 1159.115 1165.411 1172.827
1185.434 1198.876 1206.442 1213.441 1220.028 1224.717 18*1225 1215.076
1215.017 1215.079 1225 1201.419 1193.453 1183.39 1173.178 1163.221
1152.661 1143.886 1137.711 1133.331 1129.385 1127.577 1138.624 1137.589
1137.099 1137.266 1138.16 1139.581 1141.99 1144.939 1148.421 1153.464
1160.26 1168.167 1177.748 1191.196 1202.695 1209.715 1216.377 1222.486
18*1225 1215.043 1214.983 1215.048 1225 1200.274 1189.672 1179.339
1168.621 1157.159 1146.997 1139.12 1133.225 1128.939 1125.06 1125.242
1135.902 1134.772 1133.989 1133.964 1134.692 1136.197 1138.587 1141.415
1144.557 1148.24 1154.738 1163.169 1171.76 1183.859 1198.622 1206.717
1213.814 1220.383 1224.543 17*1225 1214.988 1214.929 1214.998 1225
1199.41 1187.025 1175.415 1164.56 1153.455 1144.024 1136.362 1130.734
1127.017 2*1125 1133.327 1132.042 1130.97 1130.603 1131.161 1132.542
1134.767 1137.317 1140.31 1144.579 1149.61 1157.899 1166.575 1175.702
1191.203 1203.441 1211.02 1218.093 1223.73 17*1225 1214.931 1214.872
1214.945 1225 1197.795 1183.572 1171.291 1160.775 1150.006 1141.659
1134.044 1129.478 1126.669 2*1125 1130.987 1129.387 1128.164 1127.193
1127.255 1128.485 1130.441 1132.831 1136.226 1140.733 1145.992 1152.462
1161.468 1170.819 1183.698 1199.648 1207.628 1214.945 1222.029 17*1225
1214.871 1214.813 1214.89 1225 1196.469 1182.021 1169.075 1157.649
1148.982 1145.683 1142.44 1139.251 1136.125 1133.214 1130.823 1128.758

1126.886 1125.377 1123.357 1122.944 1123.965 1125.727 1127.952 1131.787
1136.731 1142.398 1148.553 1157.279 1166.513 1176.09 1192.133 1204.096
1211.594 1218.762 1224.83 16*1225 1214.807 1214.75 1214.833 1225 1195.352
1181.655 1169.369 1158.547 1149.25 1145.586 1142.022 1138.555 1135.18
1131.893 1128.736 1126.433 1124.078 1121.218 1119.337 1118.92 1119.682
1123.3 1124.19 1127.429 1133.055 1138.919 1145.405 1153.22 1162.348
1171.357 1184.727 1200.875 1208.759 1216.208 1223.882 16*1225 1214.721
1214.666 1214.755 1225 1194.346 1181.326 1169.738 1159.62 1149.843
1145.873 1141.94 1138.094 1134.399 1130.814 1127.331 1123.569 1120.272
1117.536 1115.959 1115.638 1116.353 1121.289 1122.456 1124.266 1128.713
1134.86 1141.723 1149.361 1158.308 1167.474 1177.982 1195.314 1205.84
1213.483 1221.967 16*1225 1214.62 1214.568 1214.665 1225 1194.324
1181.354 1170.062 1160.561 1151.154 1146.325 1142.12 1137.905 1133.692
1129.556 1125.699 1121.378 1118.144 1114.916 1112.649 1112.221 1112.792
1119.594 1120.652 1122.16 1124.401 1130.12 1137.623 1146.59 1155.913
1164.781 1173.378 1188.912 1202.681 1210.299 1218.626 1224.371 15*1225
1214.514 1214.465 1214.57 1225 1196.247 1181.992 1170.348 1161.394
1152.635 1147.051 1142.765 1138.432 1134.053 1129.626 1125.151 1120.523
1117.184 1113.879 1111.296 1109.875 1108.995 1117.815 1118.597 1119.756
1121.786 1124.743 1134.116 1144.286 1153.925 1162.003 1170.295 1182.231
1197.728 1206.066 1213.732 1221.367 15*1225 1214.444 1214.397 1214.509
1225 1198.659 1184.183 1172.226 1163.726 1154.999 1148.065 1143.62
1139.126 1134.581 1129.985 1125.362 1120.492 1116.92 1113.432 1110.339
1108.852 1107.857 1115.9 1116.287 1116.97 1118.938 1122.581 1130.352
1140.357 1150.158 1158.436 1166.929 1176.103 1190.683 1202.286 1209.36
1216.421 1224.198 14*1225 1214.374 1214.329 1214.448 1225 1200.711
1188.616 1175.693 1166.653 1157.589 1149.169 1144.624 1140.047 1135.438

1130.797 1126.148 1121.101 1117.259 1113.557 1110.277 1108.221 1107.112
1113.862 1113.667 1113.894 1115.587 1119.438 1126.104 1135.953 1145.658
1154.836 1163.607 1172.427 1185.135 1199.039 1206.359 1213.144 1222.051
14*1225 1214.254 1214.213 1214.343 1225 1202.161 1192.946 1180.423
1169.843 1160.414 1150.708 1145.713 1141.062 1136.687 1132.04 1127.125
1123.663 1121.344 1119.053 1116.857 1114.83 1112.943 1111.837 1110.685
1109.851 1110.443 1115.016 1122.835 1132.193 1141.939 1151.564 1160.484
1169.532 1180.517 1193.985 1203.412 1209.82 1218.251 1224.301 13*1225
1214.123 1214.088 1214.229 1225 1203.501 1196.981 1184.833 1173.356
1163.831 1153.818 1147.59 1143.279 1138.749 1133.978 1128.946 1124.347
1121.75 1119.206 1116.726 1114.192 1111.847 1109.368 1107.04 1106.179
1107.011 1111.929 1120.021 1127.277 1136.036 1147.548 1157.097 1166.312
1176.109 1188.529 1199.748 1205.601 1213.123 1219.786 1224.158 2*1225
1224.315 1224.777 8*1225 1214.051 1214.018 1214.168 1225 1204.502
1200.3 1189.883 1178.942 1168.874 1159.641 1150.802 1145.938 1141.226
1136.249 1130.984 1125.687 1122.682 1119.874 1116.902 1113.79 1110.682
1107.462 1105.745 1105.214 1106.2 1110.793 1116.876 1121.816 1130.026
1141.994 1153.045 1162.431 1172.015 1182.868 1193.384 1201.723 1208.38
1214.527 1219.996 1223.738 1223.978 1223.152 1223.723 8*1225 1214.003
1213.971 1214.13 1225 1206.516 1202.234 1195.805 1184.861 1174.083
1165.061 1156.411 1148.904 1144.014 1138.977 1133.86 1128.682 1124.1
1120.933 1117.604 1114.103 1110.414 1106.804 1104.882 1104.148 1104.792
1108.603 1113.765 1119.019 1124.761 1136.528 1148.367 1158.247 1167.699
1177.867 1187.561 1197.267 1204.466 1210.228 1215.392 1220.299 1221.37
1221.938 1222.633 8*1225 1213.929 1213.9 1214.07 1225 1208.498 1204.163
1200.827 1191.207 1180.13 1170.385 1162.098 1153.738 1147.185 1142.097
1136.942 1131.612 1126.147 1122.282 1118.701 1114.965 1110.947 1106.801

1104.267 1102.989 1102.917 1106.033 1110.107 1115.735 1121.95 1130.437
1141.672 1151.929 1161.092 1171.792 1182.12 1191.707 1201.157 1206.73
1211.758 1216.798 1218.484 1220.627 1221.476 8*1225 1213.822 1213.799
1213.982 1214.896 1210.937 1206.484 1204.184 1198.535 1187.568 1176.574
1167.86 1159.364 1150.689 1145.249 1139.972 1134.561 1129.102 1123.957
1120.085 1115.947 1111.821 1107.742 1104.558 1102.729 1101.942 1104.197
1107.259 1111.777 1117.646 1123.178 1132.654 1142.519 1152.634 1163.894
1175.372 1184.462 1195.536 1203.036 1208.021 1213.374 1215.832 1218.629
1220.248 1224.196 7*1225 1213.72 1213.701 1213.9 1214.851 1213.351
1208.805 1207.547 1202.946 1195.341 1184.346 1173.703 1165.27 1156.509
1148.495 1143.14 1138.095 1132.727 1126.88 1122.204 1118.203 1114.178
1109.72 1105.898 1103.484 1102.056 1103.43 1105.558 1108.63 1114.051
1119.495 1123.978 1132.411 1142.757 1153.304 1164.432 1175.053 1185.308
1195.434 1202.533 1207.936 1211.162 1214.252 1218.036 1223.036 7*1225
1213.847 1213.819 1214.02 1214.994 1215.612 1211.043 1210.901 1206.615
1201.605 1192.576 1181.68 1171.625 1162.72 1153.566 1147.382 1142.348
1136.858 1130.853 1124.66 1120.577 1116.311 1111.855 1107.533 1104.583
1102.59 1103.17 1104.507 1106.665 1110.767 1115.777 1120.125 1124.143
1133.168 1143.485 1154.077 1164.679 1175.433 1185.601 1194.993 1202.98
1206.993 1210.416 1214.29 1220.598 1223.952 6*1225 1213.929 1213.894
1214.099 1215.103 1216.289 1213.609 1214.557 1210.53 1205.671 1200.581
1190.265 1179.245 1169.496 1161.22 1153.433 1147.106 1141.549 1135.576
1129.026 1123.178 1118.809 1114.299 1109.61 1106.071 1103.511 1103.311
1103.945 1105.304 1108.324 1112.731 1116.991 1120.883 1124.638 1134.687
1144.901 1155.385 1166.332 1175.402 1184.933 1196.662 1203.464 1207.415
1211.638 1218.072 1222.763 6*1225 1213.931 1213.893 1214.11 1215.152
1216.035 1214.898 1217.919 1214.241 1209.622 1204.772 1198.949 1187.905

1177.212 1168.865 1161.08 1153.41 1146.938 1140.877 1134.194 1126.895
1121.678 1117.084 1112.273 1108.049 1104.904 1103.849 1103.826 1104.433
1106.58 1109.862 1114.323 1118.385 1122.134 1126.728 1137.173 1147.337
1157.493 1166.205 1174.09 1186.548 1198.489 1204 1208.744 1215.458
1220.941 1224.639 5*1225 1213.975 1213.931 1214.157 1215.239 1215.83
1214.776 1220.491 1217.32 1213.095 1208.63 1203.641 1196.752 1186.43
1176.708 1168.636 1160.935 1153.515 1146.841 1140.125 1132.53 1124.806
1120.114 1115.591 1111.413 1107.642 1105.626 1104.966 1104.921 1106.317
1108.8 1112.971 1116.766 1120.233 1123.481 1130.209 1140.683 1149.935
1158.696 1167.515 1176.919 1188.679 1199.619 1204.416 1210.502 1215.683
1221.86 5*1225 1214.045 1213.992 1214.227 1215.349 1215.645 1214.66
1222.318 1220.57 1216.643 1212.472 1207.689 1202.605 1195.182 1185.508
1175.928 1167.899 1160.51 1153.575 1146.027 1138.224 1130.328 1123.428
1118.984 1114.654 1110.556 1107.705 1106.537 1105.906 1106.701 1108.561
1112.187 1115.646 1118.856 1122.122 1126.017 1135.624 1144.118 1152.046
1160.881 1169.986 1181.506 1192.349 1200.865 1206.45 1211.414 1217.197
1223.432 4*1225 1214.035 1213.978 1214.23 1215.404 1215.476 1214.551
1223.412 1223.708 1220.583 1216.589 1211.895 1206.821 1201.815 1193.764
1184.019 1174.402 1167.149 1159.982 1152.013 1144.01 1135.96 1127.648
1121.967 1117.765 1113.883 1111.057 1109.546 1108.292 1108.609 1110.301
1112.644 1115.376 1118.356 1121.343 1124.292 1131.566 1139.441 1146.535
1154.833 1166.267 1177.246 1187.035 1196.33 1203.199 1207.819 1213.112
1218.948 1223.022 3*1225 1213.889 1213.843 1214.126 1215.372 1215.333
1214.463 1224.523 1225 1223.823 1220.146 1215.681 1210.757 1205.924
1200.948 1192.536 1182.991 1174.234 1167.014 1158.945 1149.89 1141.744
1133.331 1124.826 1120.737 1117.254 1114.897 1113.156 1111.743 1111.596
1112.097 1102.531 1104.668 1107.562 1113.316 1120.492 1128.291 1136.081

1144.188 1153.241 1163.701 1173.415 1182.795 1192.237 1200.914 1205.366
1210.45 1216.052 1220.05 1224.703 1225 1224.866 1213.601 1213.582
1213.915 1215.255 1215.107 1214.271 3*1225 1224.157 1219.89 1215.068
1210.367 1205.341 1200.921 1192.765 1183.754 1174.958 1166.832 1157.425
1147.801 1139.287 1130.469 1123.651 1120.721 1118.342 1116.206 1114.728
1114.067 1113.941 1101.662 1103.723 1106.426 1111.083 1118.276 1126.31
1134.74 1143.189 1151.881 1161.149 1169.859 1178.492 1187.725 1196.253
1202.277 1206.997 1212.208 1216.06 1220.536 1224.527 1223.55 1213.439
1213.437 1213.815 1215.247 1214.899 1214.098 4*1225 1224.424 1219.725
1215.042 1209.859 1205.44 1201.158 1192.819 1183.563 1175.003 1164.835
1154.818 1145.426 1136.86 1129.307 1123.917 1121.292 1118.762 1117.098
1116.129 1115.637 1101.455 1103.539 1106.052 1109.651 1116.87 1125.189
1133.697 1142.225 1150.776 1159.081 1166.807 1174.015 1182.52 1190.77
1198.539 1203.574 1208.392 1212.124 1216.395 1220.272 1221.561 1213.318
1213.332 1213.757 1215.289 1214.89 1214.139 5*1225 1223.392 1218.775
1213.527 1209.139 1204.981 1199.54 1190.262 1181.25 1172.094 1162.002
1151.883 1143.363 1135.919 1128.347 1123.235 1120.809 1119.052 1117.891
1117.173 1102.376 1103.266 1105.57 1108.635 1115.093 1123.546 1132.279
1141.16 1150.178 1157.551 1164.454 1170.929 1177.515 1185.422 1193.128
1200.511 1205.007 1208.654 1212.778 1216.602 1218.172 1212.558 1213.168
1213.659 1215.312 1214.919 1214.219 5*1225 1224.704 1221.958 1216.704
1212.39 1208.403 1203.039 1196.121 1187.221 1178.504 1169.164 1159.034
1149.149 1141.275 1133.06 1124.861 1122.511 1120.712 1119.419 1118.573
1102.852 1102.889 1104.847 1107.596 1112.925 1121.433 1130.312 1139.688
1149.746 1156.282 1162.232 1167.895 1173.317 1180.146 1187.726 1195.633
1201.901 1205.493 1209.569 1213.433 1215.368 1210.904 1212.922 1213.505
1215.309 1214.975 1214.321 6*1225 1222.966 1219.373 1215.164 1211.384

1205.949 1200.682 1192.095 1183.716 1175.988 1166.175 1155.645 1146.443
1138.108 1129.514 1123.943 1122.161 1120.822 1119.847 1104.416 1102.99
1104.027 1106.152 1110.018 1118.087 1126.44 1135.997 1146.03 1153.715
1159.442 1164.886 1169.8 1174.555 1181.927 1189.61 1196.328 1201.564
1205.451 1209.226 1211.475 1208.307 1210.249 1212.731 1215.591 1215.087
1214.479 6*1225 1223.292 1220.978 1217.427 1213.794 1208.271 1202.839
1196.187 1188.221 1180.43 1171.801 1161.656 1152.117 1143.465 1134.795
1126.121 1123.472 1122.068 1121.014 1106.535 1104.441 1102.894 1104.283
1106.712 1114.025 1121.926 1130.48 1141.236 1151.301 1156.359 1161.299
1165.87 1170.354 1175.295 1182.098 1188.641 1195.533 1201.603 1205.348
1207.976 1206.178 1208.033 1210.389 1214.136 1215.189 1214.622 6*1225
1223.946 1221.625 1219.155 1216.264 1210.604 1204.96 1199.736 1192.027
1184.525 1176.522 1167.051 1157.834 1149.114 1140.269 1131.491 1124.627
1123.235 1122.15 1109.125 1106.671 1104.314 1103.781 1105.28 1111.064
1118.051 1124.582 1135.2 1145.496 1152.86 1157.274 1161.223 1165.551
1169.985 1174.481 1180.853 1188.144 1195.981 1201.955 1205.144 1204.84
1206.825 1209.335 1213.235 1215.202 1214.664 7*1225 1223.626 1221.111
1218.378 1214.032 1208.005 1202.347 1196.967 1189.268 1180.948 1172.034
1163.187 1153.976 1144.884 1136.401 1128.717 1124.352 1123.201 1112.678
1109.901 1107.185 1105.091 1104.897 1109.086 1114.653 1120.291 1127.474
1137.711 1147.197 1152.225 1156.05 1160.111 1164.202 1168.599 1173.497
1180.507 1188.352 1196.521 1202.1 1203.315 1205.455 1208.147 1212.209
1215.161 1214.644 8*1225 1223.779 1221.05 1218.19 1211.686 1205.352
1201.314 1194.719 1186.348 1177.409 1168.13 1158.703 1149.11 1141.104
1133.726 1126.933 1124.171 1116.626 1113.591 1110.575 1108.248 1106.71
1108.306 1112.373 1116.58 1121.372 1127.937 1135.61 1143.406 1150.39
1154.144 1158.119 1162.458 1167.648 1173.267 1180.406 1188.754 1197.266

1201.473 1203.703 1206.487 1210.539 1215.102 1214.604 9*1225 1224.451
1221.521 1215.985 1208.865 1204.578 1200.581 1193.067 1183.769 1173.399
1163.749 1153.751 1145.22 1138.642 1132.055 1124.984 1120.57 1117.424
1114.172 1110.594 1107.962 1107.76 1109.771 1112.404 1115.775 1119.619
1124.588 1133.014 1140.492 1146.893 1151.718 1156.243 1162.059 1167.677
1173.364 1181.271 1189.757 1198.181 1201.784 1204.596 1208.516 1214.997
1214.511 11*1225 1222.026 1213.737 1208.945 1204.526 1200.501 1191.424
1180.204 1169.146 1159.815 1150.543 1143.785 1136.681 1129.04 1125.984
1122.51 1118.999 1115.126 1111.473 1109.723 1110.16 1111.012 1111.995
1114.073 1117.623 1123.882 1131.724 1138.443 1144.158 1150.868 1156.672
1162.441 1168.54 1174.343 1183.198 1191.847 1199.422 1202.54 1206.164
1214.898 1214.425 11*1225 1224.943 1218.787 1213.648 1208.962 1204.899
1200.405 1189.345 1177.278 1167.683 1158.345 1149.024 1142.063 1135.948
1132.507 1128.174 1124.153 1120.05 1115.979 1112.586 1111.547 1111.15
1110.62 1110.846 1112.643 1117.639 1124.215 1131.379 1138.287 1145.102
1151.683 1158.239 1164.465 1171.084 1178.675 1186.757 1194.375 1200.862
1204.161 1214.797 1214.335 12*1225 1220.205 1218.219 1213.55 1209.59
1205.374 1200.457 1188.911 1176.344 1166.624 1157.354 1148.38 1142.648
1138.131 1133.704 1128.946 1124.34 1119.968 1115.802 1113.073 1111.514
1109.872 1108.873 1109.461 1113.328 1118.688 1125.663 1133.091 1140.637
1148.119 1154.845 1161.477 1168.306 1174.996 1183.03 1191.086 1199.164
1202.96 1214.704 1214.254 12*1225 1221.297 1219.333 1217.761 1214.208
1210.372 1205.948 1200.507 1188.295 1176.09 1166.564 1156.783 1148.23
1143.297 1138.477 1133.719 1128.985 1124.209 1119.518 1115.891 1113.125
1110.602 1108.692 1108.389 1111.291 1115.658 1121.835 1129.796 1137.297
1145.04 1152.587 1159.395 1165.992 1172.389 1180.004 1188.261 1196.136
1201.711 1214.642 1214.204 12*1225 1222.444 1220.509 1219.028 1217.857

1214.588 1210.834 1206.119 1200.004 1187.835 1176.479 1166.468 1156.088
1148.005 1143.142 1138.351 1133.635 1128.828 1123.75 1119.223 1115.757
1112.563 1110.036 1109.912 1111.223 1114.805 1120.471 1128.575 1136.212
1143.762 1151.109 1157.873 1164.704 1171.606 1178.975 1186.49 1193.688
1200.305 1214.589 1214.162 12*1225 1223.599 1221.685 1220.276 1220.122
1218.957 1215.735 1211.611 1205.551 1198.91 1187.61 1175.872 1165.404
1155.248 1147.716 1143.089 1138.368 1133.463 1128.466 1123.235 1119.345
1115.692 1113.382 1112.979 1113.228 1115.906 1121.31 1129.004 1135.955
1142.841 1149.712 1156.789 1163.911 1171.024 1178.222 1185.544 1192.875
1200.104 1214.525 1214.109 12*1225 1224.757 1222.848 1221.491 1221.553
1222.051 1221.294 1217.63 1211.467 1205.146 1198.402 1186.627 1174.517
1164.421 1154.979 1147.915 1143.153 1138.522 1133.544 1128.829 1124.272
1120.028 1117.535 1116.771 1116.634 1118.033 1122.954 1130.195 1137.348
1144.414 1151.308 1157.733 1164.177 1170.78 1177.731 1185.14 1192.558
1199.985 1214.464 1214.058 13*1225 1224.015 1222.704 1222.982 1223.869
1224.588 1223.893 1217.623 1211.088 1204.912 1197.945 1185.766 1173.474
1164.051 1155.149 1148.514 1143.98 1139.362 1134.816 1130.38 1126.368
1123.833 1123.048 1122.708 1123.653 1128.111 1133.728 1139.431 1146.142
1153.104 1159.728 1166.205 1172.533 1179.11 1186.013 1193.079 1200.073
1214.398 1214.002 14*1225 1223.917 1224.411 3*1225 1224.337 1217.522
1211.067 1204.982 1197.829 1184.972 1172.608 1163.988 1156.715 1149.891
1145.355 1140.818 1136.831 1133.317 1131.718 1130.948 1130.941 1131.863
1134.038 1139.868 1144.708 1149.942 1155.214 1161.998 1168.634 1175.085
1181.726 1188.484 1195.361 1200.87 1214.337 1213.949 20*1225 1223.656
1217.229 1211.11 1205.172 1197.704 1183.867 1172.808 1165.478 1158.698
1152.019 1146.856 1143.818 1141.022 1139.151 1138.341 1138.657 1139.724
1141.729 1145.17 1150.381 1155.289 1159.992 1165.137 1171.571 1177.994

1184.311 1190.837 1197.568 1201.599 1214.301 1213.922 21*1225 1221.482
1215.785 1210.412 1204.677 1196.422 1184.291 1174.193 1167.683 1161.045
1155.443 1151.671 1148.692 1146.368 1145.713 1146.348 1147.478 1149.663
1152.157 1156.495 1161.126 1165.278 1170.039 1175.246 1181.046 1187.273
1193.408 1199.674 1202.215 1214.253 1213.884 21*1225 1223.912 1219.56
1214.85 1209.784 1203.845 1196.734 1186.536 1177.361 1170.694 1165.592
1161.245 1157.551 1154.344 1153.657 1154.762 1156.146 1158.624 1161.063
1163.733 1167.53 1171.457 1174.91 1180.504 1185.684 1190.565 1196.683
1200.819 1202.969 1214.176 1213.813 21*1225 1223.896 1221.936 1218.746
1214.346 1208.857 1203.924 1198.226 1188.945 1182.309 1175.146 1170.254
1166.555 1163.199 1162.36 1163.765 1165.416 1167.704 1170.027 1172.318
1174.59 1178.325 1181.822 1186.17 1191.303 1196.034 1200.088 1201.477
1203.193 1214.047 1213.688 21*1225 1224.271 1222.713 1221.177 1219.109
1213.887 1209.267 1204.675 1200.702 1195.672 1189.165 1182.058 1175.726
1171.946 1170.97 1172.67 1174.656 1176.837 1178.831 1180.818 1182.707
1185.665 1188.881 1192.629 1197.355 1200.279 1200.91 1201.942 1203.253
2*1200 1211.766 1211.837 1211.897 1211.932 1211.968 1212.007 1212.035
1212.064 1212.055 1212.026 1212.091 1212.258 1212.708 1212.905 1213.049
1213.107 1213.171 1213.224 1213.287 1213.412 1213.577 1213.738 1213.928
1214.143 1214.434 1213.765 1210.655 1207.36 1204.652 1203.198 1201.342
1197.316 1190.64 1184.425 1182.333 1183.386 1184.784 1186.023 1187.45
1189.229 1190.919 1193.273 1196.24 1199.023 1200.773 6*1200 1212.033
1212.111 1212.178 1212.223 1212.268 1212.317 1212.356 1212.397 1212.403
1212.39 1212.469 1212.646 1213.093 1213.299 1213.456 1213.533 1213.619
1213.698 1213.789 1213.94 1214.131 1214.322 1214.542 1214.789 1215.103
1215.682 1215.057 1211.589 1208.825 1207.824 1206.349 1204.408 1201.921
1199.71 1196.047 1194.965 1195.18 1195.401 1196.165 1197.731 1199.218

1200.414 1201.342 1201.904 1202.505 4*1200

** 0 = null block, 1 = active block

NULL IJK

1	1:12	1	0	13	1	1	0
1	22:61	1	0	13	39:61	1	0
2	1:09	1	0	14	1	1	0
2	24:61	1	0	14	41:61	1	0
3	1:07	1	0	15	1	1	0
3	26:61	1	0	15	43:61	1	0
4	1:05	1	0	16	1	1	0
4	28:61	1	0	16	44:61	1	0
5	1:04	1	0	17	1:02	1	0
5	29:61	1	0	17	45:61	1	0
6	1:03	1	0	18	1:02	1	0
6	30:61	1	0	18	47:61	1	0
7	1:02	1	0	19	1:03	1	0
7	32:61	1	0	19	48:61	1	0
8	1:02	1	0	20	1:03	1	0
8	33:61	1	0	20	49:61	1	0
9	1	1	0	21	1:04	1	0
9	34:61	1	0	21	50:61	1	0
10	1	1	0	22	1:05	1	0
10	35:61	1	0	22	51:61	1	0
11	1	1	0	23	1:06	1	0
11	36:61	1	0	23	52:61	1	0
12	1	1	0	24	1:07	1	0
12	38:61	1	0	24	53:61	1	0

25	1:09	1	0	40	1:35	1	0
25	54:61	1	0	41	1:36	1	0
26	1:11	1	0	42	1:37	1	0
26	55:61	1	0	43	1:39	1	0
27	1:13	1	0	43	61	1	0
27	56:61	1	0	44	1:40	1	0
28	1:15	1	0	44	61	1	0
28	57:61	1	0	45	1:41	1	0
29	1:18	1	0	45	61	1	0
29	58:61	1	0	46	1:42	1	0
30	1:20	1	0	46	61	1	0
30	59:61	1	0	47	1:43	1	0
31	1:22	1	0	47	60:61	1	0
31	60:61	1	0	48	1:44	1	0
32	1:24	1	0	48	59:61	1	0
32	60:61	1	0	49	1:45	1	0
33	1:26	1	0	49	58:61	1	0
33	60:61	1	0	50	1:47	1	0
34	1:27	1	0	50	56:61	1	0
34	61	1	0	51	1:49	1	0
35	1:28	1	0	51	53:61	1	0
35	61	1	0	1	1:12	2	0
36	1:29	1	0	1	22:61	2	0
36	61	1	0	2	1:09	2	0
37	1:30	1	0	2	24:61	2	0
38	1:31	1	0	3	1:07	2	0
39	1:33	1	0	3	26:61	2	0

4	1:05	2	0	17	45:61	2	0
4	28:61	2	0	18	1:02	2	0
5	1:04	2	0	18	47:61	2	0
5	29:61	2	0	19	1:03	2	0
6	1:03	2	0	19	48:61	2	0
6	30:61	2	0	20	1:03	2	0
7	1:02	2	0	20	49:61	2	0
7	32:61	2	0	21	1:04	2	0
8	1:02	2	0	21	50:61	2	0
8	33:61	2	0	22	1:05	2	0
9	1	2	0	22	51:61	2	0
9	34:61	2	0	23	1:06	2	0
10	1	2	0	23	52:61	2	0
10	35:61	2	0	24	1:07	2	0
11	1	2	0	24	53:61	2	0
11	36:61	2	0	25	1:09	2	0
12	1	2	0	25	54:61	2	0
12	38:61	2	0	26	1:11	2	0
13	1	2	0	26	55:61	2	0
13	39:61	2	0	27	1:13	2	0
14	1	2	0	27	56:61	2	0
14	41:61	2	0	28	1:15	2	0
15	1	2	0	28	57:61	2	0
15	43:61	2	0	29	1:18	2	0
16	1	2	0	29	58:61	2	0
16	44:61	2	0	30	1:20	2	0
17	1:02	2	0	30	59:61	2	0

31	1:22	2	0	47	60:61	2	0
31	60:61	2	0	48	1:44	2	0
32	1:24	2	0	48	59:61	2	0
32	60:61	2	0	49	1:45	2	0
33	1:26	2	0	49	58:61	2	0
33	60:61	2	0	50	1:47	2	0
34	1:27	2	0	50	56:61	2	0
34	61	2	0	51	1:49	2	0
35	1:28	2	0	51	53:61	2	0
35	61	2	0	1	1:12	3	0
36	1:29	2	0	1	22:61	3	0
36	61	2	0	2	1:09	3	0
37	1:30	2	0	2	24:61	3	0
38	1:31	2	0	3	1:07	3	0
39	1:33	2	0	3	26:61	3	0
40	1:35	2	0	4	1:05	3	0
41	1:36	2	0	4	28:61	3	0
42	1:37	2	0	5	1:04	3	0
43	1:39	2	0	5	29:61	3	0
43	61	2	0	6	1:03	3	0
44	1:40	2	0	6	30:61	3	0
44	61	2	0	7	1:02	3	0
45	1:41	2	0	7	32:61	3	0
45	61	2	0	8	1:02	3	0
46	1:42	2	0	8	33:61	3	0
46	61	2	0	9	1	3	0
47	1:43	2	0	9	34:61	3	0

10	1	3	0	23	52:61	3	0
10	35:61	3	0	24	1:07	3	0
11	1	3	0	24	53:61	3	0
11	36:61	3	0	25	1:09	3	0
12	1	3	0	25	54:61	3	0
12	38:61	3	0	26	1:11	3	0
13	1	3	0	26	55:61	3	0
13	39:61	3	0	27	1:13	3	0
14	1	3	0	27	56:61	3	0
14	41:61	3	0	28	1:15	3	0
15	1	3	0	28	57:61	3	0
15	43:61	3	0	29	1:18	3	0
16	1	3	0	29	58:61	3	0
16	44:61	3	0	30	1:20	3	0
17	1:02	3	0	30	59:61	3	0
17	45:61	3	0	31	1:22	3	0
18	1:02	3	0	31	60:61	3	0
18	47:61	3	0	32	1:24	3	0
19	1:03	3	0	32	60:61	3	0
19	48:61	3	0	33	1:26	3	0
20	1:03	3	0	33	60:61	3	0
20	49:61	3	0	34	1:27	3	0
21	1:04	3	0	34	61	3	0
21	50:61	3	0	35	1:28	3	0
22	1:05	3	0	35	61	3	0
22	51:61	3	0	36	1:29	3	0
23	1:06	3	0	36	61	3	0

37	1:30	3	0	2	24:61	4	0
38	1:31	3	0	3	1:07	4	0
39	1:33	3	0	3	26:61	4	0
40	1:35	3	0	4	1:05	4	0
41	1:36	3	0	4	28:61	4	0
42	1:37	3	0	5	1:04	4	0
43	1:39	3	0	5	29:61	4	0
43	61	3	0	6	1:03	4	0
44	1:40	3	0	6	30:61	4	0
44	61	3	0	7	1:02	4	0
45	1:41	3	0	7	32:61	4	0
45	61	3	0	8	1:02	4	0
46	1:42	3	0	8	33:61	4	0
46	61	3	0	9	1	4	0
47	1:43	3	0	9	34:61	4	0
47	60:61	3	0	10	1	4	0
48	1:44	3	0	10	35:61	4	0
48	59:61	3	0	11	1	4	0
49	1:45	3	0	11	36:61	4	0
49	58:61	3	0	12	1	4	0
50	1:47	3	0	12	38:61	4	0
50	56:61	3	0	13	1	4	0
51	1:49	3	0	13	39:61	4	0
51	53:61	3	0	14	1	4	0
1	1:12	4	0	14	41:61	4	0
1	22:61	4	0	15	1	4	0
2	1:09	4	0	15	43:61	4	0

16	1	4	0	29	58:61	4	0
16	44:61	4	0	30	1:20	4	0
17	1:02	4	0	30	59:61	4	0
17	45:61	4	0	31	1:22	4	0
18	1:02	4	0	31	60:61	4	0
18	47:61	4	0	32	1:24	4	0
19	1:03	4	0	32	60:61	4	0
19	48:61	4	0	33	1:26	4	0
20	1:03	4	0	33	60:61	4	0
20	49:61	4	0	34	1:27	4	0
21	1:04	4	0	34	61	4	0
21	50:61	4	0	35	1:28	4	0
22	1:05	4	0	35	61	4	0
22	51:61	4	0	36	1:29	4	0
23	1:06	4	0	36	61	4	0
23	52:61	4	0	37	1:30	4	0
24	1:07	4	0	38	1:31	4	0
24	53:61	4	0	39	1:33	4	0
25	1:09	4	0	40	1:35	4	0
25	54:61	4	0	41	1:36	4	0
26	1:11	4	0	42	1:37	4	0
26	55:61	4	0	43	1:39	4	0
27	1:13	4	0	43	61	4	0
27	56:61	4	0	44	1:40	4	0
28	1:15	4	0	44	61	4	0
28	57:61	4	0	45	1:41	4	0
29	1:18	4	0	45	61	4	0

46	1:42	4	0	49	1:45	4	0
46	61	4	0	49	58:61	4	0
47	1:43	4	0	50	1:47	4	0
47	60:61	4	0	50	56:61	4	0
48	1:44	4	0	51	1:49	4	0
48	59:61	4	0	51	53:61	4	0

** 0 = pinched block, 1 = active block

PINCHOUTARRAY CON 1

POR CON 0.2

PERMI CON 50

PERMJ EQUALSI

PERMK EQUALSI * 0.37

PRPOR 14300

CPOR 4E-06

**The following is the fluid component

**property data in GEM format.

**The unit system and fluid compositions should

**be specified in the I/O control section.

**The units and compositions specified in WinProp

**are included here as comments for informational purposes.

** PLEASE DO NOT REMOVE THE FOLLOWING PVT UNIT COMMENT LINE

** PVT UNITS CONSISTENT WITH *INUNIT *SI

**COMPOSITION *PRIMARY

** 0.01150000 0.00000000 0.00000000 0.00000000 0.02280000

** 0.91450000 0.03210000 0.01210000 0.00240000 0.00300000

** 0.00090000 0.00070000

**COMPOSITION *SECOND

** 0.00000000 0.00000000 0.00000000 0.00000000 0.00000000

** 0.00000000 0.00000000 0.00000000 0.00000000 0.00000000

** 0.00000000 0.00000000

** Model and number of components

MODEL PR

NC 12 12

COMPNAME 'CO2' 'TraceCH4' 'H2' 'TraceH2' 'N2' 'CH4' 'C2H6' 'C3H8' 'IC4' 'NC4' 'IC5' 'NC5'

** The Hydrocarbon component flag values: 1 - Hydro-Carbon, 0 - non Hydro-Carbon

**

** The read-in HC-HC BIN values will be overwritten by the internal GEM calculated

** values for these HC-HC pairs, if the original *HCFLAG values are used.

** This is fine if there is only 1 HC-HC group defined in the original WinProp

** data set. Otherwise, all-zero *HCFLAG will be output here in order to use the

** full read-in BIN values.

** The original WinProp HC-flags:

** *HCFLAG 3 1 0 0 0 1 1 1 1 1 1 1

HCFLAG

0 1 0 0 0 1 1 1 1 1 1

TRES 68.80000

PVC3 1.20000000E+00

VISCOR HZYT

MIXVC 1.0000000E+00

VISCOEFF

1.0230000E-01 2.3364000E-02 5.8533000E-02 -4.0758000E-02 9.3324000E-03

MW

4.4010000E+01 1.6043000E+01 2.0159000E+00 2.0159000E+00 2.8013000E+01
1.6043000E+01 3.0070000E+01 4.4097000E+01 5.8124000E+01 5.8124000E+01
7.2151000E+01 7.2151000E+01

AC

2.2500000E-01 8.0000000E-03 -2.1400000E-01 -2.1400000E-01 4.0000000E-02
8.0000000E-03 9.8000000E-02 1.5200000E-01 1.7600000E-01 1.9300000E-01
2.2700000E-01 2.5100000E-01

PCRIT

7.2800000E+01 4.5400000E+01 1.2980000E+01 1.2980000E+01 3.3500000E+01
4.5400000E+01 4.8200000E+01 4.1900000E+01 3.6000000E+01 3.7500000E+01
3.3400000E+01 3.3300000E+01

VCRIT

9.4000000E-02 4.5723553E-01 6.6952000E-02 4.5723553E-01 8.9500000E-02
9.9000000E-02 1.4800000E-01 2.0300000E-01 2.6300000E-01 2.5500000E-01
3.0600000E-01 3.0400000E-01

TCRIT

3.0420000E+02 1.9060000E+02 3.3180000E+01 3.3180000E+01 1.2620000E+02
1.9060000E+02 3.0540000E+02 3.6980000E+02 4.0810000E+02 4.2520000E+02
4.6040000E+02 4.6960000E+02

PCHOR

7.8000000E+01 7.7000000E+01 3.1000000E+01 3.1000000E+01 4.1000000E+01
7.7000000E+01 1.0800000E+02 1.5030000E+02 1.8150000E+02 1.8990000E+02
2.2500000E+02 2.3150000E+02

SG

8.1800000E-01 2.6541973E-01 7.1070000E-02 3.0135395E-02 8.0900000E-01
3.0000000E-01 3.5600000E-01 5.0700000E-01 5.6300000E-01 5.8400000E-01
6.2500000E-01 6.3100000E-01

TB

-7.8450000E+01 0.0000000E+00 -2.5276000E+02 0.0000000E+00 -
1.9575000E+02 -1.6145000E+02 -8.8650000E+01 -4.2050000E+01 -
1.1850000E+01 -4.5000000E-01 2.7850000E+01 3.6050000E+01

OMEGA

4.5723553E-01 1.0000000E+00 4.5723553E-01 1.0000000E+00 4.5723553E-01
4.5723553E-01 4.5723553E-01 4.5723553E-01 4.5723553E-01 4.5723553E-01
4.5723553E-01 4.5723553E-01

OMEGB

7.7796074E-02 3.0000000E-01 7.7796074E-02 7.1070000E-02 7.7796074E-02
7.7796074E-02 7.7796074E-02 7.7796074E-02 7.7796074E-02 7.7796074E-02
7.7796074E-02 7.7796074E-02

VSHIFT

0.0000000E+00 1.0000000E+01 0.0000000E+00 1.0000000E+01 0.0000000E+00
0.0000000E+00 0.0000000E+00 0.0000000E+00 0.0000000E+00 0.0000000E+00
0.0000000E+00 0.0000000E+00

VISVC

9.4000000E-02 7.7796074E-02 6.6952000E-02 7.7796074E-02 8.9500000E-02
9.9000000E-02 1.4800000E-01 2.0300000E-01 2.6300000E-01 2.5500000E-01
3.0600000E-01 3.0400000E-01

BIN

0.0000000E+00

-1.6220000E-01 1.5600000E-02

-1.6220000E-01 1.5600000E-02 0.0000000E+00

0.0000000E+00 0.0000000E+00 0.0000000E+00 0.0000000E+00

1.0500000E-01 3.7867687E-02 1.5600000E-02 1.5600000E-02 2.5000000E-02

1.3000000E-01 2.0861464E-02 0.0000000E+00 0.0000000E+00 1.0000000E-02
2.6890022E-03

1.2500000E-01 1.0895695E-02 0.0000000E+00 0.0000000E+00 9.0000000E-02
8.5370405E-03 1.6620489E-03

1.2000000E-01 5.0775026E-03 0.0000000E+00 0.0000000E+00 9.5000000E-02
1.5715316E-02 5.4857876E-03 1.1165976E-03

1.1500000E-01 5.6579875E-03 0.0000000E+00 0.0000000E+00 9.5000000E-02
1.4748531E-02 4.9143360E-03 8.6625350E-04 1.5903506E-05

1.1500000E-01 2.6826142E-03 0.0000000E+00 0.0000000E+00 1.0000000E-01
2.0878892E-02 8.7338646E-03 2.8007353E-03 3.8207590E-04 5.5378054E-04

1.1500000E-01 2.7707405E-03 0.0000000E+00 0.0000000E+00 1.1000000E-01
2.0640839E-02 8.5779330E-03 2.7121325E-03 3.4971119E-04 5.1467786E-04
7.1665797E-07

ENTHCOEF

9.6880000E-02 1.5884300E-01 -3.3712000E-05 1.4810500E-07 -9.6620300E-11
2.0738320E-14

-2.8385700E+00 5.3828500E-01 -2.1140900E-04 3.3927600E-07 -1.1643220E-10
1.3896120E-14

0.0000000E+00 9.2577979E-01 -1.3929922E-03 -5.1310000E-08 0.0000000E+00
0.0000000E+00

0.0000000E+00 9.2577979E-01 -1.3929922E-03 -5.1310000E-08 0.0000000E+00
0.0000000E+00

-6.5665000E-01 2.5409800E-01 -1.6624000E-05 1.5302000E-08 -3.0995000E-12
1.5167000E-16

-2.8385700E+00 5.3828500E-01 -2.1140900E-04 3.3927600E-07 -1.1643220E-10
1.3896120E-14

-1.4220000E-02 2.6461200E-01 -2.4568000E-05 2.9140200E-07 -1.2810330E-10
1.8134820E-14

6.8715000E-01 1.6030400E-01 1.2608400E-04 1.8143000E-07 -9.1891300E-11
1.3548500E-14

1.4595600E+00 9.9070000E-02 2.3873600E-04 9.1593000E-08 -5.9405000E-11
9.0964500E-15

7.2281400E+00 9.9687000E-02 2.6654800E-04 5.4073000E-08 -4.2926900E-11
6.6958000E-15

1.7694120E+01 1.5946000E-02 3.8244900E-04 -2.7557000E-08 -1.4303500E-11
2.9567700E-15

9.0420900E+00 1.1182900E-01 2.2851500E-04 8.6331000E-08 -5.4464900E-11
8.1845000E-15

DENW 1000.497

CW 3.5e-06

REFPW 14300

SOLUBILITY HENRY

** HENRYC calculated at 68.80 deg C

HENRYC

4.2857537E+05 7.2984645E+06 9.0417E+06 9.0417E+06 0 7.2984645E+06
7.9044751E+06 1.1319890E+07 1.2254463E+07 1.2255691E+07 2.8296143E+07
2.8650787E+07

REFPH

1.4300000E+04 1.4300000E+04 8.8000000E+03 8.8000000E+03 8.8000000E+03
1.4300000E+04 1.4300000E+04 1.4300000E+04 1.4300000E+04 1.4300000E+04
1.4300000E+04 1.4300000E+04

VINFINITY

3.5239305E-02 3.5392618E-02 0.037 0.037 3.2032109E-02 3.5392618E-02
5.2058686E-02 7.1467383E-02 9.1037133E-02 9.1057055E-02 1.1012343E-01
1.1259989E-01

*AQUEOUS-DENSITY *LINEAR

DIFFC-AQU 0 3.75e-05 8.5e-05 8.5e-05 0 3.75e-05 0 0 0 0 0 0

DIFFC-GAS 0 4.46e-05 4.46e-05 4.46e-05 0 4.46e-05 0 0 0 0 0 0

ROCKFLUID

RPT 1

** Sw krw krow

SWT

0 0 1

0.1 0.007 0.9

0.9 0.9 0.1

1 1 0

** Sg krg krog

SGT

0 0 1

0.1 0.1 0.9

```
0.9       0.9     0.007
1         1       0

HYSKRG 0.45
BSWCRIT CON          0.1
INITIAL

VERTICAL DEPTH_AVE WATER_GAS NOTRANZONE EQUIL
ZGAS
0.0115 0 0 0 0.0228 0.9145  0.0321 0.0121 0.0024 0.003 0.0009 0.0007

REFPRES
  14300

REFDEPTH
  1259

DWGC
  3000

SWOC
  0.1

GASZONE NOOIL
NUMERICAL
TWOPTFLUX
RUN
```

```
DATE 1997 9 1'
**
WELL  'NM1'
PRODUCER 'NM1'
PWELLBORE  MODEL
** wdepth  wlength  rel_rough  whtemp  bhtemp  wradius
   1136.84  1136.84  0.000742  15.0  68.8  0.2032
OPERATE  MIN  BHP  200.0  CONT
**          rad  geofac  wfrac  skin
GEOMETRY  K  0.0762  0.37  1.0  0.0
     PERF      GEOA  'NM1'
** UBA              ff         Status  Connection
   28 40 1        1.0  OPEN    FLOW-TO  'SURFACE'  REFLAYER
   28 40 2        1.0  OPEN    FLOW-TO  1
   28 40 3        1.0  OPEN    FLOW-TO  2
   28 40 4        1.0  OPEN    FLOW-TO  3
LAYERXYZ  'NM1'
** perf geometric data: UBA, block entry(x,y,z) block exit(x,y,z), length
   28 40 1  1787.500000  2567.500000  1102.990000  1787.500000  2567.500000
1111.740000  8.750000
   28 40 2  1787.500000  2567.500000  1111.740000  1787.500000  2567.500000
1120.490000  8.750000
   28 40 3  1787.500000  2567.500000  1120.490000  1787.500000  2567.500000
1129.240000  8.750000
   28 40 4  1787.500000  2567.500000  1129.240000  1787.500000  2567.500000
1137.990000  8.750000
         WELL  'NM3'
PRODUCER 'NM3'
OPERATE  MIN  BHP  200.0  CONT
```

```
**         rad  geofac  wfrac  skin
GEOMETRY  K  0.0762  0.37  1.0  0.0
    PERF     GEOA  'NM3'
** UBA            ff        Status  Connection
   40 52 1       1.0  OPEN    FLOW-TO  'SURFACE'  REFLAYER
   40 52 2       1.0  OPEN    FLOW-TO  1
   40 52 3       1.0  OPEN    FLOW-TO  2
   40 52 4       1.0  OPEN    FLOW-TO  3
LAYERXYZ  'NM3'
** perf geometric data: UBA, block entry(x,y,z) block exit(x,y,z), length
   40 52 1  2567.500000  3347.500000  1122.954000  2567.500000  3347.500000
1131.704000  8.750000
   40 52 2  2567.500000  3347.500000  1131.704000  2567.500000  3347.500000
1140.454000  8.750000
   40 52 3  2567.500000  3347.500000  1140.454000  2567.500000  3347.500000
1149.204000  8.750000
   40 52 4  2567.500000  3347.500000  1149.204000  2567.500000  3347.500000
1157.954000  8.750000
        WELL  'NM4'
PRODUCER 'NM4'
PWELLBORE  MODEL
** wdepth  wlength  rel_rough  whtemp  bhtemp  wradius
   1120.44  2119.85  0.000742  15.0  68.8  0.2032
OPERATE  MIN  BHP  200.0  CONT
**         rad  geofac  wfrac  skin
GEOMETRY  K  0.0762  0.37  1.0  0.0
    PERF     GEOA  'NM4'
** UBA            ff        Status  Connection
   20 27 1       1.0  OPEN    FLOW-TO  'SURFACE'  REFLAYER
```

```
   20 27 2        1.0  OPEN    FLOW-TO  1

   20 27 3        1.0  OPEN    FLOW-TO  2

   20 27 4        1.0  OPEN    FLOW-TO  3

LAYERXYZ  'NM4'

** perf geometric data: UBA, block entry(x,y,z) block exit(x,y,z), length

   20 27 1  1267.500000  1722.500000  1102.729000  1267.500000  1722.500000
1111.479000  8.750000

   20 27 2  1267.500000  1722.500000  1111.479000  1267.500000  1722.500000
1120.229000  8.750000

   20 27 3  1267.500000  1722.500000  1120.229000  1267.500000  1722.500000
1128.979000  8.750000

   20 27 4  1267.500000  1722.500000  1128.979000  1267.500000  1722.500000
1137.729000  8.750000

         WELL  'NM5'

PRODUCER 'NM5'

OPERATE  MIN  BHP  200.0  CONT

**         rad  geofac  wfrac  skin

GEOMETRY  K  0.0762  0.37  1.0  0.0

     PERF      GEOA  'NM5'

** UBA             ff         Status  Connection

   27 48 1        1.0  OPEN    FLOW-TO  'SURFACE'  REFLAYER

   27 48 2        1.0  OPEN    FLOW-TO  1

   27 48 3        1.0  OPEN    FLOW-TO  2

   27 48 4        1.0  OPEN    FLOW-TO  3

LAYERXYZ  'NM5'

** perf geometric data: UBA, block entry(x,y,z) block exit(x,y,z), length

   27 48 1  1722.500000  3087.500000  1138.131000  1722.500000  3087.500000
1146.881000  8.750000

   27 48 2  1722.500000  3087.500000  1146.881000  1722.500000  3087.500000
1155.631000  8.750000
```

27 48 3 1722.500000 3087.500000 1155.631000 1722.500000 3087.500000 1164.381000 8.750000

27 48 4 1722.500000 3087.500000 1164.381000 1722.500000 3087.500000 1173.131000 8.750000

WELL 'NM6'

PRODUCER 'NM6'

OPERATE MIN BHP 200.0 CONT

** rad geofac wfrac skin

GEOMETRY K 0.0762 0.37 1.0 0.0

PERF GEOA 'NM6'

** UBA ff Status Connection

37 41 1 1.0 OPEN FLOW-TO 'SURFACE' REFLAYER

37 41 2 1.0 OPEN FLOW-TO 1

37 41 3 1.0 OPEN FLOW-TO 2

37 41 4 1.0 OPEN FLOW-TO 3

LAYERXYZ 'NM6'

** perf geometric data: UBA, block entry(x,y,z) block exit(x,y,z), length

37 41 1 2372.500000 2632.500000 1156.359000 2372.500000 2632.500000 1165.109000 8.750000

37 41 2 2372.500000 2632.500000 1165.109000 2372.500000 2632.500000 1173.859000 8.750000

37 41 3 2372.500000 2632.500000 1173.859000 2372.500000 2632.500000 1182.609000 8.750000

37 41 4 2372.500000 2632.500000 1182.609000 2372.500000 2632.500000 1191.359000 8.750000

WELL 'NM7'

PRODUCER 'NM7'

OPERATE MIN BHP 200.0 CONT

** rad geofac wfrac skin

GEOMETRY I 0.0762 0.37 1.0 0.0

```
    PERF     GEOA  'NM7'
** UBA            ff        Status  Connection
   12 21 1       1.0  OPEN    FLOW-TO  'SURFACE'  REFLAYER
   12 21 2       1.0  OPEN    FLOW-TO  1
   12 21 3       1.0  OPEN    FLOW-TO  2
   12 21 4       1.0  OPEN    FLOW-TO  3
LAYERXYZ  'NM7'
** perf geometric data: UBA, block entry(x,y,z) block exit(x,y,z), length
   12 21 1  747.500000  1332.500000  1121.101000  747.500000  1332.500000
1129.851000  8.750000
   12 21 2  747.500000  1332.500000  1129.851000  747.500000  1332.500000
1138.601000  8.750000
   12 21 3  747.500000  1332.500000  1138.601000  747.500000  1332.500000
1147.351000  8.750000
   12 21 4  747.500000  1332.500000  1147.351000  747.500000  1332.500000
1156.101000  8.750000
        WELL  'NM8'
PRODUCER 'NM8'
OPERATE  MIN  BHP  200.0  CONT
**         rad  geofac  wfrac  skin
GEOMETRY  I  0.0762  0.37  1.0  0.0
    PERF     GEOA  'NM8'
** UBA            ff        Status  Connection
   11 26 1       1.0  OPEN    FLOW-TO  'SURFACE'  REFLAYER
   11 26 2       1.0  OPEN    FLOW-TO  1
   11 26 3       1.0  OPEN    FLOW-TO  2
   11 26 4       1.0  OPEN    FLOW-TO  3
LAYERXYZ  'NM8'
** perf geometric data: UBA, block entry(x,y,z) block exit(x,y,z), length
```

```
   11 26 1  682.500000  1657.500000  1136.942000  682.500000  1657.500000
1145.692000  8.750000

   11 26 2  682.500000  1657.500000  1145.692000  682.500000  1657.500000
1154.442000  8.750000

   11 26 3  682.500000  1657.500000  1154.442000  682.500000  1657.500000
1163.192000  8.750000

   11 26 4  682.500000  1657.500000  1163.192000  682.500000  1657.500000
1171.942000  8.750000

        WELL  'NM9'

PRODUCER 'NM9'

OPERATE  MIN  BHP  200.0  CONT

**         rad  geofac  wfrac  skin

GEOMETRY  I  0.0762  0.37  1.0  0.0

     PERF      GEOA  'NM9'

** UBA              ff         Status  Connection

   17 23 1        1.0  OPEN    FLOW-TO  'SURFACE'  REFLAYER

   17 23 2        1.0  OPEN    FLOW-TO  1

   17 23 3        1.0  OPEN    FLOW-TO  2

   17 23 4        1.0  OPEN    FLOW-TO  3

LAYERXYZ  'NM9'

** perf geometric data: UBA, block entry(x,y,z) block exit(x,y,z), length

   17 23 1  1072.500000  1462.500000  1111.847000  1072.500000  1462.500000
1120.597000  8.750000

   17 23 2  1072.500000  1462.500000  1120.597000  1072.500000  1462.500000
1129.347000  8.750000

   17 23 3  1072.500000  1462.500000  1129.347000  1072.500000  1462.500000
1138.097000  8.750000

   17 23 4  1072.500000  1462.500000  1138.097000  1072.500000  1462.500000
1146.847000  8.750000

        WELL  'NM10'
```

```
PRODUCER 'NM10'
OPERATE  MIN  BHP  8400.0  CONT
**         rad  geofac  wfrac  skin
GEOMETRY  I  0.0762  0.37  1.0  0.0
    PERF     GEOA  'NM10'
** UBA             ff         Status  Connection
   19 33 1        1.0  OPEN    FLOW-TO  'SURFACE'  REFLAYER
   19 33 2        1.0  OPEN    FLOW-TO  1
   19 33 3        1.0  OPEN    FLOW-TO  2
   19 33 4        1.0  OPEN    FLOW-TO  3
LAYERXYZ  'NM10'
** perf geometric data: UBA, block entry(x,y,z) block exit(x,y,z), length
   19 33 1  1202.500000  2112.500000  1118.984000  1202.500000  2112.500000
1127.734000  8.750000
   19 33 2  1202.500000  2112.500000  1127.734000  1202.500000  2112.500000
1136.484000  8.750000
   19 33 3  1202.500000  2112.500000  1136.484000  1202.500000  2112.500000
1145.234000  8.750000
   19 33 4  1202.500000  2112.500000  1145.234000  1202.500000  2112.500000
1153.984000  8.750000
        WELL  'NM11'
PRODUCER 'NM11'
OPERATE  MIN  BHP  200.0  CONT
**         rad  geofac  wfrac  skin
GEOMETRY  I  0.0762  0.37  1.0  0.0
    PERF     GEOA  'NM11'
** UBA             ff         Status  Connection
   27 37 1        1.0  OPEN    FLOW-TO  'SURFACE'  REFLAYER
   27 37 2        1.0  OPEN    FLOW-TO  1
```

```
   27 37 3        1.0  OPEN    FLOW-TO  2

   21 37 4        1.0  OPEN    FLOW-TO  3

LAYERXYZ  'NM11'

** perf geometric data: UBA, block entry(x,y,z) block exit(x,y,z), length

   27 37 1  1722.500000  2372.500000  1101.455000  1722.500000  2372.500000
1110.205000  8.750000

   27 37 2  1722.500000  2372.500000  1110.205000  1722.500000  2372.500000
1118.955000  8.750000

   27 37 3  1722.500000  2372.500000  1118.955000  1690.000000  2372.500000
1125.931000  33.240255

   21 37 4  1364.999999  2372.500000  1151.941000  1300.000001  2372.500000
1157.143000  65.207828

         WELL  'NM12'

PRODUCER 'NM12'

OPERATE  MIN  BHP  8400.0  CONT

**         rad  geofac  wfrac  skin

GEOMETRY  I  0.0762  0.37  1.0  0.0

     PERF      GEOA  'NM12'

** UBA             ff         Status  Connection

   25 39 1        1.0  OPEN    FLOW-TO  'SURFACE'  REFLAYER

   25 39 2        1.0  OPEN    FLOW-TO  1

   25 39 3        1.0  OPEN    FLOW-TO  2

   25 39 4        1.0  OPEN    FLOW-TO  3

LAYERXYZ  'NM12'

** perf geometric data: UBA, block entry(x,y,z) block exit(x,y,z), length

   25 39 1  1592.500000  2502.500000  1119.419000  1592.500000  2502.500000
1128.169000  8.750000

   25 39 2  1592.500000  2502.500000  1128.169000  1592.500000  2502.500000
1136.919000  8.750000
```

25 39 3 1592.500000 2502.500000 1136.919000 1592.500000 2502.500000 1145.669000 8.750000

25 39 4 1592.500000 2502.500000 1145.669000 1592.500000 2502.500000 1154.419000 8.750000

STOP

** Trajectory header

RESULTS TRAJECTORY BEGIN

RESULTS TRAJECTORY WELLNAME 'NM1'

RESULTS TRAJECTORY TRAJNAME 'NM1'

RESULTS TRAJECTORY TRAJDATE 1997 9 1

** Trajectory nodes: X, Y, Z, DEPTH-MD, BLOCK-INDEX, NODE-TYPE, PERF-TYPE

RESULTS TRAJECTORY NODE -27.65 -26.75 0.00 0.00 -1 ORIGINAL CLOSED

RESULTS TRAJECTORY NODE -27.65 -26.75 1099.61 1099.61 -1 ORIGINAL CLOSED

RESULTS TRAJECTORY NODE -27.65 -26.75 1119.91 1119.91 5127 ORIGINAL CLOSED

RESULTS TRAJECTORY NODE -27.65 -26.75 1138.53 1138.53 -1 ORIGINAL CLOSED

RESULTS TRAJECTORY END

** Trajectory header

RESULTS TRAJECTORY BEGIN

RESULTS TRAJECTORY WELLNAME 'NM10'

RESULTS TRAJECTORY TRAJNAME 'NM10'

RESULTS TRAJECTORY TRAJDATE 1997 9 1

** Trajectory nodes: X, Y, Z, DEPTH-MD, BLOCK-INDEX, NODE-TYPE, PERF-TYPE

RESULTS TRAJECTORY NODE -157.65 1793.25 0.00 0.00 -1 ORIGINAL CLOSED

RESULTS TRAJECTORY NODE -157.65 1793.25 1195.22 1195.22 -1 ORIGINAL CLOSED

RESULTS TRAJECTORY NODE -157.65 1793.25 1215.62 1215.62 3697 ORIGINAL CLOSED

RESULTS TRAJECTORY NODE -179.32 1728.25 1211.83 1284.24 6859 ORIGINAL CLOSED

RESULTS TRAJECTORY NODE -579.08 528.97 1141.86 2550.32 10882 ORIGINAL CLOSED

RESULTS TRAJECTORY NODE -590.99 493.25 1139.78 2588.04 7821 ORIGINAL CLOSED

RESULTS TRAJECTORY NODE -607.24 444.50 1136.93 2639.51 7872 ORIGINAL CLOSED

RESULTS TRAJECTORY NODE -613.19 426.62 1135.89 2658.38 4761 ORIGINAL CLOSED

RESULTS TRAJECTORY END

** Trajectory header

RESULTS TRAJECTORY BEGIN

RESULTS TRAJECTORY WELLNAME 'NM11'

RESULTS TRAJECTORY TRAJNAME 'NM11'

RESULTS TRAJECTORY TRAJDATE 1997 9 1

** Trajectory nodes: X, Y, Z, DEPTH-MD, BLOCK-INDEX, NODE-TYPE, PERF-TYPE

RESULTS TRAJECTORY NODE -92.65 1663.25 0.00 0.00 -1 ORIGINAL CLOSED

RESULTS TRAJECTORY NODE -92.65 1663.25 1196.25 1196.25 -1 ORIGINAL CLOSED

RESULTS TRAJECTORY NODE -92.65 1663.25 1216.65 1216.65 3800 ORIGINAL CLOSED

RESULTS TRAJECTORY NODE -109.61 1598.25 1213.36 1283.90 6962 ORIGINAL CLOSED

RESULTS TRAJECTORY NODE -121.62 1552.21 1211.02 1331.54 10124 ORIGINAL CLOSED

RESULTS TRAJECTORY NODE -445.86 309.31 1148.06 2617.58 11088 ORIGINAL CLOSED

RESULTS TRAJECTORY NODE -453.69 279.29 1146.54 2648.64 11087 ORIGINAL CLOSED

RESULTS TRAJECTORY NODE -465.70 233.25 1144.21 2696.28 8027 ORIGINAL CLOSED

RESULTS TRAJECTORY NODE -478.41 184.50 1141.74 2746.72 8078 ORIGINAL CLOSED

RESULTS TRAJECTORY NODE -483.08 166.62 1140.83 2765.22 4967 ORIGINAL CLOSED

RESULTS TRAJECTORY END

** Trajectory header

RESULTS TRAJECTORY BEGIN

RESULTS TRAJECTORY WELLNAME 'NM12'

RESULTS TRAJECTORY TRAJNAME 'NM12'

RESULTS TRAJECTORY TRAJDATE 1997 9 1

** Trajectory nodes: X, Y, Z, DEPTH-MD, BLOCK-INDEX, NODE-TYPE, PERF-TYPE

RESULTS TRAJECTORY NODE -27.65 1533.25 0.00 0.00 -1 ORIGINAL CLOSED

RESULTS TRAJECTORY NODE -27.65 1533.25 1197.48 1197.48 -1 ORIGINAL CLOSED

RESULTS TRAJECTORY NODE -27.65 1533.25 1217.88 1217.88 3903 ORIGINAL CLOSED

RESULTS TRAJECTORY NODE -36.13 1468.25 1214.33 1283.52 7065 ORIGINAL CLOSED

RESULTS TRAJECTORY NODE 7116 ORIGINAL CLOSED -44.61 1403.25 1210.79 1349.17

RESULTS TRAJECTORY NODE 7167 ORIGINAL CLOSED -53.09 1338.25 1207.25 1414.81

RESULTS TRAJECTORY NODE 10329 ORIGINAL CLOSED -58.74 1294.91 1204.89 1458.58

RESULTS TRAJECTORY NODE 11142 ORIGINAL CLOSED -198.11 226.39 1146.67 2537.73

RESULTS TRAJECTORY NODE 11193 ORIGINAL CLOSED -205.70 168.25 1143.50 2596.45

RESULTS TRAJECTORY NODE 8133 ORIGINAL CLOSED -214.18 103.25 1139.96 2662.09

RESULTS TRAJECTORY NODE 8184 ORIGINAL CLOSED -220.53 54.50 1137.30 2711.33

RESULTS TRAJECTORY NODE 5073 ORIGINAL CLOSED -222.87 36.62 1136.33 2729.38

RESULTS TRAJECTORY END

** Trajectory header

RESULTS TRAJECTORY BEGIN

RESULTS TRAJECTORY WELLNAME 'NM3'

RESULTS TRAJECTORY TRAJNAME 'NM3'

RESULTS TRAJECTORY TRAJDATE 1997 9 1

** Trajectory nodes: X, Y, Z, DEPTH-MD, BLOCK-INDEX, NODE-TYPE, PERF-TYPE

RESULTS TRAJECTORY NODE 1 ORIGINAL CLOSED -30.90 -23.50 0.00 0.00 -

RESULTS TRAJECTORY NODE 5127 ORIGINAL CLOSED -30.90 -23.50 1119.83 1119.83

RESULTS TRAJECTORY NODE 5127 ORIGINAL CLOSED -11.40 -43.00 1120.33 1147.41

RESULTS TRAJECTORY NODE 37.35 -91.75 1121.58 1216.37
8290 ORIGINAL CLOSED

RESULTS TRAJECTORY NODE 102.35 -156.75 1123.24 1308.31
8342 ORIGINAL CLOSED

RESULTS TRAJECTORY NODE 167.35 -221.75 1124.91 1400.25
8394 ORIGINAL CLOSED

RESULTS TRAJECTORY NODE 232.35 -286.75 1126.57 1492.18
8446 ORIGINAL CLOSED

RESULTS TRAJECTORY NODE 297.35 -351.75 1128.23 1584.12
8498 ORIGINAL CLOSED

RESULTS TRAJECTORY NODE 362.35 -416.75 1129.90 1676.06
8550 ORIGINAL CLOSED

RESULTS TRAJECTORY NODE 427.35 -481.75 1131.56 1768.00
8602 ORIGINAL CLOSED

RESULTS TRAJECTORY NODE 492.35 -546.75 1133.22 1859.94
8654 ORIGINAL CLOSED

RESULTS TRAJECTORY NODE 557.35 -611.75 1134.89 1951.88
11817 ORIGINAL CLOSED

RESULTS TRAJECTORY NODE 622.35 -676.75 1136.55 2043.82
8758 ORIGINAL CLOSED

RESULTS TRAJECTORY NODE 687.35 -741.75 1138.22 2135.76
8810 ORIGINAL CLOSED

RESULTS TRAJECTORY NODE 736.10 -790.50 1139.46 2204.71
5751 ORIGINAL CLOSED

RESULTS TRAJECTORY NODE 753.97 -808.38 1139.92 2229.99
5751 ORIGINAL CLOSED

RESULTS TRAJECTORY END

** Trajectory header

RESULTS TRAJECTORY BEGIN

RESULTS TRAJECTORY WELLNAME 'NM4'

RESULTS TRAJECTORY TRAJNAME 'NM4'

RESULTS TRAJECTORY TRAJDATE 1997 9 1

** Trajectory nodes: X, Y, Z, DEPTH-MD, BLOCK-INDEX, NODE-TYPE, PERF-TYPE

RESULTS TRAJECTORY NODE -25.49 -30.00 0.00 0.00 - 1 ORIGINAL CLOSED

RESULTS TRAJECTORY NODE -25.49 -30.00 1119.91 1119.91 5127 ORIGINAL CLOSED

RESULTS TRAJECTORY NODE -38.49 -10.50 1119.93 1143.35 5127 ORIGINAL CLOSED

RESULTS TRAJECTORY NODE -54.74 13.87 1119.94 1172.64 5076 ORIGINAL CLOSED

RESULTS TRAJECTORY NODE -76.40 46.37 1119.96 1211.70 5075 ORIGINAL CLOSED

RESULTS TRAJECTORY NODE -108.90 95.12 1119.99 1270.29 8135 ORIGINAL CLOSED

RESULTS TRAJECTORY NODE -130.57 127.62 1120.01 1309.35 1912 ORIGINAL CLOSED

RESULTS TRAJECTORY NODE -157.65 168.25 1120.04 1358.18 1861 ORIGINAL CLOSED

RESULTS TRAJECTORY NODE -184.74 208.87 1120.06 1407.00 1810 ORIGINAL CLOSED

RESULTS TRAJECTORY NODE -206.40 241.37 1120.08 1446.07 1809 ORIGINAL CLOSED

RESULTS TRAJECTORY NODE -238.90 290.12 1120.12 1504.66 1758 ORIGINAL CLOSED

RESULTS TRAJECTORY NODE -260.57 322.62 1120.14 1543.72 1757 ORIGINAL CLOSED

RESULTS TRAJECTORY NODE -287.65 363.25 1120.16 1592.54 4817 ORIGINAL CLOSED

RESULTS TRAJECTORY NODE -314.74 403.87 1120.19 1641.37 4766 ORIGINAL CLOSED

RESULTS TRAJECTORY NODE -336.40 436.37 1120.21 1680.43 4765 ORIGINAL CLOSED

RESULTS TRAJECTORY NODE -368.90 485.12 1120.24 1739.02 4714 ORIGINAL CLOSED

RESULTS TRAJECTORY NODE -390.57 517.62 1120.26 1778.08 4713 ORIGINAL CLOSED

RESULTS TRAJECTORY NODE -417.65 558.25 1120.29 1826.90 4662 ORIGINAL CLOSED

RESULTS TRAJECTORY NODE -444.74 598.87 1120.31 1875.73 4611 ORIGINAL CLOSED

RESULTS TRAJECTORY NODE -466.40 631.37 1120.33 1914.79 4610 ORIGINAL CLOSED

RESULTS TRAJECTORY NODE -498.90 680.12 1120.36 1973.38 7670 ORIGINAL CLOSED

RESULTS TRAJECTORY NODE -520.57 712.62 1120.38 2012.44 4558 ORIGINAL CLOSED

RESULTS TRAJECTORY NODE -547.65 753.25 1120.41 2061.26 4507 ORIGINAL CLOSED

RESULTS TRAJECTORY NODE -571.49 789.00 1120.43 2104.23 7567 ORIGINAL CLOSED

RESULTS TRAJECTORY END

** Trajectory header

RESULTS TRAJECTORY BEGIN

RESULTS TRAJECTORY WELLNAME 'NM5'

RESULTS TRAJECTORY TRAJNAME 'NM5'

RESULTS TRAJECTORY TRAJDATE 1997 9 1

** Trajectory nodes: X, Y, Z, DEPTH-MD, BLOCK-INDEX, NODE-TYPE, PERF-TYPE

RESULTS TRAJECTORY NODE -27.25 -23.50 0.00 0.00 - 1 ORIGINAL CLOSED

RESULTS TRAJECTORY NODE -27.25 -23.50 1119.70 1119.70 5127 ORIGINAL CLOSED

RESULTS TRAJECTORY NODE -29.68 -43.00 1121.01 1139.39 8238 ORIGINAL CLOSED

RESULTS TRAJECTORY NODE -35.78 -91.75 1124.31 1188.63 8289 ORIGINAL CLOSED

RESULTS TRAJECTORY NODE -43.90 -156.75 1128.70 1254.28 8340 ORIGINAL CLOSED

RESULTS TRAJECTORY NODE -52.03 -221.75 1133.09 1319.94 8391 ORIGINAL CLOSED

RESULTS TRAJECTORY NODE -58.12 -270.50 1136.39 1369.18 8442 ORIGINAL CLOSED

RESULTS TRAJECTORY NODE -62.18 -303.00 1138.58 1402.00 8441 ORIGINAL CLOSED

RESULTS TRAJECTORY NODE -68.28 -351.75 1141.88 1451.24 8492 ORIGINAL CLOSED

RESULTS TRAJECTORY NODE -76.40 -416.75 1146.27 1516.90 8543 ORIGINAL CLOSED

RESULTS TRAJECTORY NODE -84.53 -481.75 1150.66 1582.55 8594 ORIGINAL CLOSED

RESULTS TRAJECTORY NODE -90.62 -530.50 1153.96 1631.79 5534 ORIGINAL CLOSED

RESULTS TRAJECTORY NODE -92.86 -548.38 1155.17 1649.84 5534 ORIGINAL CLOSED

RESULTS TRAJECTORY END

** Trajectory header

RESULTS TRAJECTORY BEGIN

RESULTS TRAJECTORY WELLNAME 'NM6'

RESULTS TRAJECTORY TRAJNAME 'NM6'

RESULTS TRAJECTORY TRAJDATE 1997 9 1

** Trajectory nodes: X, Y, Z, DEPTH-MD, BLOCK-INDEX, NODE-TYPE, PERF-TYPE

RESULTS TRAJECTORY NODE -30.90 -26.39 0.00 0.00 -
1 ORIGINAL CLOSED

RESULTS TRAJECTORY NODE -30.90 -26.39 1119.62 1119.62
5127 ORIGINAL CLOSED

RESULTS TRAJECTORY NODE -11.40 -28.56 1121.40 1139.32
8238 ORIGINAL CLOSED

RESULTS TRAJECTORY NODE 37.35 -33.98 1125.84 1188.57
8239 ORIGINAL CLOSED

RESULTS TRAJECTORY NODE 102.35 -41.20 1131.77 1254.24
8240 ORIGINAL CLOSED

RESULTS TRAJECTORY NODE 167.35 -48.42 1137.70 1319.91
11352 ORIGINAL CLOSED

RESULTS TRAJECTORY NODE 232.35 -55.64 1143.63 1385.58
8242 ORIGINAL CLOSED

RESULTS TRAJECTORY NODE 297.35 -62.86 1149.56 1451.24
11405 ORIGINAL CLOSED

RESULTS TRAJECTORY NODE 362.35 -70.09 1155.49 1516.91
8295 ORIGINAL CLOSED

RESULTS TRAJECTORY NODE 427.35 -77.31 1161.42 1582.58
8296 ORIGINAL CLOSED

RESULTS TRAJECTORY NODE 492.35 -84.53 1167.35 1648.25
5186 ORIGINAL CLOSED

RESULTS TRAJECTORY NODE 541.10 -89.95 1171.80 1697.50
5187 ORIGINAL CLOSED

RESULTS TRAJECTORY NODE 558.97 -91.93 1173.43 1715.56
5187 ORIGINAL CLOSED

RESULTS TRAJECTORY END

** Trajectory header

RESULTS TRAJECTORY BEGIN

RESULTS TRAJECTORY WELLNAME 'NM7'

RESULTS TRAJECTORY TRAJNAME 'NM7'

RESULTS TRAJECTORY TRAJDATE 1997 9 1

** Trajectory nodes: X, Y, Z, DEPTH-MD, BLOCK-INDEX, NODE-TYPE, PERF-TYPE

RESULTS TRAJECTORY NODE -417.65 2183.25 0.00 0.00 -1 ORIGINAL CLOSED

RESULTS TRAJECTORY NODE -417.65 2183.25 1196.07 1196.07 -1 ORIGINAL CLOSED

RESULTS TRAJECTORY NODE -417.65 2183.25 1216.47 1216.47 3387 ORIGINAL CLOSED

RESULTS TRAJECTORY NODE -444.74 2142.62 1213.21 1265.41 6549 ORIGINAL CLOSED

RESULTS TRAJECTORY NODE -466.40 2110.12 1210.60 1304.55 9659 ORIGINAL CLOSED

RESULTS TRAJECTORY NODE -513.63 2039.29 1204.90 1389.88 9710 ORIGINAL CLOSED

RESULTS TRAJECTORY NODE -986.40 1330.12 1147.90 2244.09 10263 ORIGINAL CLOSED

RESULTS TRAJECTORY NODE -1018.90 1281.37 1143.98 2302.81 10314 ORIGINAL CLOSED

RESULTS TRAJECTORY NODE -1040.57 1248.87 1141.37 2341.96 7202 ORIGINAL CLOSED

RESULTS TRAJECTORY NODE -1056.82 1224.50 1139.41 2371.32 7253 ORIGINAL CLOSED

RESULTS TRAJECTORY NODE -1068.74 1206.62 1137.97 2392.85 4142 ORIGINAL CLOSED

RESULTS TRAJECTORY END

** Trajectory header

RESULTS TRAJECTORY BEGIN

RESULTS TRAJECTORY WELLNAME 'NM8'

RESULTS TRAJECTORY TRAJNAME 'NM8'

RESULTS TRAJECTORY TRAJDATE 1997 9 1

** Trajectory nodes: X, Y, Z, DEPTH-MD, BLOCK-INDEX, NODE-TYPE, PERF-TYPE

RESULTS TRAJECTORY NODE -352.65 2118.25 0.00 0.00 -1 ORIGINAL CLOSED

RESULTS TRAJECTORY NODE -352.65 2118.25 1196.62 1196.62 -1 ORIGINAL CLOSED

RESULTS TRAJECTORY NODE -352.65 2118.25 1217.02 1217.02 3439 ORIGINAL CLOSED

RESULTS TRAJECTORY NODE -379.17 2076.27 1214.88 1266.72 6601 ORIGINAL CLOSED

RESULTS TRAJECTORY NODE -410.98 2025.90 1212.30 1326.35 9711 ORIGINAL CLOSED

RESULTS TRAJECTORY NODE -1066.34 988.24 1159.30 2554.79 10517 ORIGINAL CLOSED

RESULTS TRAJECTORY NODE -1085.61 957.73 1157.75 2590.90 10568 ORIGINAL CLOSED

RESULTS TRAJECTORY NODE -1106.14 925.23 1156.09 2629.38 7456 ORIGINAL CLOSED

RESULTS TRAJECTORY NODE -1122.39 899.50 1154.77 2659.84 7507 ORIGINAL CLOSED

RESULTS TRAJECTORY NODE -1133.68 881.62 1153.86 2681.00 4396 ORIGINAL CLOSED

RESULTS TRAJECTORY END

** Trajectory header

RESULTS TRAJECTORY BEGIN

RESULTS TRAJECTORY WELLNAME 'NM9'

RESULTS TRAJECTORY TRAJNAME 'NM9'

RESULTS TRAJECTORY TRAJDATE 1997 9 1

** Trajectory nodes: X, Y, Z, DEPTH-MD, BLOCK-INDEX, NODE-TYPE, PERF-TYPE

RESULTS TRAJECTORY NODE -1 ORIGINAL CLOSED	-287.65	2053.25	0.00	0.00
RESULTS TRAJECTORY NODE -1 ORIGINAL CLOSED	-287.65	2053.25	1198.32	1198.32
RESULTS TRAJECTORY NODE 3491 ORIGINAL CLOSED	-287.65	2053.25	1218.72	1218.72
RESULTS TRAJECTORY NODE 6653 ORIGINAL CLOSED	-311.49	2002.18	1214.01	1275.27
RESULTS TRAJECTORY NODE 9763 ORIGINAL CLOSED	-326.65	1969.68	1211.01	1311.26
RESULTS TRAJECTORY NODE 9814 ORIGINAL CLOSED	-355.67	1907.50	1205.28	1380.11
RESULTS TRAJECTORY NODE 9865 ORIGINAL CLOSED	-378.30	1859.01	1200.81	1433.81
RESULTS TRAJECTORY NODE 10269 ORIGINAL CLOSED	-629.45	1320.83	1151.21	2029.77
RESULTS TRAJECTORY NODE 10320 ORIGINAL CLOSED	-640.82	1296.46	1148.96	2056.76
RESULTS TRAJECTORY NODE 10319 ORIGINAL CLOSED	-655.99	1263.96	1145.96	2092.75
RESULTS TRAJECTORY NODE 10370 ORIGINAL CLOSED	-681.99	1208.25	1140.83	2154.45
RESULTS TRAJECTORY NODE 7310 ORIGINAL CLOSED	-703.65	1161.82	1136.55	2205.86
RESULTS TRAJECTORY NODE 7309 ORIGINAL CLOSED	-718.82	1129.32	1133.55	2241.85
RESULTS TRAJECTORY NODE 7360 ORIGINAL CLOSED	-735.07	1094.50	1130.34	2280.41
RESULTS TRAJECTORY NODE 4249 ORIGINAL CLOSED	-743.41	1076.62	1128.70	2300.20

RESULTS TRAJECTORY END

RESULTS SPEC 'Grid Top'

RESULTS SPEC SPECNOTCALCVAL -99999

RESULTS SPEC REGION 'Layer 1 - Whole layer'

RESULTS SPEC REGIONTYPE 'REGION_LAYER'

RESULTS SPEC LAYERNUMB 1

RESULTS SPEC PORTYPE 1

RESULTS SPEC MAP

RESULTS SPEC 'C:\Users\LABUSER\Desktop\HG\After\NMBNA.bna'

RESULTS SPEC

RESULTS SPEC 1

RESULTS SPEC UNITSTRING 'm'

RESULTS SPEC SPECKEEPMOD 'YES'

RESULTS SPEC STOP

RESULTS SPEC 'Permeability J'

RESULTS SPEC SPECNOTCALCVAL -99999

RESULTS SPEC REGION 'All Layers (Whole Grid)'

RESULTS SPEC REGIONTYPE 'REGION_WHOLEGRID'

RESULTS SPEC LAYERNUMB 0

RESULTS SPEC PORTYPE 1

RESULTS SPEC EQUALSI 0 1

RESULTS SPEC SPECKEEPMOD 'YES'

RESULTS SPEC STOP

RESULTS SPEC 'Permeability K'

RESULTS SPEC SPECNOTCALCVAL -99999

RESULTS SPEC REGION 'All Layers (Whole Grid)'

RESULTS SPEC REGIONTYPE 'REGION_WHOLEGRID'

RESULTS SPEC LAYERNUMB 0

RESULTS SPEC PORTYPE 1

RESULTS SPEC EQUALSI 1 0.37

RESULTS SPEC SPECKEEPMOD 'YES'

RESULTS SPEC STOP

F. Hydrogen Properties

Table 8.1 Hydrogen Properties Table (Dinçer et al. (2021))

Hydrogen Properties	Value	Unit
Molecular Weight	2.02	g/mol
Critical Pressure	13.15	bar
Critical Temperature	33.2	K
Density at the Critical Point	0.0324	g/mL
Normal Boiling Point (NBP)	20,268	K
Liquid Density @NBP	0.0708	g/mL
Vapor Density @NBP	0.000134	g/mL
Triple Point Pressure	0.0965	atm
Triple Point Temperature	13,803	K
Triple Point Solid Density	0.0865	g/mL
Triple Point Liquid Density	0.077	g/mL
Triple Point Vapor Density	0.0001256	g/mL
Melting Heat	58.23	J/g
Heat of Sublimation	507.39	J/g
Heat of Evaporation	445.59	J/g
Vapor Density @NTP	0.0838	kg/m3
Liquid Specific Heat Capacity @NBP	9.69	J/g*K
Gas Specific Heat Capacity@NTP	14.89	J/g*K
Liquid Heat Capacity Ratio @NBP	1,688	-
Gas Heat Capacity Ratio @NTP	1,383	-
Liquid Viscosity @NBP	0.000133	g/cm*s
Gas Viscosity @NTP	0.0000875	g/cm*s

Table 8.1 Continued…

Liquid Phase Surface Tension @NBP	0.00193	N/m
Liquid Phase Heat Conductivity @NBP	1	mW/cm*K
Gaseous Phase Heat Conductivity @NTP	1,897	mW/cm*K
Z gas compressibility factor @NTP	1.0006	-
Z liquid compressibility factor @NBP	0.01712	-
Coefficient of expansion for liquid @NBP	40.7037	ml*atm/g*K
Stochiometric Abundance in Air	29.53	% by volume
Explosion limit in Air	18.3-59	% by volume
Minimum Ignition Energy	0.02	mJ
Hot Air Jet Ignition Temperature	943	K
Ignition Temperature	844	K
Ignition Range in Air	4.1-74	% by volume
Adiabatic Flame Temperature	2318	K
Radiative Heat from Flame	17-25	%
Flame speed @NTP	265-325	cm/s
Explosion speed @NTP	1.48-2.15	km/s
Molecular Diffisuvity in Air @NTP	0.000061	m2/s
Diffusion Speed @NTP	2	cm/s
Lower Calorific Value by Mass	120	MJ/kg
Lower Calorific Value by Volume @1 atm	11	MJ/m3
Higher Calorific Value by Mass	142	MJ/kg
Higher Calorific Value by Volume @1 atm	13	MJ/m3
Wobbe Index	45.86	MJ/m3

G. UHS Project Risk Factors and Potential Outcomes

List of risk factors and potential outcomes (modified from RAG Austria AG et al., 2017).

1) Component Risk
    a) Hydrogen Embrittlement (steel)
        Leakage occuring at valves, compressors, casing, tubing, pipes or wellhead
    b) Diffusion into Facility Components
        Diffusion into packers or pipes
    c) Blistering (Elastomers)
        Leakage occuring at packers or sealing rings
    d) Corrosion (Steel)
        Leakage occuring at valves, compressors, casing, tubing, pipes or wellhead
    e) Viscous Cement Flow
        Cement Leakage
    f) Cement Diffusion
        Cement Leakage
    g) Nearby Wells Connected to the Reservoir
        Leakage into other regions
    h) Poorly Abandoned Nearby Wells
        Leakage through other regions
2) Human Risk
    a) Poor SCADA
        Overfilling the reservoir or missing out irregularities
    b) Poor Equipment Maintenance
        Leakage due to Maintenance
    c) Unsuitable Material from Supplier
        Leakage due to supplier
    d) Lack of Quality Checking of Material
        Leakage due to supplier

e) 3rd Party Interference

   Leakage due to sabotage

f) Misbehaviour from Contractors

   Leakage due to contractors

g) Bad Signage

   Leakage due to misconception

3) Environment Risk
   a) Flood
   b) Subsidence
   c) Earthquake
4) Non-Equipment Risk
   a) Viscous Fingering/Lateral Spreading

      Escape from trap

   b) Reservoir not being Isolated

      Escape from trap

   c) Existing Faults and Fractures

      Leakage to surrounding rocks, surface or groundwater

   d) Induced Shear or Hydraulic Fractures

      Leakage to surrounding rocks, surface, groundwater or destruction of the geological system

   e) Induced Capillary Pressure

      Leakage to surrounding rocks, surface or groundwater

   f) Methanogenesis, Homoacetogenesis, Sulphate Reduction

      Loss of gas

   g) Biomass Accumulation

      Destruction of the pore space

   h) Change of Mineral Composition, Aqueous Components or pH

      Destruction of the pore space

5) Risk Inducing Factors

a) H2S Generation

   Increasing risks of corrosion, embrittlement, blistering, cement leakage, fatality

b) Static Demixing

   Increasing risks of blistering, embrittlement, diffusion, cement leakage, cap rock leakage, viscous fingering

c) Dynamic Demixing (Pipes)

   Increasing risks of embrittlement and diffusion

d) Dynamic Demixing (Reservoir)

   Increasing risks of viscous fingering, cap rock leakage, cement leakage, blistering, and diffusion

e) Overfilling

   Increasing the risk of cap rock leakage

f) Too High Injection Rate

   Increasing the risk of viscous fingering

H. Comparison of Withdrawn Energy for Methane and Hydrogen Cycles

During the methane cycles between 15.11.2007 and 15.11.2032, 1663919489064 gmoles of CH_4 was produced. Taking 16.043 g/mole as the molecular weight of CH_4, 26.69 million tons of CH_4 can said to be produced.

During the hydrogen cycles between 15.11.2032 and 15.03.2057, 1500331507700 gmoles of H_2 was produced. Taking 2.0159 g/mole as the molecular weight of H_2, 3.17 million tons of H_2 can said to be produced. During hydrogen cycles 0.88 million tons of CH_4 was also produced.

Since their proportion was trivial, by neglecting the other gases in the stream, and taking 13.9 KWh/kg energy density for CH_4 and 33.6 KWh/kg for H_2, the withdrawn energy amounts are calculated as 371.05 TWhs for methane cycles and 119 (106.65_{H2}+12.25_{CH4}) TWhs for hydrogen cycles. In the end, 3.12 times more energy was withdrawn in the methane cycles compared to the hydrogen cycles.

Table 8.2 Summary Table for the 25 years Cycling Periods

Years (25 Cycles)	2007-2032	2032-2057	
Cycled Gas	CH4	H2	CH4
Production (gmoles)	$1.66392x10^{12}$	$1.57457x10^{12}$	54980640700
Production (million tons)	26.69	3.17	0.88
Produced Energy (TWh)	371.05	106.65	12.25

I. Flame Visibility

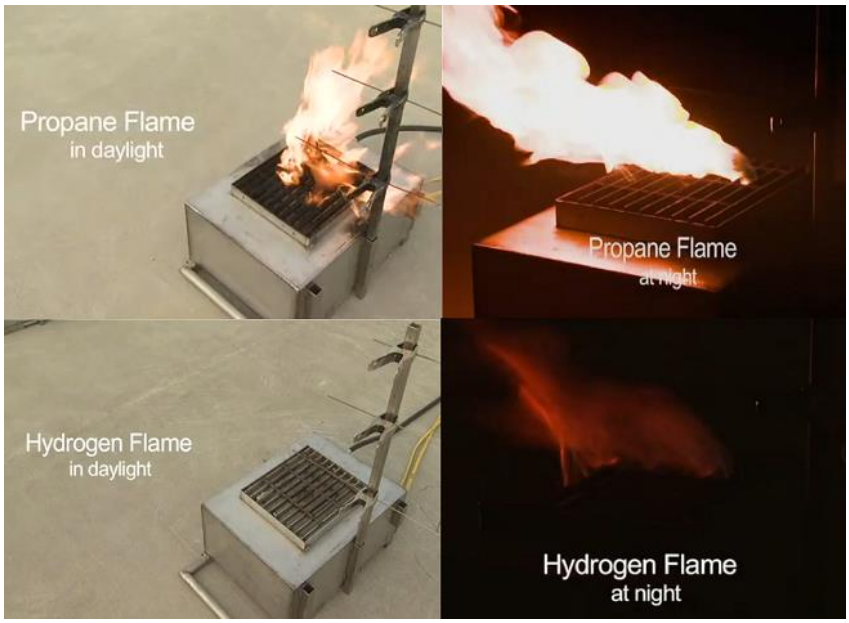

Figure 8.3. Propane Flame vs Hydrogen Flame (AIChE Academy, 2020)

Figure 8.4. Water Heater and Furnace burning simulation (Glanville et al., 2022)

J. Electrical Reliability of Solar and Wind

The map below shows that even in best case development scenarios, no country can fully rely on solar and wind to meet their electricity demand unless there is some form of storage (Tong et al., 2021 as cited in Sabine Hossenfelder, 2022).

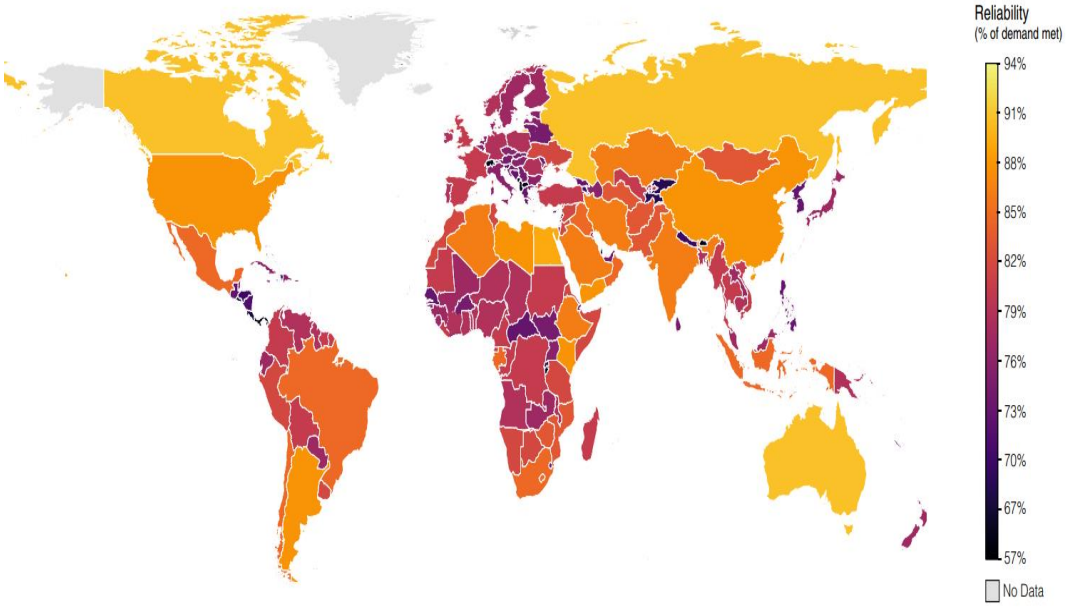

Figure 8.5. Countries' map of electricity system reliability under the most reliable solar-wind mix without excess generation or energy storage (Tong et al., 2021)

K. Worldwide UHS Projects

Table 8.3 Compilation of some UHS projects (Dopffel et al., 2021; Kruck et al., 2013; Zivar et al., 2021).

Project Name	Country	Since (year)	Storage Media	Working Conditions	Depth	Volume (1000 m^3)	H_2 (%)
Teeside	UK	1972	Bedded Salt	45 bar	365	3x70	95
Clemens	USA	1983	Domal Salt	70-137 bar	930	580	95
Moss Bluff	USA	2007	Domal Salt	55-152 bar	822	566	-
Spindletop	USA	-	Domal Salt	68-202 bar	1340	906	95
Kiel	Germany	1971	Salt	80-100 bar	1330	32	60
Ketzin*	Germany	1964 -2000	Aquifer	-	250	130000	Town Gas
Beynes*	France	1956 -1972	Aquifer	-	430	330000	50
STOPIL-H_2	France	ongoing	Salt	60-240 bar	-	90	-
Lobodice*	Czech Republic	1989	Aquifer	90 bar 34 °C	400	-	50
HyChico*	Argentina	2010	Depleted Gas Res.	26.5 bar 50 °C	815	750	10
Underground Sun*	Austria	2017	Depleted Gas Res.	78 bar 40 °C	1200	115	10

* denotes that the field has reported microbial activity

There are also five planned projects in Germany with one of them being under construction. USA has two, Denmark, Sweden, and Czech Republic each have one project in perspective (Advanced Energy Technologies, 2020).

L. Visualisation of European Hydrogen Projects

The European Network of Transmission System Operators for Gas (ENTSOG) have initiated a platform that visualises European hydrogen projects on a map and gives general information. A screenshot taken from the platform is given below in Figure 8.6. (ENTSOG, 2022)

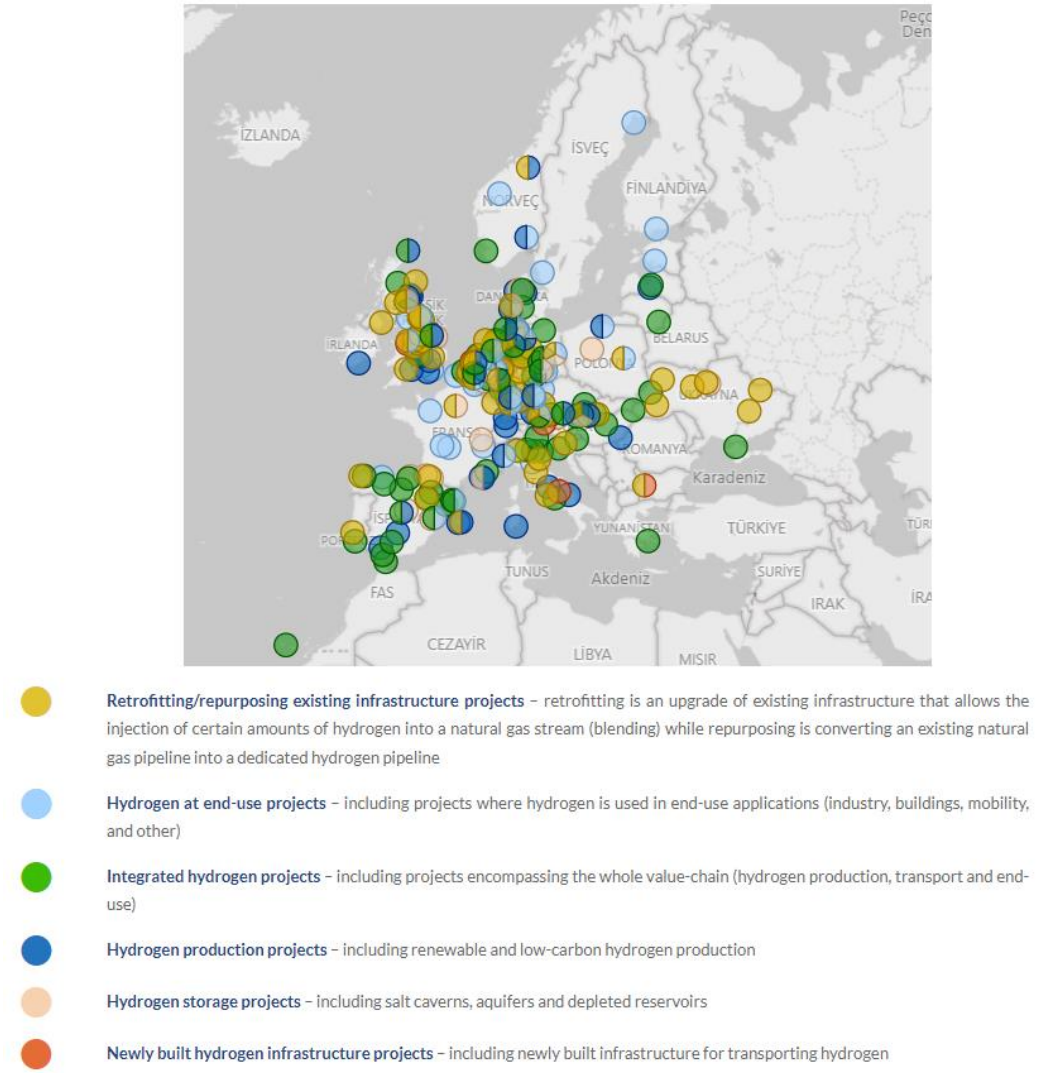

Figure 8.6. Visualisation of European Hydrogen Projects